

UNIVERSITÀ
DEGLI STUDI
DI PADOVA

Sede Amministrativa: Università degli Studi di Padova

Dipartimento di Geoscienze

CORSO DI DOTTORATO DI RICERCA IN SCIENZE DELLA TERRA
XXXI CICLO

**GAS EMISSION CENTRES ON MARS SURFACE AND
PUTATIVE BIOLOGICAL CONTRIBUTION: INSIGHTS
ON HYDROTHERMAL FLUID CIRCULATION IN THE
UPPER CRUST**

Coordinatore: Prof. Claudia Agnini
Supervisore: Prof. Matteo Mssironi
Co-Supervisore: Dr. Gabriele Cremonese
Dr. Francesco Mazzarini

Dottorando: Barbara De Toffoli

Barbara De Toffoli

**GAS EMISSION CENTRES ON MARS SURFACE
AND PUTATIVE BIOLOGICAL
CONTRIBUTION: INSIGHTS ON
HYDROTHERMAL FLUID CIRCULATION IN
THE UPPER CRUST**

“The open road still softly calls, like a nearly forgotten song of childhood. This appeal, I suspect, has been meticulously crafted by natural selection as an essential element in our survival. Long summers, mild winters, rich harvests, plentiful game—none of them lasts forever.

Herman Melville, in Moby Dick, spoke for wanderers in all epochs and meridians; he said: “I am tormented with an everlasting itch for things remote. I love to sail forbidden seas ...”

Maybe it’s a little early. Maybe the time is not quite yet. But those other worlds—promising untold opportunities—beckon.”

C.Sagan – Pale blue dot

“Because the history of evolution is that life escapes all barriers. Life breaks free. Life expands to new territories. Painfully, perhaps even dangerously. But life finds a way.”

M.Crichton – Jurassic Park

Index

<i>Outline</i>	pg 9
<i>Introduction</i>	pg 15
Chapter 1: Investigation method	
<i>Introduction</i>	pg 19
<i>Estimate of depths of source fluids related to mound fields on Mars</i>	pg 25
Chapter 2: Application to Mars exploration through orbiters' data	
<i>Introduction</i>	pg 47
<i>Surface expressions of subsurface sediment mobilization rooted into gas hydrate-rich cryosphere</i>	pg 49
<i>Evidence of mud volcanism related to gas hydrate-rich cryosphere on Mars</i>	pg 67
Chapter 3: From orbiter to field exploration	
<i>Introduction</i>	pg 103
<i>Comparative planetary structural asset analysis: insights on Martian sulfate vein networks and the Bletterbach site, N-E Italy</i>	pg 105
Appendix: Future developments	
<i>Introduction</i>	pg 125
<i>Looking for water-related environments on Mars: analysis of reflectance spectra for present and future exploration</i>	pg 129
<i>Young flows producing aqueous alteration in Ladon basin, Mars, observed by the CaSSIS imaging system on the ExoMars Trace Gas Orbiter</i>	pg 139
<i>Conclusions</i>	pg 147
<i>Acknowledgments</i>	pg 151

Outline

The herein presented work aims to develop and expand Mars geological exploration in a search for life prospective and, accordingly, water resurgence features and possible degassing centers have been given a central role in the target selection and process investigation. Hydrothermal fluid circulation in the Martian crust is among the natural processes characterized by the combined involvement of fluids such water and methane so defining a potential set of environments prone to biosphere growth and flourish. Subsurface fluid flow is a key area of planetary science research because fluids affect almost every physical, chemical, mechanical and thermal property of the upper crust. Hydrothermal systems are closely bond to the transport of mass, heat, nutrients and chemical species in hydrogeological systems making these mechanisms central in fields such as volcano-tectonic, deep-biosphere and water/ice cycle.

To step forward toward a new generation of planetary exploration that aims, not only to analyse and map the surfaces of planetary bodies other than Earth, but also to push the survey down in depth, in the *first chapter* we successfully test the efficiency of a rising technique that allows to probe the subsurface starting from surface case studies: fractal analysis. This method was firstly applied on many different study cases on Earth to investigate the location at depth of magma chambers and sediment source layers beneath volcanic vent and mud volcano fields. We thus took this technique and applied it to many different well-known morphologically convergent features on Mars, but with very different inferred formation process, in order to test if fractal analysis were an efficient methodology to identify spatial patterns linked to system of percolating connected fractures and drained material source depth by outputting the expected outcomes for the different cases. Thanks to the successfully obtained results we fostered the implementation of such method in the planetary exploration research field.

In the *second chapter* is reported the produced work concerning the exploration and investigation aimed to identify new regions on Mars with a high astrobiological potential through the usage of classic and fractal analyses. Since the main objective of the herein presented work is to spot emission centers linked to water and methane release, we set our starting point on the search for fields of pitted mounds, which are good candidate morphologies for our purposes. Many different areas, with large

coverages and very different geological context showed a relationship with systems of connected fractures extending many kilometres beneath the surface. We were not just able to profitably analyse different areas and locate several interesting vast regions, but we observed a systematic linkage between large fields of pitted mounds on the surface and the shallowest interface between gas hydrate-rich cryosphere and hydrosphere hypothesised for the Martian subsurface, so discovering the potential key role of clathrates on a, geologically speaking, recent Mars.

The intriguing results produced and displayed in the first two chapters of this work led to a spectrum of unsolved questions concerning the processes that could be involved in such kind of phenomena. We thus choose to approach this topic from the structural side aiming to produce structural asset interpretations based on fluid circulation evidence, where information is available. In the *third chapter*, we hence face a propaedeutic explorative study which has the objective to compare sulfate vein networks on several locations on Earth with sulfate veins outcropping in the Gale crater (Curiosity Rover landing site, Mars), that represent the only case of close up acquisitions of Martian features that surely experienced fluid circulation. A better understanding of the structural asset on portions of the Martian surface will progressively lead to a contextualisation of the forces that could have contributed to drive the fluid flows in the upper Martian crust and again pushing the exploration toward the subsurface realm and to the identification of outgassing and water related environments.

In the *fourth chapter* are exposed preliminary works that further pursue the aim of identify and investigate environments that experienced fluid circulation, backbone of this thesis. On one side, we moved on in exploring the Martian surface throughout the observation of the freshly acquired four-colours images of the CaSSIS camera we are involved in, with remarkable outcomes thanks to the location of light-toned ridges possibly linked to hydrothermal fluid percolation and connected rocks alteration. Contextually, we also approached the question from the compositional side by enhancing spectral libraries with the production of spectral signatures, on ultraviolet-far infrared wavelength span, of minerals belonging to environments that, on Earth, are linked to low temperature hydrothermal circulation and of rare bio-mineralisation features that are siliceous stromatolites.

Outline

-Italian Version-

Il lavoro presentato ha lo scopo di sviluppare ed espandere l'esplorazione geologica di Marte nell'ottica di ricerca di ambienti adatti allo sviluppo della vita e, di conseguenza, centri di risalita di acqua e centri di degassamento hanno avuto un ruolo centrale nella selezione degli obiettivi di indagine. La circolazione idrotermale nella crosta marziana è tra i processi naturali caratterizzati dal coinvolgimento combinato di fluidi quali acqua e metano, definendo così un potenziale insieme di ambienti inclini alla crescita e allo sviluppo della biosfera. La circolazione di fluidi nel sottosuolo è un'area chiave nel contesto delle scienze planetarie perché essi influenzano quasi ogni proprietà fisica, chimica, meccanica e termica della crosta superiore. I sistemi idrotermali sono strettamente legati al trasporto di massa, calore, sostanze nutritive e specie chimiche nei sistemi idrogeologici, rendendo questi meccanismi centrali in campi quali il ciclo vulcano-tettonico, la biosfera profonda e il ciclo acqua / ghiaccio.

Per sviluppare una nuova generazione di esplorazione planetaria che mira non solo ad analizzare e mappare le superfici dei corpi planetari diversi dalla Terra, ma anche a sondarne le profondità, nel primo capitolo testiamo con successo l'efficienza di una nuova tecnica che permette di investigare il sottosuolo partendo dalle osservazioni di superficie: l'analisi frattale. Questo metodo è stato applicato per la prima volta sulla Terra per indagare la profondità delle camere magmatiche e degli strati sorgente che alimentano vulcanesimo magmatico e vulcani di fango. Abbiamo quindi applicato questa tecnica a diverse strutture di superficie su Marte con caratteristiche morfologicamente convergenti, ma con processi di formazione molto diversi, al fine di verificare se l'analisi frattale fosse una metodologia efficiente per identificare la presenza di un sistema percolante di fratture connesse e la profondità della sorgente del materiale drenato. I risultati sono stati positivi promuovendone così l'implementazione nel processo di esplorazione planetaria.

Nel secondo capitolo viene riportato il lavoro prodotto relativo all'esplorazione volto a identificare nuove regioni ad alto potenziale su Marte attraverso l'uso di analisi classiche e frattali. Poiché l'obiettivo principale del presente lavoro presentato è quello di individuare i centri di emissione legati al rilascio di acqua e metano,

poniamo il nostro punto di partenza nella ricerca di campi di pitted mounds, che sono ottimi candidati per i nostri scopi. Varie aree, con grandi coperture e un contesto geologico molto diverso, hanno mostrato una relazione con sistemi di fratture connesse con estensioni fino a svariati chilometri di profondità. Non solo siamo stati in grado di analizzare proficuamente aree diverse e localizzare vaste regioni ad alto interesse, ma abbiamo osservato un collegamento sistematico tra grandi campi di pitted mounds sulla superficie e l'interfaccia più superficiale tra la criosfera ricca in clatrati e l'idrosfera ipotizzata per il sottosuolo marziano, scoprendo così il ruolo chiave che i clatrati potrebbero aver avuto su Marte in un passato geologicamente recente.

I risultati promettenti prodotti e mostrati nei primi due capitoli di questo lavoro hanno portato a uno spettro di domande riguardanti i processi che potrebbero essere coinvolti in questo tipo di fenomeni. Scegliamo quindi di affrontare questo argomento tramite l'interpretazione dell'assetto strutturale basato su evidenze di circolazione di fluidi, in aree in cui tali informazioni sono disponibili. Nel terzo capitolo, quindi, affrontiamo uno studio esplorativo propedeutico che ha l'obiettivo di confrontare sistemi di vene a solfati in diverse località sulla Terra con le vene a solfati affioranti nel Gale crater, che rappresentano l'unico caso di acquisizioni ravvicinate di strutture marziane che sicuramente hanno sperimentato circolazione di fluidi. Una migliore comprensione dell'assetto strutturale su porzioni della superficie marziana può portare progressivamente ad una contestualizzazione delle forze che potrebbero aver contribuito a guidare i flussi di fluido nella crosta superiore marziana e inoltre a migliorare la corrente conoscenza del sottosuolo marziano nonché all'identificazione di ambienti legati all'acqua.

Nel quarto capitolo sono esposti i lavori preliminari che hanno come obiettivo quello di identificare e indagare ambienti che hanno subito la circolazione di fluidi, spina dorsale di questa tesi. Da un lato, siamo andati avanti nell'esplorazione della superficie marziana attraverso l'osservazione delle immagini a quattro colori appena acquisite della camera CaSSIS, con esiti notevoli grazie all'individuazione di creste probabilmente legate alla percolazione di fluido idrotermale e all'alterazione delle rocce incassanti. Contestualmente, abbiamo anche affrontato la questione dal lato compositivo migliorando le librerie spettrali con la produzione di firme spettrali, in lunghezze d'onda dall'ultravioletto al lontano infrarosso, di minerali appartenenti

ad ambienti che, sulla Terra, sono legati alla circolazione idrotermale a bassa temperatura e di rare bio-mineralizzazioni quali le stromatoliti silicee.

Introduction

Planetary geology is an interdisciplinary research field which aims to explore and investigate planets other than Earth. This branch of geology is based on terrestrial geologic approaches and merges them with tools and technologies belonging to different fields, such as astronomy or engineering. Thus, rooted in classic geology principles, it needs to rely on remote sensing acquired data more than on field observations, even remaining deeply bonded to investigation processes grounded on experiments, modelling and comparison to terrestrial analogue realms. This discipline is hence focused on solid-surface bodies that orbit the Sun, i.e. planets, dwarf planets, satellites and small bodies. As of today, humankind put landers on two planets beyond Earth, Venus and Mars, two moons, Earth's Moon and Titan (Saturn's moon), one asteroid and two comets and have orbited and surveyed from remote many other bodies among which planet Mercury, Mars's moons, asteroid belt's bodies, Jupiter's icy moons and Pluto. Presently, Mars and Moon, immediately followed by gas giants' icy moons, are the primary targets of future exploration and in situ operations, both robotic and human, aiming to establish future bases for fundamental research related to geologic and life evolution and their intricate interplay.

In planetary exploration the importance of the analogy is invaluable; this principle, on which all sciences rely upon, implies possible links between similar features and is based on the comparison of newly discovered phenomena and features to the ones already known and understood. In the specificity of this branch of research, unknown environments are observed on alien planets and shared characteristics with terrestrial counterparts are identified. This starts a multiple hypotheses-based investigation process that allows scientists to infer likely potential interpretations and reconstructions. This procedure is clearly more than a mere look-alike exercise, it is the kick-off of the pioneer journey of exploration and, even where similarities are detected and considered, consistency needs to be shown by always keeping into account intrinsically different conditions occurring whenever analysing planetary bodies other than Earth. In the work herein presented, being the overall focus on the exploration of Mars, we commonly refer to Earth's environments as terrestrial analogues.

Planet Mars will be in the spot light of this work. It is the most far rocky planet orbiting the Sun, that is by definition a celestial body orbiting the Sun, mainly constituted by silicate rocks, with a sufficient mass to show self-gravity and overcome rigid body forces, thus reaching the hydrostatic equilibrium shape (nearly spherical), and have typically cleaned the space around their orbit. Being sited in the habitable zone and carrying undoubtable marks of past presence of large quantity of water on its surface, Mars covers a special place in space exploration. The habitable zone is a distance range around a star where liquid water can be supported given a sufficient atmospheric pressure. Hence, given the intimate relationship between liquid water and terrestrial biosphere, planets orbiting within this distance are considered pivotal targets for exploration for life forms. On Mars, the presence of water in the deep geological past is no question (until ~ 2 Ga), morphologies and formations linked to fluvial and lacustrine environments are today well-known in the collected data record. Progressively over the last 4 Gy, Mars experienced atmosphere loss resulting in a decrease of atmospheric pressure and temperature making liquid water unstable on the surface, this producing a retreat of water in solid form toward the poles and in the subsurface, where the Martian crust acts as a reservoir due to the impact-generated megaregolith high porosity. During the Noachian time ($\sim 4.6 - 3.7$ Ga) a hydrological cycle including surface runoff and precipitations was likely to be active, but from the Hesperian period ($\sim 3.7 - 3$ Ga) onward it started to be affected by drastic climate changes (linked for instance to a global decrease of the volcanic activity) that led to the loss of 95-99% of surface water and thus water release from the subsurface reservoirs to the surface started to be driven only by complex paroxysmal processes (e.g. outflow channels discharge). A diverse and abundant geological evidence population of water-related features is present on the Martian surface and covers a key role in understanding the evolution of the planet and in investigating the putative development of an extinct or extant biosphere.

Along with water, also methane covers a central role to address questions about the concurrent evolution of lithosphere and biosphere and it has been detected more than once in the Martian atmosphere by several means since 2004. The relevance of such discovery lies in the fact that this gas is produced in Earth's atmosphere predominantly through biological processes, along with a minor contribution of non-

biological geological mechanisms, among which the most efficient are serpentinization, geothermal activity and release from subsurface clathrates.

References

- Cockell, C.S., 2015. *Astrobiology*. John Wiley & Sons Ltd, 472 pp.
- Faure, G. and Mensing, T.M., 2007. *Introduction to Planetary Science: The Geological Perspective*. Springer, Dordrecht, The Netherlands, 526 pp.
- Formisano, V., Atreya, S., Encrenaz, T., Ignatiev, N., Giuranna, M., 2004. Detection of methane in the atmosphere of Mars. *Science* 306, 1758–1761.
- Geminale, A., Formisano, V., Giuranna, M., 2008. Methane in Martian atmosphere: Average spatial, diurnal, and seasonal behaviour. *Planet. Space Sci.* 56, 1194–1203. doi:16/j.pss.2008.03.004
- Judd, A.G., Hovland, M., 2007. *Seabed Fluid Flow: The Impact on Geology, Biology and the Marine Environment*. University Press, Cambridge. 475 pp.
- Mumma, M.J., Novak, R.E., DiSanti, M.A., Bonev, B.P., Dello Russo, N., 2004. Detection and mapping of methane and water on Mars. American Astronomical Society, 36th Division of Planetary Science Meeting, 8–12 November, 2004, Louisville. *Bull. American Astronomical Society* 36 (4), Abstract No. 26.02.
- Mumma, M.J., Villanueva, G.L., Novak, R.E., Hewagama, T., Bonev, B.P., Disanti, M. a, Mandell, A.M., Smith, M.D., 2009. Strong release of methane on Mars in northern summer 2003. *Science* 323, 1041–1045. doi:10.1126/science.1165243
- Rossi, A.P., 2018. *Planetary Geology*. doi.org/10.1007/978-3-319-65179-8
- Webster, C.R., Mahaffy, P.R., Atreya, S.K., Flesch, G.J., Mischna, M.A., Meslin, P., Farley, K.A., Conrad, P.G., Christensen, L.E., Pavlov, A.A., Martín-torres, J., Zorzano, M., McConnochie, T.H., Owen, T., Eigenbrode, J.L., Glavin, D.P., Steele, A., Malespin, C.A., Jr, P.D.A., Sutter, B., Coll, P., Bridges, J.C., Navarro-gonzalez, R., Gellert, R., 2015. Mars methane detection and variability at Gale crater. *Science* (80-.). 347, 415–417. <https://doi.org/10.1126/science.1261713>

Chapter 1: *Investigation method*

Introduction

The complexity of geosciences has inspired the development of many innovative concepts and techniques improving our understanding and modelling capacities of our complex environment. Euclidean geometrical shapes, such as by instance circles, spheres, rectangles or cones, rarely describe the reality of nature and can be considered mostly artificial models and approximations. Fractal geometry is, on the other hand, a geometry that allows the description of rough irregular shapes common constituents of the natural world.

The word fractal has been first used by Mandelbrot (1975, 1967) to refer to entities that could be broken down in finer elements regardless of the scale. Fractals have been initially described as mathematical entities, laying their roots in differential calculus and thus on the concept of infinitesimals, whose main properties are to be infinitely long and detailed and devoid of regularity. To understand these unceasing changing curves, it is necessary to bear in mind some concepts like the Cantor's continuum space concept, that explains the existence of different kinds of infinite sets (e.g. the lack of biunivocal correspondence between natural and real numbers), and, similarly, the Cantor set (Fig.1). This last is extremely useful to the understanding of fractal geometry; it can be graphically represented by drawing a straight line and then drawing the same line taking out the middle third, so two separate segments will thus be obtained. The Cantor set is ultimately obtained by repeating infinitely this same procedure for each drawn line. Even if this process can be undertaken infinitely, in the end the sum of the lengths of the removed intervals is equal to the length of the original interval. In addition to depict and highlight how infinite sets of different sizes co-exist, the invaluable concept introduced by this mathematical entity is self-similarity. This means that looking at a single step of the cut-out procedure it will always be similar to the former one, independently from the step we are considering. Bright examples of infinite self-similar curves are by instance the Peano curve, which thins the boundary between the geometrical concepts of line and plane, and the Koch curve (Fig.1). This second one, also known as Snowflake curve, is one of the best known graphical examples to picture fractals. It is a curve so densely folded to be infinitely long even if contained in a limited space (i.e. the length of the curve in-

between any two given points is always infinite) and its peculiar characteristic is that it appears constantly the same in spite of what scale we look at it.

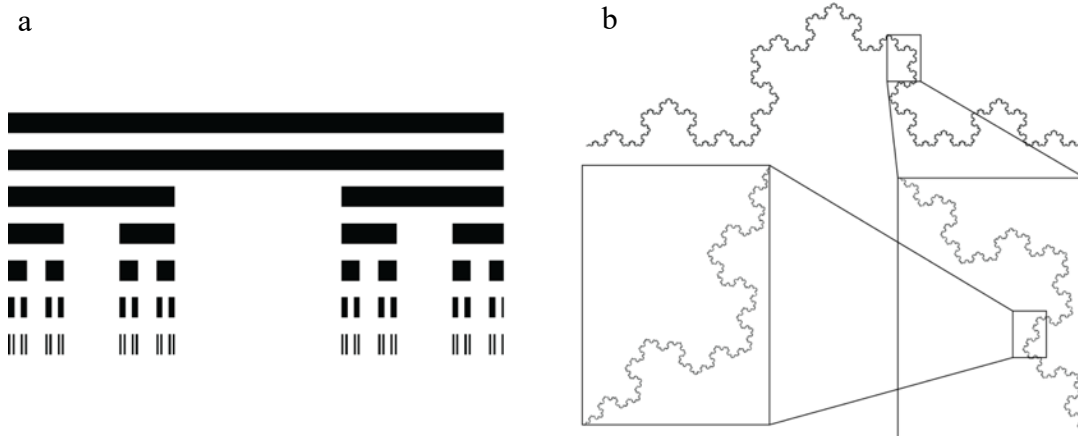


Fig.1 Cantor set (a) and Koch curve (b)

Richardson (1961) applied fractal geometry to the description of a natural system that became an emblematic example of the further leap of actual description of reality through this new method. In his work, Richardson assesses that the exact length of the Great Britain coast is undefinable and it tends to infinity, so declaring that the object of his interest and geological formations are best described by fractal. This case study underscores how the concept of length starts making little sense when it comes to fractals and the common concept of dimension starts fading. Objects residing in Euclidean geometry are usually intended to be mono, bi or three dimensional and so on (for example, a segment in mono-dimensional, a square is bi-dimensional and a cube is three-dimensional), but fractals are irregular objects and thus require an increased complexity introduced by fractional values (Fig.2). Accordingly, a line residing in the Euclidean domain has a dimension $D=1$, while in the case of a fractal entity the irregularity grows and the dimension along with it, so the fractal dimension will assume increasing fractional values (non-whole values) with the rising roughness. In the case of Richardson's work, the line describing the Great Britain coast's length results to have a fractal dimension $D=1.26$, that is almost identical to the Koch curve's.

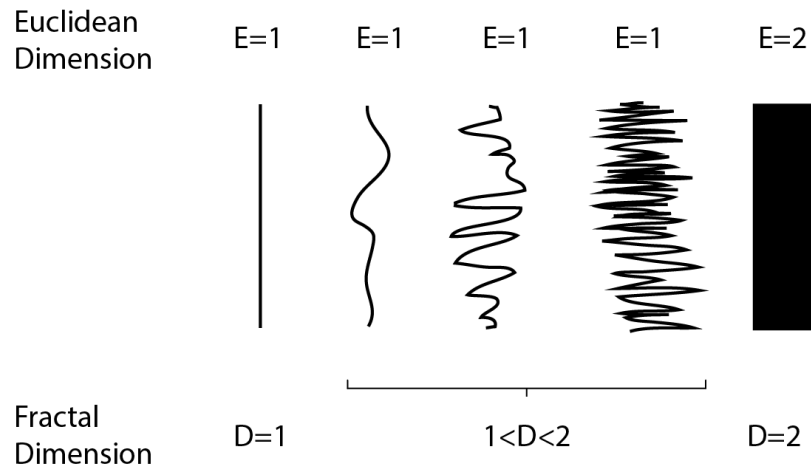


Fig.2. Fractal dimension is represented by increasing fractional values constrained between 1 and 2 with the increasing complexity of the line.

Despite the complexity of these structures, real natural fractal systems are finite entities, so they show irregular dimension and self-similarity within a size range of existence. This size range of existence is limited by the magnitude of the smallest element and the magnitude of the whole system. These physical limits could be visualized referring to practical examples in many natural realms, i.e. geography: one single channel - the entire drainage basin; living world: the ammonite's single living chamber - the whole shell. These instances are trivial, but highly complicated systems occur in nature whose fractal behaviour and size range are not immediately detectable so making this intimate connection, between fractal distribution and size range, a pivotal tool for the geological investigation. Among natural systems following fractal distributions, there are networks of connected fractures that will be one of the central focuses of the studies herein collected. As presented further on in the main section of this chapter, the analysis through singularities mapping has been proved to be a very effective tool to characterize the local structural properties of spatial patterns and methodologies have been developed to infer the existence range of fractal systems by seeking and analysing their fractal behaviour, thus providing invaluable clues on the entirety of the frame when only limited portions of it are detectable. The purpose of the following study is therefore to assess the applicability and usefulness of such methodologies, based on fractal analyses, for the investigation of planetary surfaces. This branch of fractal concepts applied to geosciences is based on the percolation theory which in turn relies on connectivity of voids in a given medium). Connectivity is relevant to a number of processes that involve flow or transport of material from

one place to another, or to whether a rigid portion of a medium connects across a system, accordingly, percolation theory has potential relevance while studying flows of materials. In nature, the development of drainage networks is an active process that connects paths through a medium leading to flux optimization that can be reached by the construction of an optimal network in space, or it may reflect the selection of an optimal path through a disordered network.

References

- Ghanbarian, B. and Hunt, A.G., 2017. *FRACTALS: Concepts and Applications in Geosciences*. CRC Press
- Mandelbrot, B., 1967. How Long Is the Coast of Britain ? Statistical Self-Similarity and Fractional Dimension. *Science* 156, 636–638
- Mandelbrot, B., 1975. Stochastic models for the Earth 's relief , the shape and the fractal dimension of the coastlines , and the number-area rule for islands. *Proc. Natl. Acad. Sci.* 72, 3825–3828
- Richardson, L F, 1961. The problem of contiguity: An appendix to statistics of deadly. *General Systems Yearbook* 6, 139–187.
- Stauffer, D. and A. Aharony. 1994. *Introduction to Percolation Theory*. Taylor and Francis, London

***ESTIMATE OF DEPTHS OF SOURCE FLUIDS RELATED TO
MOUND FIELDS ON MARS***

Barbara De Toffoli ^{a,b,*}, Riccardo Pozzobon ^{a,b}, Francesco Mazzarini ^c,
Csilla Orgel ^d, Matteo Massironi ^{a,b}, Lorenza Giacomini ^e, Nicolas Mangold ^f,
Gabriele Cremonese ^b

^a Department of Geosciences, University of Padova, Via Gradenigo 6, Padova 35131, Italy

^b INAF, Osservatorio Astronomico di Padova, Vicolo dell'Osservatorio 3, Padova I-35122, Italy

^c Istituto Nazionale di Geofisica e Vulcanologia, Via Della Faggiola 32, Pisa 56100, Italy

^d Institute of Geological Sciences, Planetary Sciences and Remote Sensing, Freie Universitat, Berlin, Germany

^e INAF, Istituto di Astrofisica e Planetologia Spaziali, via Fosso del Cavaliere 100, Roma 00133, Italy

^f Laboratoire de Planetologie et Geodynamique, Universite de Nantes, Nantes, France

De Toffoli, B., Pozzobon, R., Mazzarini, F., Orgel, C., Massironi, M., Giacomini, L., Mangold, N., Cremonese, G., 2018. Estimate of depths of source fluids related to mound fields on Mars. *Planet. Space Sci.* 164–173. <https://doi.org/10.1016/j.pss.2018.07.005>

Abstract

The investigation of the Martian surface through remote sensing allowed the identification of mound-like topographically positive features that, based on geomorphological observations, have been ascribed to different phenomena. New observations will be performed in the forthcoming future to look for possible methane sources, hence discriminating morphologically similar features is a key objective to efficiently investigate and target the Martian surface. Here, we performed fractal analysis on five Martian fields of mound-like features that have been interpreted respectively as mud volcanoes, pingos, tumuli, rootless cones and monogenetic volcanic vents successfully validating the major interpretations of these features and in turn, the applicability of the fractal clustering method for discriminating among such features. Indeed, this technique is able to assess if the analysed features are directly related to underlying systems of connected percolating fracture networks and estimates their extension in the subsurface. Accordingly, volcanic vents and mud volcanoes appeared to be connected to percolating systems involving several kilometers of crust, pingos and tumuli resulted to be unequivocally unrelated to active

percolating fractures while rootless cones outputted weak relationship with shallow active fracture systems.

1. Introduction

The analysis of the spatial clustering of vents and/or fractures, on rocky and icy planetary surfaces, can provide information about the fracture network exploited by fluids during their flow up and their linkage with the possible fluid source at depth. In particular, the analysis of the self similar (fractal) clustering, either applies to fractures themselves or to eruption vents, has been already used to explore the fluid source depth and the crust mechanical layering on Earth, Mars and Enceladus (Mazzarini, 2004; Mazzarini & Isola, 2010; Le Corvec et al., 2013; Pozzobon et al., 2015, Lucchetti et al., 2017). Thus, besides the investigation of fractures (e.g. Renshaw, 1999; Bonnet et al., 2001; Mazzarini & Isola, 2010), this method has been recognized as a valid technique to be applied to features that have a well-known relationship with subsurface flows of materials providing insights on the application of the method to estimate the depths of the reservoirs, such as volcanic vents (Mazzarini, 2004; Mazzarini & Isola, 2010), mud volcanoes (Bonini & Mazzarini, 2010) and on volcanic dykes on Mars (Pozzobon et al., 2015).

In this work we test the reliability of this technique for discriminating mound features on Mars apt to be confused due to their morphological similarities. Accordingly, we have applied the fractal methodology on case studies where there is wide consensus on the interpretation of the morphologies. Our work is therefore focused on providing an innovative tool to distinguish features related to near-surface vs. deep-rooted phenomena and additionally provide a more solid interpretation. Specifically, herein are considered: monogenic volcanic vents, mud volcanoes, pingos, rootless cones and tumuli (Hargitai and Kereszturi, 2015). Indeed, all of these morphologies during their evolution stages can come to appear as mounds, organized within large fields, and, undergoing a cross comparison process with terrestrial analogue features, uncertainties arise due to the presence of characteristics that can lead to more than just one interpretation. The technique presented in this work provides information on the occurrence of a deep-rooted pathway hydraulically connecting the surface to deep reservoir systems. Therefore, it can be used to distinguish between formation mechanisms that are related or unrelated to connected fracture networks, providing also estimates about the fluid source depths when the

connectivity exists, so leading to a discrimination of different types of resurgence products and mechanisms.

2. Background

To address the objective of providing a new tool unbiased by geomorphological observations to help the discrimination of mound-like morphologically convergent features, we herein undertook the analyses only on samples of structures which interpretation has been well accepted among the scientific community so to leave the focus on the efficiency of the method.

Specifically, volcanic vents, mud volcanoes, pingos, rootless cones and tumuli will be under examination since all of them can appear as mound-like topographically positive features and all of them have been observed on the Martian surface (Fig. 1; Fig. 2; Fig. 3 and references therein).

The comparative process of investigation between well-known regions, in this case on Earth, and the ones under examination on Mars is crucial and leads to a better understanding of objects on both sides. In this work frame, we concurrently addressed some terrestrial analogue features to investigate more deeply those categories that have never undergone fractal analysis before, that is to say rootless cones, tumuli and pingos. The methodology herein discussed is indeed meant to provide information about fracture-related phenomena, thus allowing the user to tell apart processes that involve widely different crustal thicknesses. Accordingly, in the past, it has been applied only where fracture systems were already known to underlie the surface structures (e.g. Bonini and Mazzarini, 2010; Mazzarini and Isola, 2007, 2010) leaving unexplored very shallow process expressions. Thus, we selected one terrestrial analogue region for each unexplored feature category choosing areas where fields large enough are recognizable through the observation of satellite images. The analyses described in the following sections were carried out on both planets by performing manual mapping of edifices and accordingly applying fractal analysis. Although we performed consistent and comparable procedures, throughout the mapping process terrestrial and Martian environments showed different limitations. On Mars an easier identification of mound fields is facilitated by a wide continuous coverage of the surface by mid-resolution (MRO CTX, ~ 6 m/pixel) images and due to favourable environmental conditions, i.e. absence of disturbance factors such as vegetation covering or clouds. On Earth, remote observation of the surface faces

stricter limits such as smaller dimensions of features, because of gravity difference in comparison to Mars, vegetation covering and/or more intense weathering degradation. Terrestrial analogues are sites showing geological and environmental conditions resembling the ones that characterize locations of interest on Mars; although this allows to collect a broader amount of information, differences mainly driven by gravity occur. On Mars gravity is around one third (3711 m/s^2) of Earth's counterpart and this substantially affects morphologies and dimensions of features, particularly when considering resurgence processes. In fact, lower gravity impacts material traits such density and compaction, leading fluid masses to more easily rise buoyantly when less dense than the surrounding rock, and it affects volumes involved in resurgence processes as well, that end up being larger since more mass is needed to crack the host medium and let the buoyant materials rise; accordingly, to accommodate such increased volumes, thicknesses of lithosphere wider than their terrestrial counter- part may be involved (e.g. Carr, 2006). We herein chose to analyse shallow-processes terrestrial features which identification and interpretation is already assessed and accepted among the scientific community so to leave, once more, the focus on the efficiency of the method. On this base, we considered the following terrestrial locations (Fig. 2): (i) 1783-84 Laki lava flow in Iceland for rootless cones (Hamilton et al., 2010; Bruno et al., 2006); (ii) Llacanelo Volcanic Field, Mendoza, Argentina for tumuli (Nemeth et al., 2008); (iii) Kolyma Lowland, North Asia for pingos (Grosse and Jones, 2011).

Overall, all the investigated features on Mars and on Earth, although similar in shape, may result from significantly different processes as the upwelling of materials and fluids from beneath, (with varying thickness of medium and natures of the extruded materials) or from thermo- mechanical processes (Fig. 3). By the application of fractal analysis, we hence aim to provide insights about the possible presence of connectivity between mounds and fractures and so distinguishing between fracture-related or fracture-unrelated processes, thus integrating and strengthening the information datasets that concur to the interpretation of mound-like features, particularly where actual connection with percolating systems occur and further details about the fluid source depths can be inferred.

2.1 *Monogenetic volcanic vents*

Monogenetic vents are volcanoes that, according to several authors (e.g. Smith and Nemeth, 2017; Nemeth and Kereszturi, 2015; Nemeth, 2010; Connor and Conway, 2000) are the product of single episodes short lived, small-volume and normally deep-sourced, hence mafic, volcanic activity. They are associated to feeder dykes fed from deep sources sitting at several tens of kilometres in the subsurface and have no real associated to shallower magma chambers. The feeding systems of monogenetic vents are connected to magmatic reservoirs sited at depth within the lithosphere. We herein analysed the monogenetic volcanic vents located in the Tharsis region (Pavonis Mons South and South-Eastern Volcanic Fields) described and mapped by Bleacher et al. (2009) and (2007a).

2.2 *Mud volcanoes*

Mud volcanoes are the result of upflows of gases, water and sediments from the subsurface that occur when the buoyancy forces that push the mixtures exceed the confining lithostatic pressure (van Loon, 2010; Kopf, 2002). The rapid sedimentation and low permeability of surrounding strata can lead to store undercompacted levels at depth and therefore overpressured and buoyant. The resurgence can be triggered by new fluid supply, increasing of pore pressures and a decrease of viscosity that could be produced by various events such as tectonic loading, impact cratering unloading, hydrothermal pulses, hydrocarbon generation, or injection of gas through dissociation of clathrates (Dimitrov, 2002; Kopf, 2002; Prieto-Ballestreros et al., 2006; Skinner and Tanaka, 2007; Skinner and Mazzini, 2009; Oehler and Allen, 2010 and references therein). Mud volcanoes are topographically positive features that can come in single or coalescent mounds, dome or pie shaped (depending on the flattening grade estimated on slope angles, specifically the term mud pie is usually applied when less than 5° (e.g. Kopf, 2002; Mazzini and Etiope, 2017)). This phenomenon has been herein addressed by mapping and investigating a sample of Acidalia Planitia cones interpreted as mud volcanoes (e.g. Oehler and Etiope, 2017; Oehler and Allen, 2010). Thousands of mud volcanoes have been observed in that area, showing the typical

mud volcano dome shape, circular base, light albedo, low thermal inertia, central pit and flow features (Oehler and Allen, 2010, 2012).

2.3. *Pingos*

Pingos are periglacial landforms produced by the upwelling of freezing water that results in transient hill shaped morphologies. Such appearance is, indeed, due to the volume increase during the transition from liquid water, capillary up-flowing, to solid state ice close to the surface and are usually subjected to apex collapse due to the subaerial exposition and destabilization of the ice core. Pingos go through different evolution stages that affect their morphology. They firstly appear like surface bulges with no summit depressions; later, during the growth process, the surface dissects leading to the beginning of the mound collapse, thus orthogonal, tensional single or multiple intersecting cracks propagate downslope from their tops; after the melting process, the remnants of pingos appear like shallow, rimmed depressions whose margins can merge forming overlapping, lobate, irregular features (e.g. Page and Murray, 2006; Burr et al., 2009; Dundas and McEwen, 2010). As case study, we mapped a group of features interpreted as pingos in Athabasca Valles from their shape and localization inside a flood valley (Page and Murray, 2006; Balme and Gallagher, 2009).

2.4. *Rootless cones*

Rootless cones (or pseudocraters) are volcanic exit points of pyro- clasts derived from an explosive interplay, produced for instance by the interaction between volatile-rich substrates and lava flows (Thorarisson, 1953), and are characterized by a lack of vertical magmatic feeder networks (Bruno et al., 2004; Sheth et al., 2004; Lanagan et al., 2001; Keszthelyi and Self, 1998). The definition of “rootless” lays in the absence of magma chambers feeding the cones. These can come in single, double or multiple concentric and/or coalescent cones with steep sides and summit crater (Noguchi et al., 2016). Distribution of rootless cones on the surface can be clustered, but their non-random arrangement is ascribed to lava pathways (Bruno et al., 2004). We addressed rootless cones investigation by mapping a portion of a rootless cone field in the Phlegra Dorsa region from their localization at the edge of lava flows (e.g. Bruno et al., 2006; Lanagan et al., 2001).

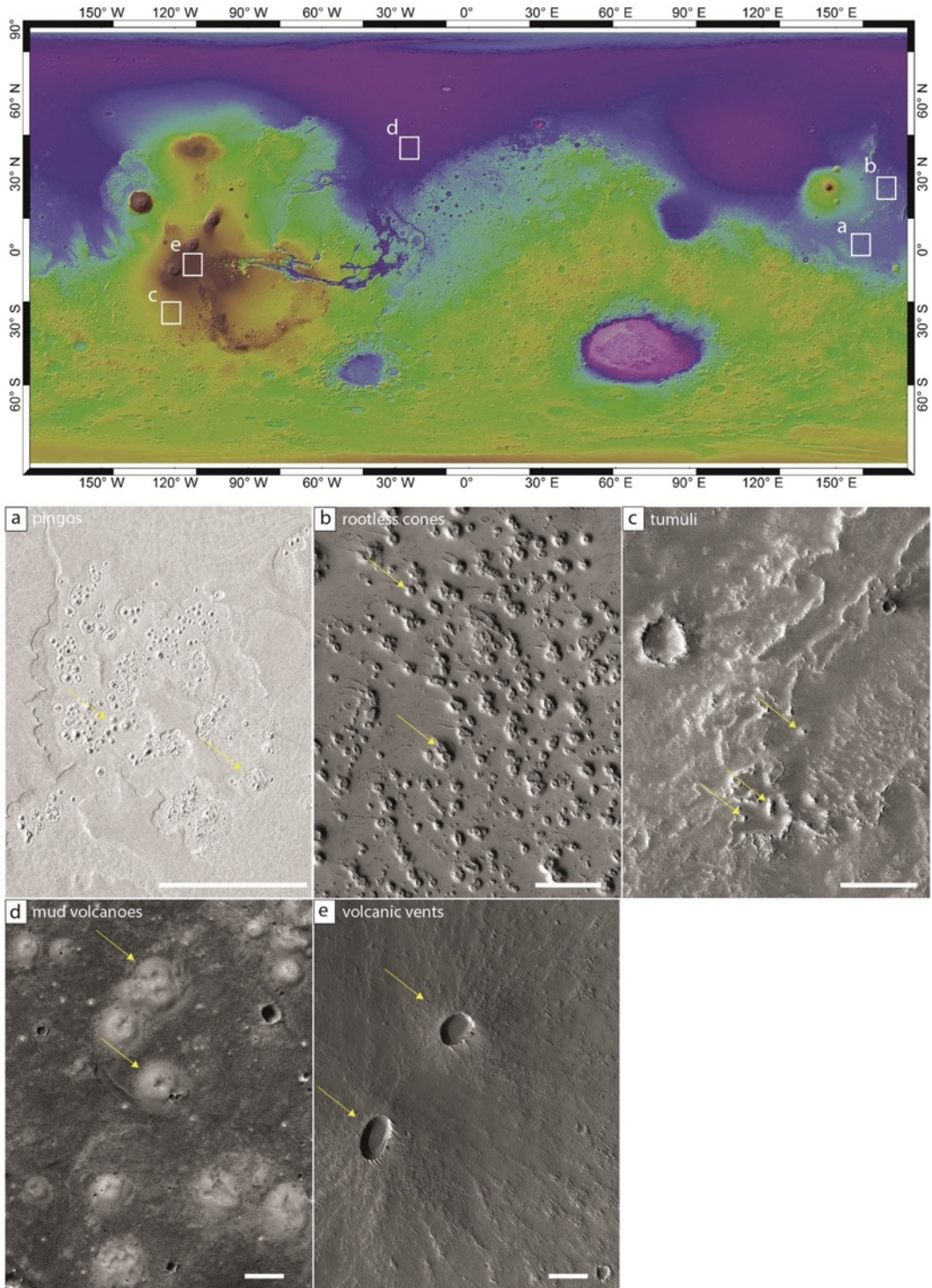


Fig. 1. On the map, locations of the study areas are indicated by white boxes. Samples of features interpreted as a) pingos (PSP_009280_1905) in Athabasca Valles (Balme and Gallagher, 2009), b) rootless cones (ESP_047085_2060) in Phlegra Dorsa region (Bruno et al., 2004), c) tumuli (PSP_002711_1550) in Daedalia Planum (Giacomini et al., 2009), d) mud volcanoes (PSP_008522_2210) in Acidalia Planitia (Oehler and Allen, 2010) and d) monogenetic volcanic vents (ESP_014037_1760) in the Tharsis Province (Bleacher et al., 2009). Arrows highlight single and, where present, coalescent structures of each object type. (scale bars: 500 m).

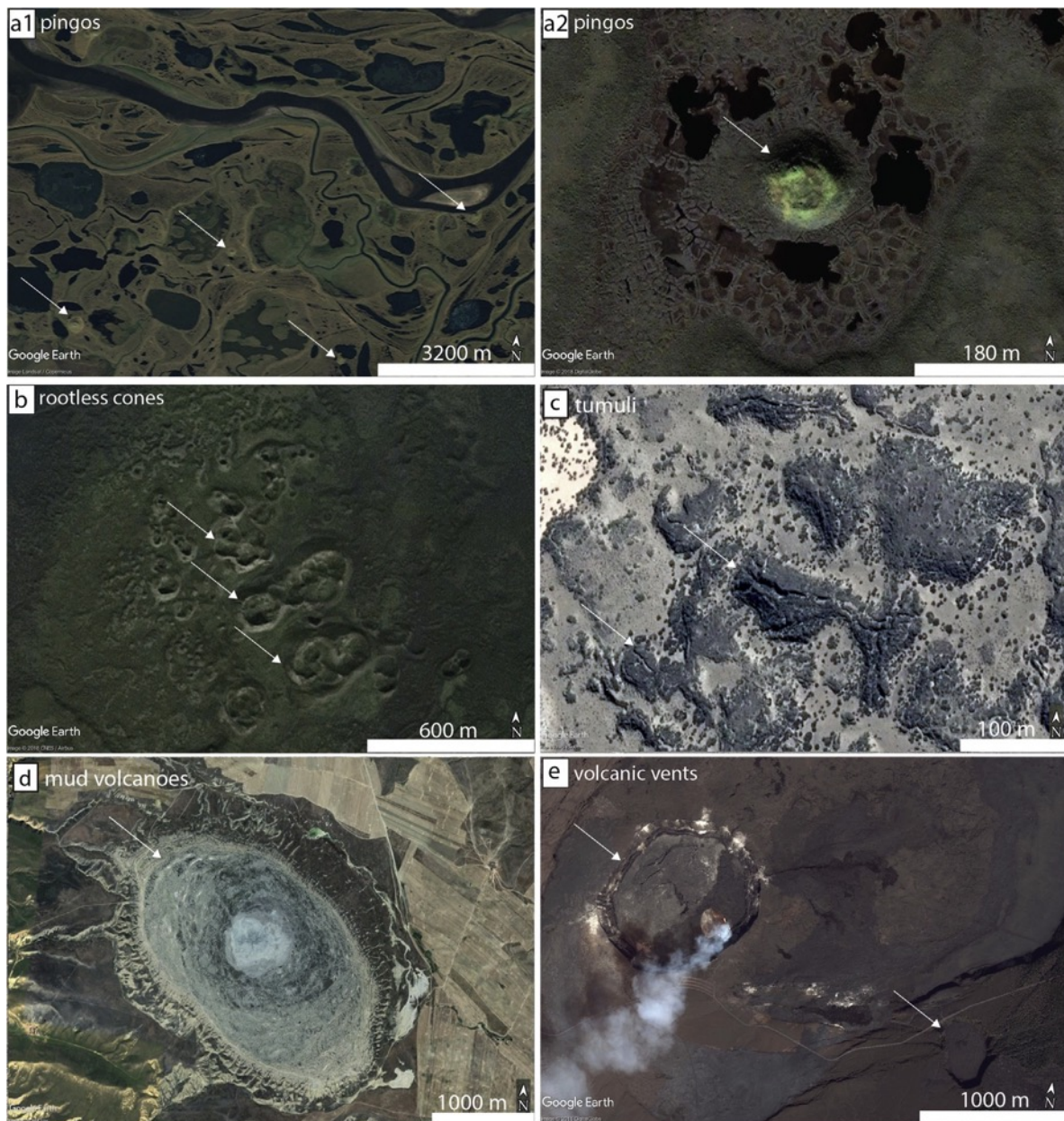


Fig. 2. Terrestrial analogues: a1) Pingos, North Asia (Grosse and Jones, 2011); a2) single pingo, Mackenzie delta, Canada (Balme and Gallagher, 2009); b) rootless cones, Iceland (Hamilton et al., 2010); c) tumuli, Argentina (Nemeth et al., 2008); d) mud volcanoes, Azerbaijan (Mazzini and Etiope, 2017); e) volcanic vents, Kilauea, Hawaii.

2.5. Tumuli

Tumuli are circular to elliptical knobby positive features displaying clefts on the top that are produced on lava flows' surface due to magmatic overpressure which can locally induce uplift on the sealing crust (Nemeth et al., 2008, 2017; Mattsson and Hoskuldsson, 2005; Rossi and Gudmundsson, 1996; Walker, 1991; Ollier, 1964). In fact, the movement of inflated lava is initially distributed uniformly throughout the liquid core and then, progressively, differential cooling occurs focusing lava flux. At this stage, when obstacles are encountered by the lava flow a localized inflation may create tumuli (Hon et al., 1994). Alignments can be observed also in tumuli distribution due to preferential magma path- ways, such as lava tubes, within the inflation (Giacomini et al., 2009). A knob field located in Daedalia Planum, already ascribed to tumuli uplift process, has been herein addressed as a case study for this category (Giacomini et al., 2009; Giacomini and Massironi, 2010). In this specific case, the recognized tumuli are mounds with mainly elliptical shape and are placed on basaltic lava flows spreading on the southwestern flank of Arsia Mons. Some of these have radial or axial cracks on their top, however most of the tumuli lack well-preserved clefts, rather showing a rough surface covered in boulders (Giacomini et al., 2009).

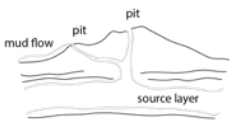
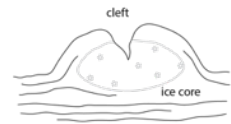
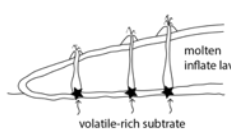

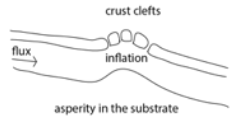
Type	Cross Section	Drives	Thickness	Case study	References
Mud Volcanoes		Sediments, water and gas resurgence triggered by new fluid supply, increasing of pore pressures and a decrease of viscosity in correspondence of undercompacted strata in the subsurface.	Systems of connected fractures are the pathways for the materials' flows. The expected thickness of fractured medium can be up to 10-20 Km.	Acidalia Planitia 41°N -24°E	Oehler & Etiopie, 2017; Fryer, 2012; Oehler & Allen, 2010; Kopf, 2002; Dia, 1999;
Pingos		Bulging of the surface due to capillar upwelling and freezing of groundwater.	No cracks or fractures are expected to lie beneath the knobs. The phenomenon is pellicular, thus just involves a few meters of the surface.	Athabasca Valles 9°N 156°E	Balme & Gallagher, 2009; Burr et al., 2009; Page & Murray, 2006
Rootless Cones		Explosive eruptions, triggered by the interaction between inflating flowing lavas and volatile-rich substrates, lead to the violent extrusion of tuffs and ashes that accumulate in cones on the surface.	The processes of trigger and eruption are bound within the thicknesses of the inflating lava flows, thus a maximum threshold can be expected around 200 metres.	Phlegra Dorsa Region 25°N 170°E	Noguchi et al., 2016; Hiesinger et al., 2007; Bruno et al., 2006; Lanagan et al., 2001;
Volcanic Vents		Fluid basaltic lavas are released on the surface from magma chambers.	Lavas upflow through networks of connected conduits that link the magma chambers to the surface. The chambers are usually expected to sit tens of kilometres below the surface.	Tharsis Province - Pavonis Mons -5°N 246°E	Bleacher et al., 2009, 2007a; Mazzarini & Isola, 2007
Tumuli		Bulging and fracturing on inflating lava flows' top. Differential cooling produces preferential magma pathways that can come to interact with asperities in the substrate producing uplifts in the sealing lava crust.	No cracks or fractures expanding in the subsurface are expected beneath these mounds since the phenomenon is limited to the very upper portions of lava flows.	Tharsis Province - Daedalia Planum -24°N 237°E	Giacomini and Massironi 2010; Giacomini et al., 2009;

Fig. 3. Specific traits are listed and sketched for each feature class highlighting the wide variety of interplays with the subsurface that these surface expressions have despite the morphological analogy

3. *Methods*

We mapped the features of interest and performed the self-similar clustering (i.e. fractal) analyses to produce comparable datasets to appreciate how the surface distribution of mounds express the eventual association with hydraulically connected fracture systems extending in the subsurface. Each feature was distinguished from the neighboring through manual identification. This mapping procedure were carried out using (i) Context Camera (on board Mars Reconnaissance Orbiter) images (Malin et al., 2007), or mosaics where necessary (produced by means of Pilot software; pilot.wr.usgs.gov), which has a resolution data capture of 6 m/pixel and provide a total coverage of the areas, and (ii) HiRISE (High Resolution Imaging Science Experiment on board the Mars Reconnaissance Orbiter mission) images to enhance the observation, when available (McEwen et al., 2007).

Where a large number of features were mapped (i.e. rootless cones), clustering of mounds was performed computing the coordinates of all the vents in MINITAB® software and applying an agglomerative hierarchical clustering method (Mazzarini, 2007). This approach is used when the number of clusters is initially unknown. The optimal number of clusters is derived by analysing the dendrogram that depicts the amalgamation of observations into one cluster. The similarity at any step is defined, in this case, by the maximum distance between points. Where the step values change abruptly, the dendrogram may be cut and accordingly the best suitable number of clusters can be inferred (Mazzarini, 2007). The coordinates used for the analysis were extrapolated by sinusoidal projections of the surface of Mars centered on the observed area, for this reason the procedure was separately repeated for each area. Then for each defined cluster the self-similar cluster analysis has been performed.

Fractal analysis is a methodology that, starting from the observation of fractures or vents, allows to infer the extension of the connected fracture network actually draining the fluids from the deep source toward the surface. In fact, fractures' length and their spatial distribution control the overall permeability of fracture networks (e.g. Darcel et al., 2003). The percolation theory quantifies a critical fracture density threshold that defines the limit above which the fracture network is connected (Mazzarini and Isola, 2010 and references therein). When the fracture network is actually percolating its spatial distribution is fractal and its self-similarity is defined in a specific lengths range bounded by a lower and an upper cutoff (e.g. Mandelbrot, 1982). Such analysis evaluates

the scaling properties of the systems and, in particular, the derived upper cutoff is assumed to represent the distance between the surface and the fluid source at depth (e.g. Mazzarini and Isola, 2010).

We performed self-similar clustering (i.e. how the features fill the space; Fig. 4) of the datasets of interest by applying the following scaling equation:

$$C(l) \propto l^{-D} \quad (1)$$

where $C(l)$ is the correlation sum, defined as $C(l) = 2N(l)/N(N-1)$ where $N(l)$ are the pairs of points whose distance is less than l , and D is the fractal exponent. The D exponent is defined as the slope of the tangent to the $\log(C(l))$ vs. $\log(l)$ curve (equation (1)); high D values imply increasingly homogeneous distribution of fractures, low values imply increasingly clustered distribution of fractures (Darcel et al., 2003 Mazzarini and Isola, 2010).

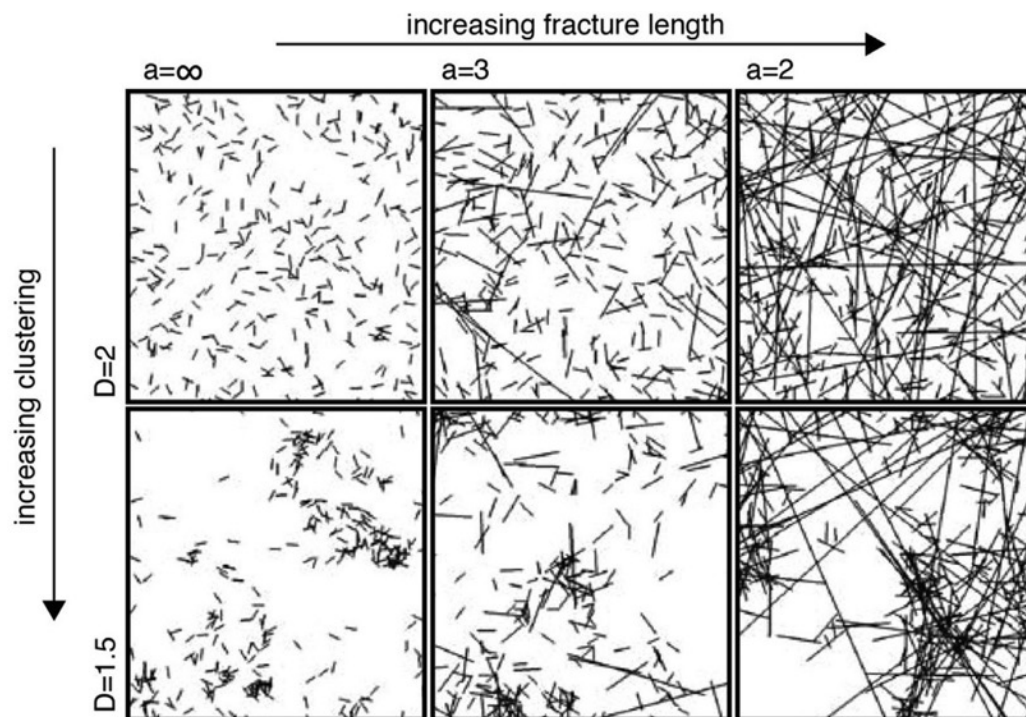


Fig. 4. Simulations representing network connectivity controlled by fracture length and clustering. Varying parameters are the fractal exponents (i) D , that controls the degree of self-similar clustering ($D=2$ weakly clustered; $D=1.5$ strongly clustered) and (ii) a , that controls the power-law distribution for fracture length (increasing lengths from $a = \infty$ -short- to $a = 2$ -long-). Adapted from Darcel et al. (2003) and Mazzarini and Isola, 2010.

The fractal distribution can be inferred from the analysis of a $\log(C(l))$ v. $\log(l)$ diagram (Bonnet et al., 2001). Since the upper cutoff (Uco) scales as the maximum thickness of the fractured medium, this is the specific parameter to investigate in order to shed light on the extension of the phenomenon and thus on possible fracturing processes (e.g. wide plumbing system, shallow fracturing, overpressure fracturing, etc.; Mazzarini and Isola, 2010 and references therein). The size range, bound within the lower and upper cutoffs, is detectable as a linear fit (a plateau) in a local slope $\Delta\log(C(l)/\Delta\log(l))$ vs. $\log(l)$ diagram (Fig. 5 a-1; Walsh and Watterson, 1993). Thus, the Uco (upper cutoff; i.e. the highest plateau breaking point) is defined by the maximum value of the size range, which is the maximum extension of the pipeline connecting the reservoirs to the surface, thus it represents the depth of the fluids source (Mazzarini and Isola, 2010 and references therein). The goodness of the Uco picking was estimated on the basis of the maximum values of the coefficient R^2 defined as the proportion of data variability in cutoffs' interval. R^2 is defined as shown in equation (2)

$$R^2 = 1 - \frac{SS_{res}}{SS_{tot}} \quad (2)$$

where SS_{res} represents the residuals sum of squares, which is meant to be minimized in proportion to the normalization coefficient SS_{tot} (total sum of squares) in accordance to the order of magnitude involved in the calculation. We detected the depth range corresponding to the higher values of R^2 , thus describing the values of best-fit for the Upper cutoff. The error of the measure was estimated calculating the half-difference between the maximum and the minimum Uco's values depths where the R^2 shows the best-fit value providing to ensure the largest size range. To make the analysis more robust, we also produced a cross check among the $\Delta\log(C(l)/\Delta\log(l))$ vs. $\log(l)$ diagrams (where the eventual fractal behaviour is displayed by a plateau) and plots of all possible $\Delta\log(l)$ (i.e. size range) and R^2 values. In this second diagram, a significant break in the slope should be detected when fractal clustering occurs and, the higher the R^2 value is in correspondence of the breaking point, the higher is the reliability of the information. Hence this additional analysis tests the reliability of the Lco-Uco extension estimate giving a graphic quantitative measure of the reliability of the cutoffs picking (Fig. 5).

Therefore, if no plateau is recognizable in the diagram, the examined features have no fractal behaviour and, therefore, no relationship with system of connected

fractures at depth. In order to produce meaningful estimates, the sample size effect needed to be taken into account. As a rule of thumb, at least 50 samples are required to extract robust parameter estimates (Clauset et al., 2009) and, accordingly, in our study the number of observed mounds spans between a minimum of 65 to a maximum of 1428 per single cluster (Table 1).

Feature	n° units	Uco [Km]
Mars		
Volcanic vents	217	32 ± 4 ; 200 ± 22
Mud Volcanoes	174	12 ± 3
Rootless Cones	1428	–
• cluster1 RC	462	–
• cluster2 RC	566	1.2 ± 0.2
• cluster3 RC	281	–
• cluster4 RC	118	–
Pingos	281	–
Tumuli	75	–
Earth		
Rootless Cones	65	–
Pingos	103	–
Tumuli	105	–

Table 1. Number of units and Uco estimates for each feature group

Indeed, this large number of observations ensure a robust estimate of the fractal distribution parameters. In particular, Mazzarini and Isola (2010) showed that removing a random sample of 20% of the vents from large (i.e. > 200 vents) datasets does not affect the estimation of the fractal exponent (less than 0.01% of variation) and the error introduced into the estimation of the cut-offs is less than 1%–2%. In Mazzarini et al. (2013) the effect of uncertainties in point (mound) locations has been tested by adding random errors to the sampled points. In their test, the added errors (in the 0–100 m, 0–300 m and 0–500 m ranges) were as high as five to twenty-five times that of the coarsest image resolution used to locate vents. The 0–100 m errors generate fractal exponent and cut off value identical to those computed for the original dataset. In the case of 0–500 m random errors, the resulting fractal exponent is 3% higher than that computed for the original dataset, and the cut offs are very similar to those computed for the original dataset. We performed analyses on clusters exceeding the minimum number of 50 units, thus keeping the error on the scaling parameter smaller than 1%.

4. Results

Based on the interpretation of the different groups of features, the outputs of fractal analysis were expected to highlight a different involvement of the subsurface below the fields. From the deepest to the shallowest: (i) monogenetic vents are expected to be linked to very deep fluid (magma) reservoirs sitting several tens of kilometres below the surface; (ii) mud volcanoes, scaling the inferred depths of source layers on Earth (Dia, 1999; Fryer et al., 1999; Kopf, 2002; Fryer, 2012) to the lower Martian gravity, are expected to involve a portion of fractured medium that can significantly vary within the first 20 km of subsurface; (iii) rootless cones are a phenomenon which extends up to the thickness of the inflat lava flows that are estimated to reach a few tens of meters depths (Hiesinger et al., 2007), hence they are not linked to percolating networks recognizable by means of fractal analysis and it is to be expected a significant chance to have no visible plateau in return; (iv) pingos, that are driven by capillarity processes, are not expected to show any effective plateau in the fractal analysis; (v) tumuli are the result of a pellicular uplift of inflated magma, not even related to effective materials flow-up, thus they are not expected to produce any fractal clustering as well.

Below the results are presented listed for each feature class.

Volcanic vents: the magmatic reservoir is situated up to 32 ± 4 km of depth (Uco corresponding to $\log(l) = 4.5$). Despite the flattened tendency of the data distribution is notably marked within the data describing the first tens of kilometres, a second plateau is also visible and suggests the presence of a deeper reservoir (i.e. a possible two magma chambers feeding). This seems to extend deeper than 200 ± 22 km (Uco corresponding to $\log(l) = 5.4$), however reliability decreases as R^2 values drop down (Fig. 5a, m, n).

Mud volcanoes: fractal analysis on the mud volcano cluster showed a clear plateau, noisy close to the Lco but displaying a well recognizable slope break for the Uco; accordingly connected fractures are estimated to reach a depth of 12 ± 3 km (Uco corresponding to $\log(l) = 4.08$; Fig. 5b, o).

Rootless cones: in the $\log(C(l))$ v. $\log(l)$ diagram a constant descending trend is displayed (Fig. 5c). No significant plateaus are clearly visible, anyway, due to a weakly flattening tendency between $\log(l)$ values of 3.1 and 3.3, we subdivided the features into four sub-clusters in order to identify eventual groups of features with a fractal behaviour. The outcomes of these further analyses (Fig. 5 i-l) displayed no plateau distribution of the data for cluster 1, 3 and 4 and confirmed that no percolating fracture network was

active. Differently, cluster 2 showed a slight flattening suggesting a possible relationship with some source located at 1.2 ± 0.2 km depth (Uco corresponding to $\log(l) = 3.07$; Fig. 5p). On the terrestrial counterpart, the $\log(C(l))$ v. $\log(l)$ diagram shows an abrupt descending trend quickly approaching the zero value, any plateau trend is clearly missing (Fig. 5f).

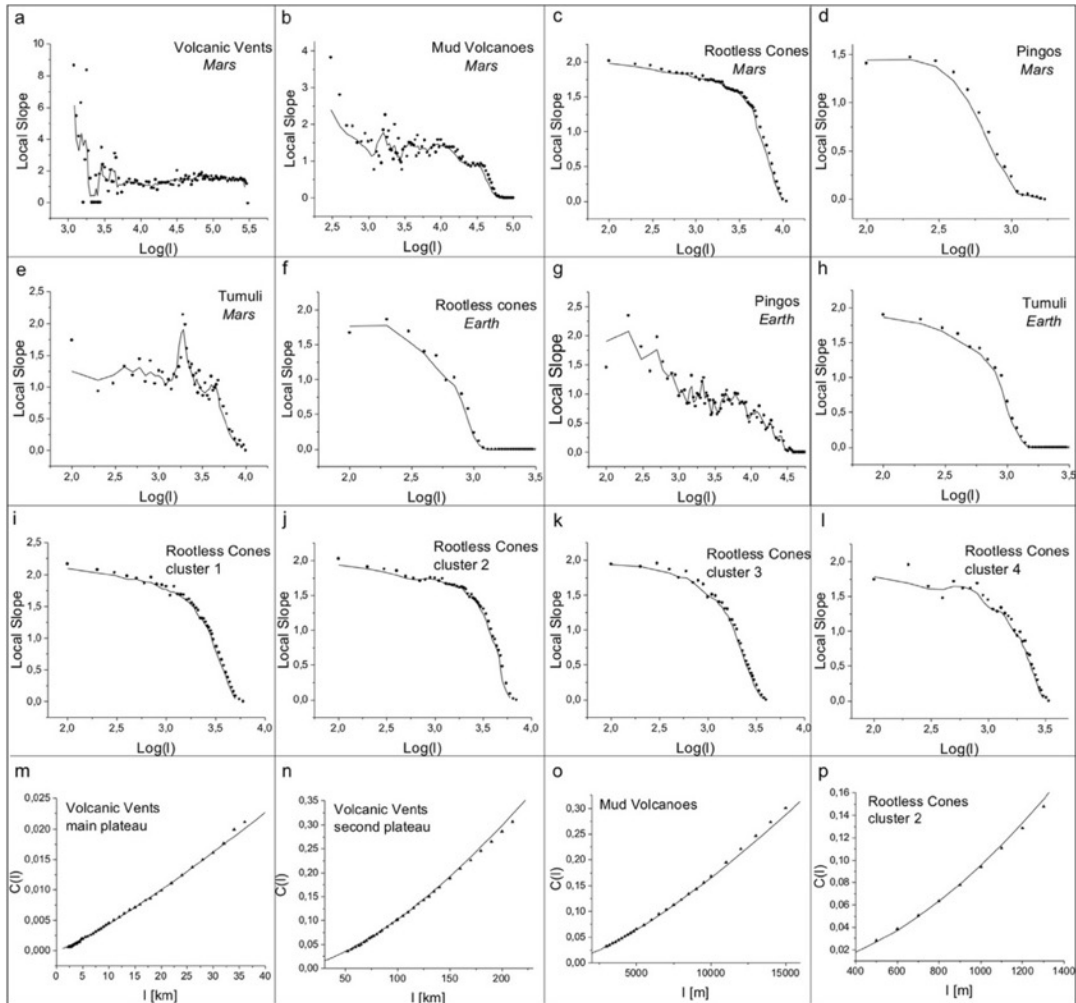


Fig. 5. Size range plots (a–l) and fracture distribution plots (m–p). Size range of interconnected fractures are represented by the plateau stage of the curve where present (a,b,c,j). Where the slope breaks the fractures' distribution stops to be fractal. The corresponding $\log(l)$ value coincides to a specific maximum thickness of the fractured medium that connects the surface to the subsurface (Uco). Graphs from m to p show the variation of fractures distribution compared to the Power Law (solid line). Here the goodness of the Uco picking in the previous graph is tested. Fractal distribution follows the Power Law, where data matches the solid line the distribution of fractures/vents is fractal. [l : fractures length; $C(l)$: correlation integral defines the correlation between point at a distance lower to l ; Local Slope: represents the $\Delta \log(C(l))/\Delta \log(l)$ ratio].

Pingos & Tumuli: fractal analysis outputted unequivocal results and we accordingly detected no plateau trend in the data (Fig. 5d and e). Hence, as expected for such features associated to different processes such as capillarity, thermo-mechanical and inflating processes, no relationship with percolating fracture network can be inferred from this investigation. Similarly to the rootless cones case discussed above in this section, the fractal analysis outcomes for pingos and tumuli terrestrial analogue sites are clearly missing plateau distributions (Fig. 5g and h). Indeed, the related diagrams display a sharp abrupt descending trend for tumuli and a noisy but unequivocally descending trend for pingos.

The results we gathered by the application of fractal analysis to the case studies, both on Mars and on Earth, allowed the verification of the geomorphological interpretations of the features of interest. In fact volcanic vent and mud volcano fields showed a relationship with systems of connected fractures, as such structures are supposed to. Martian rootless cones displayed a weak and uncertain possible interplay with shallow fractures, this marking the necessity of better caution while discussing such uncommon features; terrestrial rootless cones, pingos and tumuli instead clearly resulted to have no linkage with any fracture network hydraulically connected to fluid reservoirs at depth.

5. Discussions

The method herein presented is hence a tool that can be profitably used for the interpretation of planetary surfaces and, in the specificity of this work, effective to discriminate mound features on Mars with convergent morphologies but significantly different interplay with the subsurface. In fact, as herein reported, the outcomes of fractal clustering are confirming and validating the major interpretations of the features of interest and, where percolating fracture networks were active, the maximum extension values are well matching with complementary literature data.

Our results point towards various depths for vents consistent with previous works. In fact, volcanic vents of the Tharsis region appear to be linked to reservoirs sited around 30 and 200km under the surface reflecting what is to be expected in the magmatic plumbing systems on Mars (e.g. Grott et al., 2013) and what has been observed in the neighbouring region of Ascraeus Mons by Pozzobon et al. (2015) where multiple source depths were identified at around 10 and 80 km, drawing a solid relationship between the background data and the fractal outcomes. Similarly,

our mud volcano field case shows that the inferred vertical involvement of the crust reaches up a depth where gas hydrate-rich permafrost has been calculated to be theoretically stable and close to the hypothetical water-ice interface (~15 km) laying beneath the ice table (Clifford et al., 2010). This relationship further matches the mud volcano interpretation by highlighting a connection between landforms that are by definition linked to water and a subsurface location where water, in the form of ice and gas hydrate, is presumed to have been likely sited. Contextually, Martian rootless cones gave back more ambiguous results due to the hard identification of a plateau in the fractal analysis output diagram. In particular three sub-clusters of rootless cones out of four do not show any plateau indicating percolating systems, whereas a slight flattening of the last cluster seems to suggest an uncertain source at a depth of 1.2 km. This on one side leaves doubts about the effective connection with a percolating fracture network and its extension, but at the same time reflects what was expected to happen while applying the technique to features that may be linked to significant, but very shallow conduits. In fact, a fracture extension of 1.2 km beneath rootless cones appears to be significantly larger with the respect of what could be expected in such case, even considering the lower Martian gravity that allows the placement of thicker lava flows (Hiesinger et al., 2007). It is to be noticed though that, at the field scale where distances between mounds can reach up to tens of kilometres, a resolution quality below the kilometre is hard to pursue and, accordingly, such value could be an overestimation of a shallower process. This uncertainty arises from the very narrow span of the plateau in the Martian rootless cones case study. In fact, while in magmatic and sedimentary volcanism cases the plateaus span over one or more orders of magnitude (Fig. 5), in the rootless cones analysis the flattened tendency is confined between 3.1 and 3.3 $\log(L)$ values. Accordingly, such data portion is expressed by a little number of points making the tendency possibly mistakable with background noise (i.e. the noise produced by unavoidable mistakes made during population picking, for instance by mapping several vents fed by the same fracture, which is averagely mitigated by picking a sample of features large enough; refer to the methods section) that is normally present. This result needs thus to be coupled with further information collected on the terrestrial analogue site, where feature interpretation is no question. Hence, for the Icelandic rootless cones case study, the analysis unmistakably underscores the total lack of relationships between such

structures and putative underlying percolating fracture systems, remarking the very surficial nature of the phenomenon unrelated to networks of connected fractures.

Results of fractal analysis of features surely unrelated to percolating systems, such as inflated tumuli and periglacial pingos, unambiguously show a complete lack of any fractal distribution on both planets.

6. Conclusions

Our study provides the evidence of the efficiency of the fractal analysis application to infer the extension of percolating fracture networks starting from the distribution of eruption vents. This work validates fractal analysis as a reliable method for mound features discrimination and foster the integration of this investigation technique in future geomorphological observations and within studies intending to probe the entity of the subsurface cracking. Assessing the power of investigation of such methodology, we encourage to take it into consideration within the exploration process frame since it provides insights regardless of the usual physical limits that surveying the subsurface presents. Due to the freshness of this kind of natural systems investigation, many phenomena can be explored when percolating cracking is presumed or assessed. This allows features discrimination and fracturing mechanism deeper understanding both in the frame of already known contexts, like terrestrial environments, and on extra-terrestrial planetary landscapes, where cracking behavior at all scales can be widely different from Earth's ones, poorly understood and still limited by the surveying efficiency of today space exploration techniques.

Acknowledgments

We thank the reviewers who provided helpful and detailed suggestions to improve the manuscript. This work has been supported by the Italian Space Agency (ASI) (ASI-INAF agreement no.2017-03-17).

References

- Balme, M.R., Gallagher, C., 2009. An equatorial periglacial landscape on Mars. *Earth Planet. Sci. Lett.* 285, 1–15. <https://doi.org/10.1016/j.epsl.2009.05.031>
- Bleacher, J.E., Greeley, R., Williams, D.A., Cave, S.R., Neukum, G., 2007a. Trends in effusive style at the Tharsis Montes, Mars, and implications for the development of the Tharsis province. *J. Geophys. Res.* 112, E09005. doi:10.1029/2006JE002873
- Bleacher, J.E., Glaze, L.S., Greeley, R., Hauber, E., Baloga, S.M., Sakimoto, S.E.H., Williams, D.A., Glotch, T.D., 2009. Spatial and alignment analyses for a field of small volcanic vents south of Pavonis Mons and implications for the Tharsis province, Mars. *J. Volcanol. Geotherm. Res.* 185, 96–102. <https://doi.org/10.1016/j.jvolgeores.2009.04.008>
- Bonini, M., Mazzarini, F., 2010. Mud volcanoes as potential indicators of regional stress and pressurized layer depth. *Tectonophysics* 494, 32–47. <https://doi.org/10.1016/j.tecto.2010.08.006>
- Bonnet, E., Bour, O., Odling, N.E., Davy, P., Main, I., Cowie, P., Berkowitz, B., 2001. Scaling of Fracture System in Geological Media. *Rev. Geophys.* 39, 347–383.
- Bruno, B.C., Fagents, S.A., Hamilton, C.W., Burr, D.M., Baloga, S.M., 2006. Identification of volcanic rootless cones, ice mounds, and impact craters on Earth and Mars: Using spatial distribution as a remote sensing tool. *J. Geophys. Res. E Planets* 111, 1–16. <https://doi.org/10.1029/2005JE002510>
- Bruno, B.C., Fagents, S.A., Thordarson, T., Baloga, S.M., Pilger, E., 2004. Clustering within rootless cone groups on Iceland and Mars: Effect of nonrandom processes. *J. Geophys. Res. E Planets* 109, 1–11. <https://doi.org/10.1029/2004JE002273>
- Burr, D.M., Tanaka, K.L., Yoshikawa, K., 2009. Pingos on Earth and Mars. *Planet. Space Sci.* 57, 541–555. <https://doi.org/10.1016/j.pss.2008.11.003>
- Carr, M.H., 2006. *The Surface of Mars*, Cambridge Planetary Science Series. <https://doi.org/10.1086/518077>
- Clauset, A., Rohilla Shalizi, C., J Newman, M.E., 2009. Power-Law Distributions in Empirical Data. *SIAM Rev.* 51, 661–703. <https://doi.org/10.1214/13-AOAS710>
- Clifford, S.M., Lasue, J., Heggy, E., Boisson, J., McGovern, P., Max, M.D., 2010. Depth of the Martian cryosphere: Revised estimates and implications for the existence and detection of subpermafrost groundwater. *J. Geophys. Res.* 115, E07001. doi:10.1029/2009JE003462
- Connor, C.B., and Conway, F.M., 2000. Basaltic volcanic Fields, in Sigurdsson, H., ed., *Encyclopedia of Volcanoes*: New York, Academic Press, p. 331–343.
- Darcel, C., Bour, O., Davy, P., and de Dreuzy, J.R., 2003, Connectivity properties of two-dimensional fracture networks with stochastic fractal correlation: *Water Resources Research*, v. 39, p. 1272, doi: 10.1029/2002WR001628.
- Dia, A., 1999. Trinidad mud volcanoes: where do the expelled fluids come from? *Geochim. Cosmochim. Acta* 63, 1023–1038. [https://doi.org/10.1016/S0016-7037\(98\)00309-3](https://doi.org/10.1016/S0016-7037(98)00309-3)
- Dimitrov, L., 2002. Mud volcanoes – the most important pathways for degassing deeply buried sediments. *Earth Sci. Rev.* 59, 49–76. [https://doi.org/10.1016/S0012-8252\(02\)00069-7](https://doi.org/10.1016/S0012-8252(02)00069-7)
- Dundas, C.M., McEwen, A.S., 2010. An assessment of evidence for pingos on Mars using HiRISE. *Icarus* 205, 244–258. <https://doi.org/10.1016/j.icarus.2009.02.020>
- Fryer, P., 2012. Serpentine Mud Volcanism: Observations, Processes, and Implications. *Ann. Rev. Mar. Sci.* 4, 345–373. <https://doi.org/10.1146/annurev-marine-120710-100922>
- Fryer, P., Wheat, C.G., Mottl, M.J., 1999. Mariana blueschist mud volcanism: Implications for conditions within the subduction zone. *Geology* 27, 103–106. [https://doi.org/10.1130/0091-7613\(1999\)027](https://doi.org/10.1130/0091-7613(1999)027)
- Giacomini, L., Massironi, M., Martellato, E., Frigeri, A., Cremonese, G., 2009. Inflated flows on Daedalia Planum (Mars)? Clues from a comparative analysis with the Payen volcanic complex (Argentina). *Planet. Space Sci.* 57, 556–570. <https://doi.org/10.1016/j.pss.2008.12.001>
- Giacomini, L., Massironi, M., 2010. Tumuli and pingos : a comparative analysis between Daedalia Planum and Elysium Planitia mounds, in: *European Planetary Science Congress*. Vol. 5, p. 414.
- Grosse, G., Jones, B.M., 2011. Spatial distribution of pingos in northern Asia. *Cryosphere* 5, 13–33. <https://doi.org/10.5194/tc-5-13-2011>
- Grott, M., Baratoux, D., Hauber, E., Sautter, V., Mustard, J., Gasnault, O., Ruff, S.W., Karato, S.I., Debaille, V., Knapmeyer, M., Sohl, F., Van Hoolst, T., Breuer, D., Morschhauser, A., Toplis, M.J., 2013. Long-Term Evolution of the Martian Crust-Mantle System. *Space Sci. Rev.* 174, 49–111. <https://doi.org/10.1007/s11214-012-9948-3>
- Hamilton, C.W., Thordarson, T., Fagents, S.A., 2010. Explosive lava-water interactions I: Architecture and emplacement chronology of volcanic rootless cone groups in the 1783-1784

- Laki lava flow, Iceland. *Bull. Volcanol.* 72, 449–467. <https://doi.org/10.1007/s00445-009-0330-6>
- Hargitai, H., Kereszturi, A., (eds.), 2015. *Encyclopedia of Planetary Landforms*, Springer Science, New York, DOI 10.1007/978-1-4614-3134-3
- Hiesinger, H., Head, I.W., Neukum, G., 2007. Young lava flows on the eastern flank of Ascaraeus Mons: Rheological properties derived from High Resolution Stereo Camera (HRSC) images and Mars Orbiter Laser Altimeter (MOLA) data. *J. Geophys. Res. E Planets* 112. <https://doi.org/10.1029/2006JE002717>
- Hon, K., Kauahikaua, J., Denlinger, R., Mackay, K., 1994. Emplacement and inflation of pahoehoe sheet flows; observations and measurements of active lava flows on Kilauea Volcano, Hawaii. *GSA Bull.* 106, 351–370
- Kopf, A.J., 2002. Significance of mud volcanism. *Rev. Geophys.* 40, 1005. <https://doi.org/10.1029/2000RG000093>
- Lanagan, P.D., McEwen, A.S., Keszthelyi, L.P., Thordarson, T., 2001. Rootless cones on Mars indicating the presence of shallow equatorial ground ice in recent times. *Geophys. Res. Lett.* 28, 2365–2367. <https://doi.org/10.1029/2001GL012932>
- Le Corvec, N., Sporli, K.B., Rowland, J., Lindsay, J., 2013. Spatial distribution and alignments of volcanic centers: Clues to the formation of monogenetic volcanic fields. *Earth-Science Rev.* 124, 96–114. <https://doi.org/10.1016/j.earscirev.2013.05.005>
- Lucchetti, A., Pozzobon, R., Mazzarini, F., Cremonese, G., Massironi, M., 2017. Brittle ice shell thickness of Enceladus from fracture distribution analysis. *Icarus* 297, 252–264. <https://doi.org/10.1016/j.icarus.2017.07.009>
- Malin, M.C., Bell, J.F., III, Cantor, B.A., Caplinger, M.A., Calvin, W.M., Clancy, R.T., Edgett, K.S., Edwards, L., Haberle, R.M., and James, P.B., 2007. Context Camera investigation on board the Mars Reconnaissance Orbiter: *Journal of Geophysical Research*, v. 112, E05S04, doi: 10.1029/2006JE002808.
- Mandelbrot, B.B., 1982, *The Fractal Geometry of Nature*: San Francisco, Freeman, 468 p.
- Mattsson, H. B. and A. Hoskuldsson, 2005. Eruption reconstruction, formation of flow-lobe tumuli and eruption duration in the 5900 BP Helgafell lava field (Heimaey), south Iceland. *Journal of Volcanology and Geothermal Research* 147(1-2): 157-172
- Mazzarini, F., 2004. Volcanic vent self-similar clustering and crustal thickness in the northern Main Ethiopian Rift. *Geophys. Res. Lett.* 31, 1–4. <https://doi.org/10.1029/2003GL018574>
- Mazzarini F., Keir D., Isola I., 2013. Spatial relationship between earthquakes and volcanic vents in the central-northern Main Ethiopian Rift. *Journal of Volcanology and Geothermal Research*, 262, 123–133
- Mazzarini, F., Isola, I., 2010. Monogenetic vent self-similar clustering in extending continental crust: Examples from the East African Rift System. *Geosphere* 6, 567–582. <https://doi.org/10.1130/GES00569.1>
- Mazzarini, F., Isola, I., 2007. Hydraulic connection and fluid overpressure in upper crustal rocks: Evidence from the geometry and spatial distribution of veins at Botrona quarry, southern Tuscany, Italy. *J. Struct. Geol.* 29, 1386–1399. <https://doi.org/10.1016/j.jsg.2007.02.016>
- Mazzarini, F., 2007. Vent distribution and crustal thickness in stretched continental crust: The case of the Afar Depression (Ethiopia). *Geosphere* 3, 152–162. <https://doi.org/10.1130/GES00070.1>
- Mazzini, A., Etiope, G., 2017. Mud volcanism: An updated review. *Earth-Science Rev.* 168, 81–112. <https://doi.org/10.1016/j.earscirev.2017.03.001>
- McEwen, A.S., Eliason, E.M., Bergstrom, J.W., Bridges, N.T., Hansen, C.J., Delamere, W.A., Grant, J.A., Gulick, V.C., Herkenhoff, K.E., Keszthelyi, L., Kirk, R.L., Mellon, M.T., Squyres, S.W., Thomas, N., and Weitz, C.M., 2007, Mars Reconnaissance Orbiter's High Resolution Imaging Science Experiment (HiRISE): *Journal of Geophysical Research*, v. 112, E05S02, doi: 10.1029/2005JE002605.
- Németh, K., Haller, M.J., Martin, U., Risso, C., Massaferrò, G., 2008. Morphology of lava tumuli from Mendoza (Argentina), Patagonia (Argentina), and Al-Haruj (Libya). *Zeitschrift für Geomorphol.* 52, 181–194. <https://doi.org/10.1127/0372-8854/2008/0052-0181>
- Németh, K. 2010. Monogenetic volcanic fields: Origin, sedimentary record, and relationship with polygenetic volcanism. *The Geological Society of America Special Paper* 470: 43–66
- Németh, K. and G. Kereszturi, 2015. Monogenetic volcanism: personal views and discussion. *International Journal of Earth Sciences* 104(8): 2131–2146.
- Nemeth, K., Wu, J., Sun, C., Liu, J., 2017. Update on the Volcanic Geoheritage Values of the Pliocene to Quaternary Arxan-Chaihe Volcanic Field, Inner Mongolia, China. *Geoheritage* 9(3): 279–297.
- Noguchi, R., Höskuldsson, Á., Kurita, K., 2016. Detailed topographical, distributional, and material

- analyses of rootless cones in Myvatn, Iceland. *J. Volcanol. Geotherm. Res.* 318, 89–102.
<https://doi.org/10.1016/j.jvolgeores.2016.03.020>
- Oehler, D.Z., Allen, C.C., 2010. Evidence for pervasive mud volcanism in Acidalia Planitia, Mars. *Icarus* 208, 636–657. <https://doi.org/10.1016/j.icarus.2010.03.031>
- Oehler, D.Z., Allen, C.C., 2012. Giant Polygons and Mounds in the Lowlands of Mars: Signatures of an Ancient Ocean? *Astrobiology* 12, 601–615. <https://doi.org/10.1089/ast.2011.0803>
- Oehler, D.Z., Etiope, G., 2017. Methane Seepage on Mars: Where to Look and Why. *Astrobiology* 17, ast.2017.1657. <https://doi.org/10.1089/ast.2017.1657>
- Ollier, C. D., 1964. Tumuli and lava blisters of Victoria, Australia. *Nature* 202, 1284.
- Page, D.P., Murray, J.B., 2006. Stratigraphical and morphological evidence for pingo genesis in the Cerberus plains. *Icarus* 183, 46–54. <https://doi.org/10.1016/j.icarus.2006.01.017>
- Pozzobon, R., Mazzarini, F., Massironi, M., Marinangeli, L., 2014. Self-similar clustering distribution of structural features on Asraeus Mons (Mars): implications for magma chamber depth. *Geol. Soc. London, Spec. Publ.* <https://doi.org/10.1144/SP401.12>
- Prieto-Ballesteros, O., Kargel, J.S., Fairén, A.G., Fernández-Remolar, D.C., Dohm, J.M., Amils, R., 2006. Interglacial clathrate destabilization on Mars: Possible contributing source of its atmospheric methane. *Geology* 34, 149. <https://doi.org/10.1130/G22311.1>
- Renshaw, C.E., 1999. Connectivity of joint networks with power law length distributions. *WATER Resour. Res.* 35, 2661–2670.
- Rossi, M.J., Gudmundsson, A., 1996. The morphology and formation of flow-lobe tumuli on Icelandic shield volcanoes. *J. Volc. Geotherm. Res.* 72, 291–308.
- Skinner, J.A., Tanaka, K.L., 2007. Evidence for and implications of sedimentary diapirism and mud volcanism in the southern Utopia highland–lowland boundary plain, Mars. *Icarus* 186, 41–59. <https://doi.org/10.1016/j.icarus.2006.08.013>
- Skinner, J. a., Mazzini, A., 2009. Martian mud volcanism: Terrestrial analogs and implications for formational scenarios. *Mar. Pet. Geol.* 26, 1866–1878. <https://doi.org/10.1016/j.marpetgeo.2009.02.006>
- Smith, I. E. M. and K. Németh, 2017. Source to surface model of monogenetic volcanism: a critical review *Monogenetic Volcanism*. K. Németh, G. Carrasco-Nuñez, J. J. Aranda-Gomez and I. E. M. Smith. Bath, UK, The Geological Society Publishing House. 446
- Thorarinnsson, S. (1953), The crater groups in Iceland, *Bull. Volcanol.*, 14, 3–44.
- Walker, G. P. L., 1991. Structure, and origin by injection of lava under surface crust, of tumuli, lava rises, lava-rise pits, and lava-inflation clefts in Hawaii. *Bulletin of Volcanology* 53(7): 546-558.
- Walsh, J.J. & Watterson, J. 1993. Fractal analysis of fracture pattern using the standard box-counting technique: valid and invalid methodologies. *Journal of Structural Geology*, 15, 1509–1512, [http://dx.doi.org/10.1016/0191-8141\(93\)90010-8](http://dx.doi.org/10.1016/0191-8141(93)90010-8)

Chapter 2: *Application to Mars exploration through orbiters' data*

Introduction

Fractals applications are widespread among many scientific disciplines and have been introduced as surveying technique also in geosciences. Specifically, in the studies herein developed the fractal analyses allowed to reconstruct fracture assets in the Martian subsurface up to depths which are presently unreachable by current technologies of planetary exploration. Given this successful application, extremely compelling scientific questions regarding the Martian exploration can be address under a new prospective.

Although very different conditions, Mars shares more common characteristic with planet Earth than any other rocky planetary body, displaying many geological and morphological features akin to terrestrial landforms such as volcanoes, canyons, fluvial channels, polar ice caps but also seasonal weather patterns as well as clouds in its atmosphere. Among the countless discoveries that we have achieved about Mars, one stands out above all the others: this is the evidence of past presence of liquid water on the planet and its putative preservation until recent times, or even today. The intimate correlation observable on Earth between water and life makes this finding so remarkable to such an extent that led to the origin of an entire new field of study: astrobiology. This new-born branch sits at the convergence point of several scientific and technical disciplines such as astronomy, biology, geology, physics and engineering. Accordingly, addressing the question of the search for water on Mars thoroughly implies a contribution to enrich the knowledge about the putative arise of a biosphere possibly linked to its presence. We approached this goal from the geological side, that is to say through the investigation of water related features and environments and, specifically, we aimed to the exploration of structures that could allow us to collect new insights about water distribution in the subsurface where it can still be preserved today. In this regard, the successful application of fractal analyses to known geologic features, as discussed in Chapter 1, provided us with an innovative tool to explore new systems and regions on Mars pushing the investigation into the largely un-tackled underground domain.

References

- Cockell, C.S., 2015. *Astrobiology*. John Wiley & Sons Ltd, 472 pp.
- Faure, G. and Mensing, T.M., 2007. *Introduction to Planetary Science: The Geological Perspective*. Springer, Dordrecht, The Netherlands, 526 pp
- Ghanbarian, B. and Hunt, A.G., 2017. *FRACTALS: Concepts and Applications in Geosciences*. CRC Press
- Rossi, A.P., 2018. *Planetary Geology*. doi.org/10.1007/978-3-319-65179-8

Submitted Paper

SURFACE EXPRESSIONS OF SUBSURFACE SEDIMENT MOBILIZATION ROOTED INTO GAS HYDRATE-RICH CRYOSPHERE

Barbara De Toffoli ^{a,b,*}, Riccardo Pozzobon ^{a,b}, Matteo Massironi ^{a,b},

Francesco Mazzarini ^c, Gabriele Cremonese ^b

^a Department of Geosciences, University of Padova, Via Gradenigo 6, Padova 35131, Italy

^b INAF, Osservatorio Astronomico di Padova, Vicolo dell'Osservatorio 3, Padova I-35122, Italy

^c Istituto Nazionale di Geofisica e Vulcanologia, Via Della Faggiola 32, Pisa 56100, Italy

Abstract

Fluid circulation in the upper crust can define potential sets of environments prone to biosphere growth and flourish. Here we investigate the nature of thumbprint terrains covering a portion of Arcadia Planitia in the Martian northern hemisphere. Our analytic procedure allowed to date back to approximately only 370 Ma the thumbprint terrains under examination and to highlight a set of evidence that links these fine grained sediments edifices to percolating fracture networks extensively involving hypothesized clathrate-rich cryosphere down to its theoretical contact with the underlying hydrosphere. We conclude that the study area has a high astrobiological potential, consistent with the relevance of water and fine grained sediment preservation potential in the search for life quest.

1. Introduction

Northern lowlands are considered to have hosted large bodies of water in the Martian geological past and different studies propose various time of permanence of liquid water on the surface. Paleoshoreline interpretation of unit contacts and morphologies in the Borealis province (Fig.1) suggests the existence of an ocean on Mars during the Early Noachian age that covered one third of the planet as a consequence of thermal and hydraulic conditions hypothesised during that time (Clifford & Parker, 2001 and references therein). In a dynamic perspective of the

migration of water masses on the Martian surface, perturbations of the hydrological cycle were also suggested in the form of short-lived water bodies during the Hesperian period produced by paroxysmal outflow events that experienced freezing and sublimation rapidly after the placement (Kreslavsky & Head, 2002 and references therein).

The study area is set in Vastitas Borealis context at mid-high latitudes, centered at 47°N 184°E, close to the central portion of Arcadia Planitia at around 4 km below the mean Martian elevation (Fig.1). The Vastitas Borealis marginal and interior units, where the region of interest is set, are interpreted to be the product of Early Amazonian pervasive alteration on Late Hesperian sediment release during outflow events triggered by processes involving both lowland and highland sources, that appear to be covered in places by superimposing ejecta blankets belonging to Amazonian crater units (Tanaka et al., 2014).

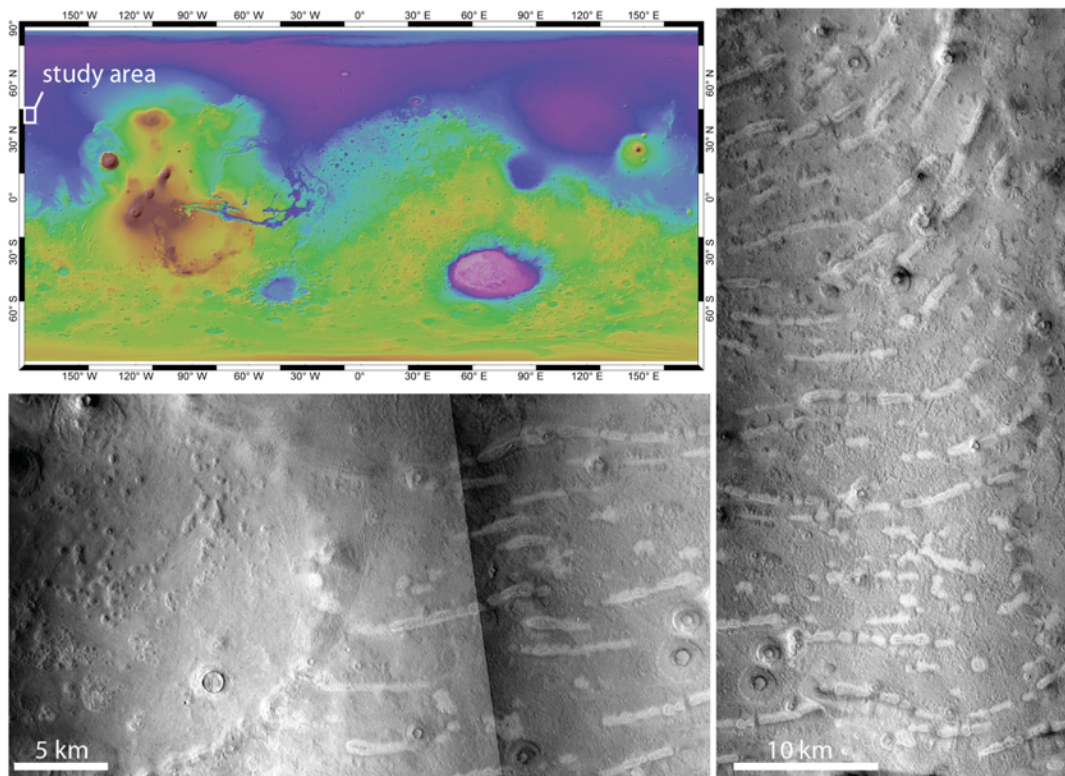


Fig. 1. On the map: location of the study area is underscored by the white box. Highlights on (a) Thumbprint Terrains (CTX: F03_036957_2301) and (b) crater displaying pitted mounds on the floor (CTX: P21_009055_2314).

Topographically positive morphologies have already been observed and reported in previous literature as mounds or, on larger scale, as knobby fields and terrains or thumbprint terrains (e.g. Pomerantz and Head, 2003; Rodriguez et al., 2010; Guidat

et al., 2015; Bernhardt et al., 2016). Specifically, thumbprint terrains (TT) are characterised by sets of curvilinear features made up of continuous and discontinuous alignments of pitted domes and are recognisable in several locations on the Northern hemisphere (Lockwood et al., 1992; Tanaka et al., 2014) with Arcadia Planitia among the main sites (e.g. Lucchitta 1981; Scott & Underwood, 1991; Kreslavsky & Head, 2002; Pomerantz & Head, 2003). The interpretation of these landforms is still widely debated, proposed suggestions include magmatic volcanism (e.g. Bridges et al., 2003; Bruno et al., 2004; Hiesinger et al., 2009; Ghent et al., 2012), mud volcanism (e.g. Skinner and Mazzini, 2009; Oehler & Allen, 2010; Ivanov et al., 2014; Orgel et al., 2015), ice-related processes (e.g. Grizzaffi and Schultz, 1989; Scott and Underwood, 1991; Lockwood et al., 1992; Ivanov et al., 2012; Guidat et al., 2015) and tsunami deposits (Rodriguez et al., 2016; Costard et al., 2017).

Herein we interpolate the geomorphological information, absolute model ages and the spatial distribution analysis of mounds on the area covered in TT to address the interpretation of such debated features and lay a background for further future investigations on their origin and thus on the evolution of a large portion the northern plains.

2. Methods

We compiled an extensive mapping of mound-like features recognisable in the study area and performed geomorphological observations, cluster and fractal analyses. By the application of the following procedures we tested the possible relationship between such morphologies and putative underlying systems of connected percolating fracture networks that could have acted as fluid pathways. We then dated these features by means of absolute model ages based on crater-size-frequency-distributions (CSFDs).

2.1 Image analyses

We designated as features of interest topographically positive mound-shaped features characterize by circular or elliptical base (coalescent mounds-like features included) above 100 m of diameter. The geomorphological observations were performed on a mosaic of 46 CTX images produced by means of USGS Astrogeology service's Pilot software (pilot.wr.usgs.gov). The images of the Mars Reconnaissance Orbiter (MRO) Context Camera (CTX) have a resolution of 6 m/pixel, hence also HiRISE (High Resolution Imaging Science Experiment) images, with a resolution of 0,25 m/pixel were consulted, when available, to enhance the observation of the mounds' morphological details. However HiRISE images were not used to regionally map the mounds because their highly uneven distribution on the study area. THEMIS Nighttime Infrared images were consulted to gather additional information of the thermic behaviour of the target features. The image analysis was performed within ArcGIS® software using sinusoidal projections centered in the study area in order to minimize spatial distortions. This region displays large fields of single and coalescent light albedo mound populations that we identified and denomitaed based on their evident characterizing morphological traits, such as low elevation, rough surface and central pit surrounded by concentric ring-like features and perimetral moats (Fig.2).

2.2 Crater Counting Methodology

On such surfaces we also performed absolute model age determination. Statistical analysis of crater size-frequency distributions (CSFD) of impact craters on planetary surfaces is a well-established method to infer absolute ages on remotely-sensed image data (e.g. Hartmann and Neukum, 2001). GIS-based measurements, by the mean of ArcMap toolbar CraterTools, coupled with further processing using the software CraterStats allowed to carry out standardize age estimation of the surfaces of interest (Kneissel et al., 2011). Cratering model ages were obtained by fitting the crater production function of Hartmann and Daubar (2016). By adopting this chronology system we properly took into account also the cumulative resurfacing correction and set diameter range limits between 200 and 1000 m for the best fit age estimation. Following Kneissl et al. (2011) we used sinusoidal map projections to avoid incorrect

area size determinations, considered resurfacing corrections and delimited impact craters by identifying two opposing points on the impact-crater rim following the illumination direction, where possible, because it provides the best contrast conditions to determine the rim's crest. Due to the peculiar surface distribution we delimited the unit area by contouring patches where the TT were effectively outcropping. We discarded the buffered-CSFD and favored the classical CSFD method because of patches proximity leading to significant buffer area overlap.

2.3 Cluster and fractal analyses

The investigation of the subsurface asset was performed on the study area by means of the application of cluster and fractal analyses on the entirety of the mapped mound populations. We mapped 2126 mounds in Arcadia, on a region of about 20.000 km² centred at N50° E175° fully covered by TT. Each feature was distinguished from the neighbouring through manual identification and mapping of pits. Where chains of coalescent mounds occurred, the pit identification was supported by the observation of recurrent associated swellings of the ridge margin and internal incision profiles on planar view.

We performed the spatial distribution analyses by following the two steps workflow of clustering and fractal behaviour investigation according to Mazzarini and Isola (2010). Accordingly, clustering of features was performed to delimitate groups of mound-like structures that could be more likely linked to the same fracture system computing their sinusoidal projections centred coordinates in MINITAB® software and applying an agglomerative hierarchical clustering method (Mazzarini, 2007). Each cluster subsequently underwent self-similar clustering analysis, i.e. fractal analysis, which investigates the spatial properties of the examined objects, thus how fractures or vents fill the space. This methodology, starting from the observation of punctual features distribution (e.g. vents), provides insights about the possible presence of connectivity between mounds and fracture networks and so allowing to distinguish between fracture-related or fracture-unrelated processes and, where such connection is recognized, this technique allows to infer the extension of the connected fracture network actually able to drain fluids from a deep source toward the surface (De Toffoli et al., 2018). When the fracture network is actually percolating its spatial distribution is fractal and its self-

similarity is defined in a specific lengths range bounded by a lower and an upper cutoff (e.g. Mandelbrot, 1982). Fractal behaviour is recognized when a plateau stage is displayed in a $\Delta \log(C(l)/\Delta \log(l))$ vs. $\log(l)$ diagram where $C(l)$ is the correlation sum, defined as $C(l)=2N(l)/N(N-1)$ and $N(l)$ are the pairs of points (i.e. the mapped central pits) whose distance is less than l (Darcel et al., 2003 Mazzarini and Isola, 2010). The starting and ending edges of such plateau stage are defined as the lower and upper cutoffs (Lco and Uco) where the upper cutoff is assumed to represent the distance between the surface and the fluid source at depth (e.g. Mazzarini and Isola, 2010). Thus, the Uco, that is the largest plateau breaking point, represents the maximum value of the size range, which is the maximum extension of the pipeline connecting the reservoirs to the surface, accordingly, Uco defines the depth of the fluids source (Mazzarini and Isola, 2010 and references therein) making it the value of interest to infer the thickness of the cracked medium between the source and the surface in the studied region.

To produce the best Uco values estimate we adopted measures to minimize the errors. Firstly, we identified the Uco depth range corresponding to the higher values of R^2 , where R^2 is defined as shown in equation (1)

$$R^2 = 1 - \frac{SS_{res}}{SS_{tot}} \quad (1)$$

where SS_{res} represents the residuals sum of squares, which is meant to be minimized in proportion to the normalization coefficient SS_{tot} (total sum of squares) in accordance to the order of magnitude involved in the calculation. The error of the measure was estimated calculating the half difference between the maximum and the minimum depths where the R^2 shows the best-fit value (De Toffoli et al., 2018). Secondly, in order to produce meaningful estimates, the sample size effect needed to be considered. As a rule of thumb, at least 50 samples are required to extract robust parameter estimates (Clauset et al., 2009) and, in accordance, in our study the number of observed mounds spans between a minimum of 309 to a maximum of 863 per single cluster. Indeed, a number of observations greater than this threshold, endure a robust estimate of the fractal distribution parameters. In fact, Mazzarini and Isola (2010) showed that removing a random sample of 20% of the vents from large (i.e. > 200 vents) datasets does not affect the estimation of the fractal exponent (less than 0.01% of variation) and the error introduced into the estimation of the cut-offs is less than 1%–2%. In Mazzarini et al. (2013) the effect of uncertainties in point (mound) locations has been tested by adding random errors (in the

0–100 m, 0–300 m and 0–500 m ranges) to the sampled points. In this test, the added errors were as high as five to twenty-five times that of the coarsest image resolution used to locate vents. The 0–100 m errors generate fractal exponent and cut off value identical to those computed for the original dataset. In the case of 0–500 m random errors, the resulting fractal exponent is 3% higher than that computed for the original dataset, and the cut offs are very similar to those computed for the original dataset. Accordingly, we performed analyses on clusters exceeding the precautionary value to keep the error on the scaling parameter smaller than 1%.

3. Results

3.1 Image analyses

In the Arcadia region, we define the mound-like objects as low light features (LLFs), according to the dominant and more evident traits and relative spatial organisation (Fig.1a,1b) we identified. LLFs show distinctly brighter albedo compared to the surrounding plane and are characterised by low elevation, perimeter moats and swellings, rough surface and central pit surrounded by concentric ring-like features manifested by multiple crestral incisions (Fig. 2 a, c, d). LLF are around 700 to 300 m in diameter, averagely rounded with irregular, blending and jagged margins not always neatly distinguishable.

The large majority of the LLF are organised in tight arcuate chains (Fig. 1 and Fig. 2 d) where each feature is significantly overlapping on its neighbouring. These ridges are averagely around 5 km long, although, lengths are variable between tens of kilometres to hundreds of metres and due to this asset moats, pit surrounding structures can often be found merged in elongated clefts. LLF that come in curvilinear ridges constitute the large majority of the dome alignments that, by definition, characterise the TT (Pomerantz & Head, 2003 and references therein). Such ridges are distributed in arcuate parallel sets shaping a pattern of overlapping fans.

Nighttime Infrared (IR) data from the Thermal Emission Imaging Spectrometer (THEMIS) on Mars Odyssey were also consulted. The mound-like population appear to be well-recognizable prominent dark linear and circular structures (Fig.3), this including

both high and lower plain-like albedo features, so depicting a common low thermal inertia behaviour (e.g. Mellon et al., 2000; Farrand et al., 2005).

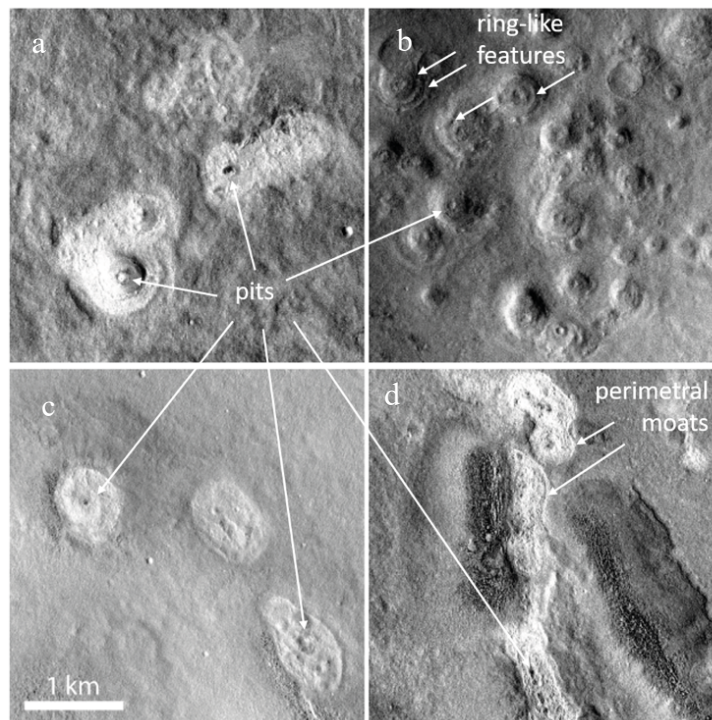


Fig. 2. The mounds in the captures display the key traits of LLFs. Single and coalescent features are shown; well-visible pivotal characteristics are: albedo, surface roughness, basal shape, pitted tops, ring-like features and perimeter moats.

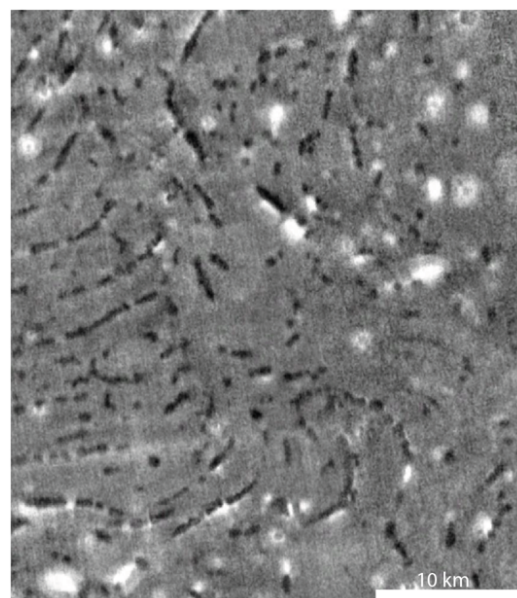


Fig.3. THEMIS Nighttime IR response. High albedo feature chains shown in Fig. 1 correspond to the dark patches in the Nighttime map well recognisable thank to the peculiar spatial organization.

Statistical analysis of crater size-frequency distributions of impact craters on planetary surfaces is a well-established method to derive absolute ages on the basis of remotely-sensed image data (e.g. Hartmann and Neukum, 2001). CSFD-based age modelling was performed on the entire LLFs assemblage as a single mound population, this allowed to date the TT surface back to 370 ± 40 Ma.

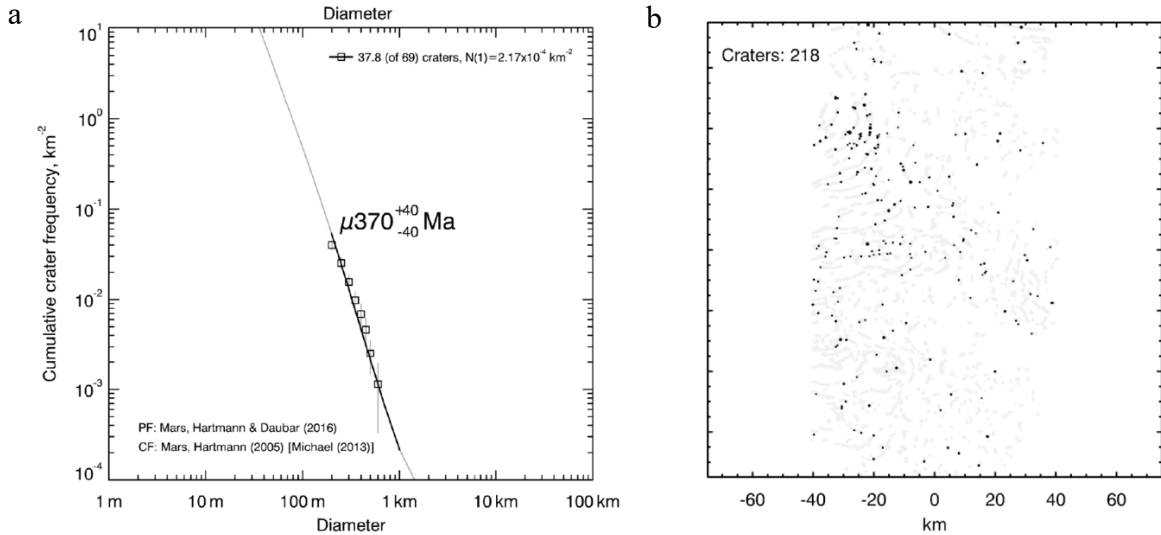


Fig.4 Fig.4 CSFD-based age modelling outputs for the whole area covered with LLF (a) and map of the TT surface distribution and the relative crater population (b).

3.2 Fractal analysis

We grouped mapped mound-like features into clusters due to the large area covered by the investigated region. In Arcadia Planitia, fractal analysis has been applied to four different clusters of LLFs (AP). The Upper cutoff identification for each cluster was derived from *local slope* v. $\log(l)$ and $C(l)$ vs. $l(m)$ diagrams used for both Lco and Uco picking. The correct selection of the cutoffs was performed identifying the wider size range with the highest correlation between $\log(l)$ and the local slope values (Mazzarini and Isola, 2010).

Among the clusters of Arcadia, three out of four show fractal distributed mounds (Tab.1). Output AP3 was too noisy and with no clear distribution pattern and, for this reason, no deductions can be made out of this group of data. Uco values are: 16 ± 2 km for AP1, 18 ± 2 km for AP2 and 20 ± 3 km for AP4 (Fig.5), which also displays a second shallow plateau with Uco at 2.5 ± 0.3 km.

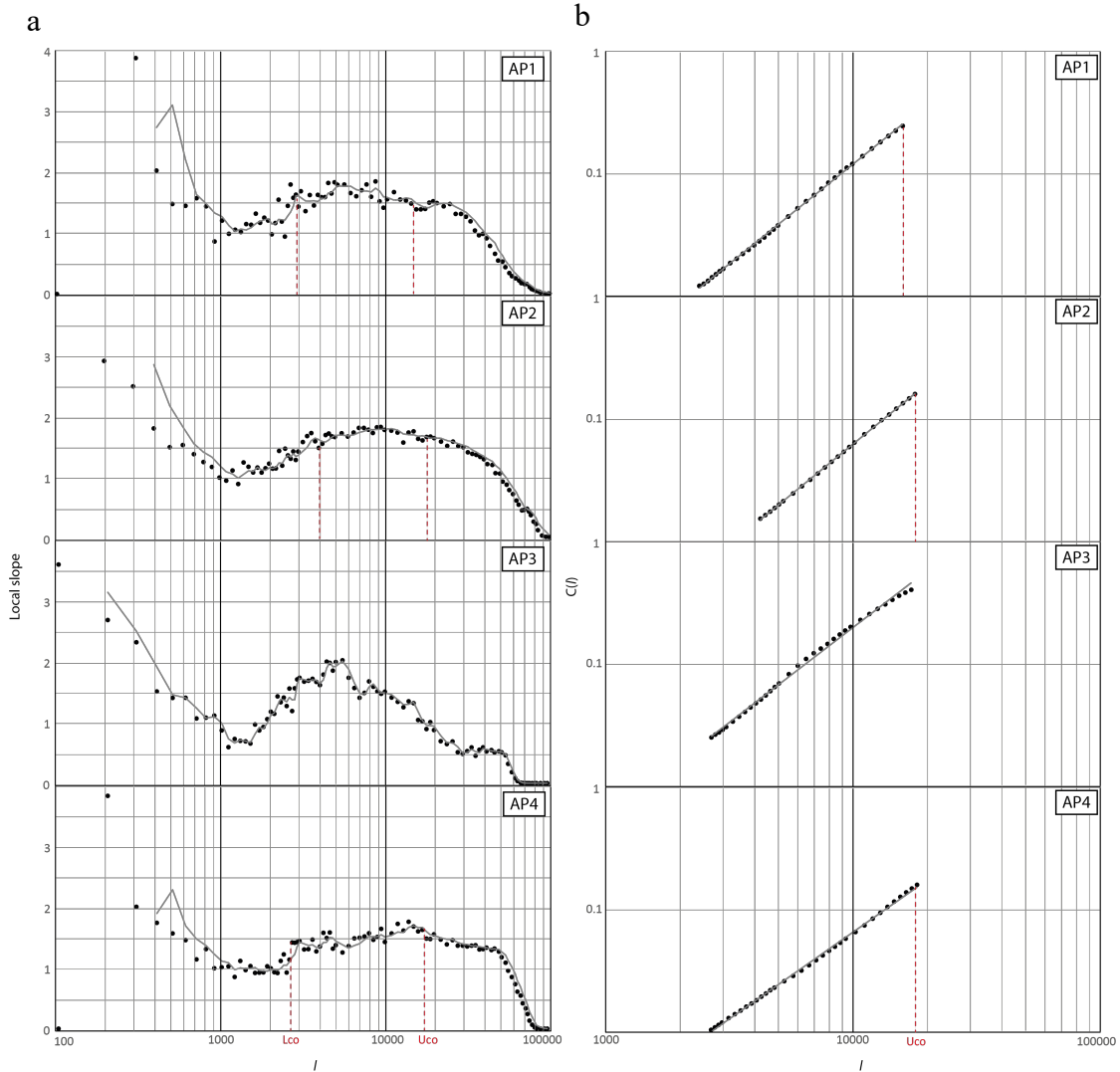


Fig5. Size range of interconnected fractures are represented by the plateau stage of the curve, where present, for all the clusters (a). Where the slope breaks the fractures' distribution stops to be fractal. The corresponding $\log(l)$ value coincides to a specific maximum thickness of the fractured medium that connects the surface to the subsurface (U_{co}). Graphs (b) show the variation of fractures distribution compared to the Power Law (solid line). Here the goodness of the U_{co} picking in the previous graph is tested. Fractal distribution follows the Power Law, where data matches the solid line the distribution of fractures/vents is fractal. [l : fractures length [m]; $C(l)$: correlation integral defines the correlation between point at a distance lower to l ; Local Slope: represents the $\Delta \log(C(l)) / \Delta \log(l)$ ratio].

CLUSTER ID	N°	LCO [km]	UCO [km]	R ²
AP1	386	2.4 ± 0.3	16 ± 2	0.9994
AP2	863	4 ± 0.5	18 ± 2	0.9999
AP3	309	-	-	-
AP4	569	2.8 ± 0.5	20 ± 3	0.9988
		1 ± 0.1	2.5 ± 0.3	0.9998

Tab 1. Fractal analyses number of units per cluster, outputs and errors.

5. Discussion

TT are still debated surface features and no agreement has been reached on their origin, for this reason we aimed to apply a nouvelle approach in order to bring new evidence that could advance the current knowledge on the topic. Specifically, the implementation of the cluster and fractal analyses gives herein an innovative prospective on the issue by taking into consideration the interplay between the surface and the subsurface.

The large majority of the mound-like objects are originally circular features merged in coalescent chains and we observed summit (and also peripheral in places) pits with several concentric annular structures suggesting an eruptive activity (e.g. Hovland et al., 1997; Oehler & Allen, 2010; Okubo, 2016). The albedo of the mounds depends on the nature of the extruded material. CTX mosaics displayed a population with bright albedo or equal to the surrounding plain, while in the Nighttime IR imagery dataset the same mound-like features appeared evidently darker than the surrounding due to their low thermal inertia. This parameter represents the ability of the subsurface to conduct and store heat energy during the exposure to sunlight and to return that heat energy to the surface during the night. Also, thermal inertia depends on the nature of the material and so it can help identifying the characteristics of the surface under examination, particularly, fine grained and loosely packed materials typically has low

value of thermal inertia, while higher values are commonly exhibited for rocks and exposed bedrock. Therefore, matching together all the collected evidence, in the specificity of this case study the mound-like mapped elements are likely to be made of localized resurgences of fine-grained loose sediments (Mellon et al., 2000; Kopf, 2002; Judd & Hovland, 2007; Skinner & Tanaka, 2007 and Oehler & Allen, 2010). This hypothesis would make such objects relevant also to astrobiological purposes due to the close relationship that, on Earth, sediment resurgences usually have with liquid water and the degassing phenomenon, specifically concerning the methane release (e.g. Milkov, 2000; Kopf, 2002; Skinner & Tanaka, 2007) two key life detection proxies in the search for life beyond Earth (e.g. Formisano et al., 2004; Atreya et al., 2007; Geminale et al., 2008; Mumma et al., 2009).

The geomorphological evidence pointing toward sediment mobilisation and eruption as formation process of Arcadia mound-like features is supported by the outcome of the fractal analysis that underscores the link between these object fields and the presence of underlying networks of connected percolating fractures draining a reservoir at depth (De Toffoli et al., 2018 and references therein). This relationship implies fluid circulation in the Martian upper crust at the moment of the genesis of these features, that according to the age model took place, in the context of the Martian timeframe, in an extremely recent geological past ~ 370 Ma. Thus, we compared the thickness of cracked medium, i.e. the location at depth of the fluid source, with estimated distribution of ice and water in the subsurface, where they are commonly hypothesised to still be present in such recent times. In fact, the cryosphere is a natural water trap in the subsurface and groundwater persists as liquid phase when its inventory exceeds the actual pore volume of the cryosphere leading to an accumulation of water in the lower portion of the crust (Clifford, 1993; Clifford et al., 2010). In our case study, the considered region is situated in a low topographic area where an actual physical contact between the cryosphere base and the groundwater reservoir is likely to be present in the subsurface, whether the H_2O inventory is sufficient (e.g. Clifford, 1993; Clifford & Parker, 2001; Clifford et al., 2010). Different brines in the Martian subsurface have different phase transition behaviours on a global scale and the basal limits of the cryosphere stability zone, displayed in Fig.6 by different lines in function of brines salinity, are representative of the best-insulated scenario modelled by Clifford et al., (2010), i.e. describing the shallowest calculated position of the isotherms marking the transition from solid to liquid phase of the brines. In fact, the authors

assumed the maximum realistic porosity ($F = 0.35$ at the surface and follows the exponential decay relationship of Clifford, (1993) in the subsurface), a low thermal conductivity value ($0.5 \text{ W m}^{-1} \text{ K}^{-1}$) of the crust and a cryosphere fully saturated of gas-hydrates instead of water-ice. Astronomically induced variations are also described in Clifford et al., (2010) but, since they are estimated to have affected the cryosphere depth just of few hundred of meters in equatorial and polar positions, these parameters are neglected in this work. Comparing the thicknesses of fractured medium involved beneath the mound fields and the cryosphere stability zone, we observed that almost all the mapped TT chains are related to fracture networks extending up to 16-18 km beneath the surface in correspondence of the modelled gas-hydrate rich cryosphere-hydrosphere transition (Clifford et al., 2010).

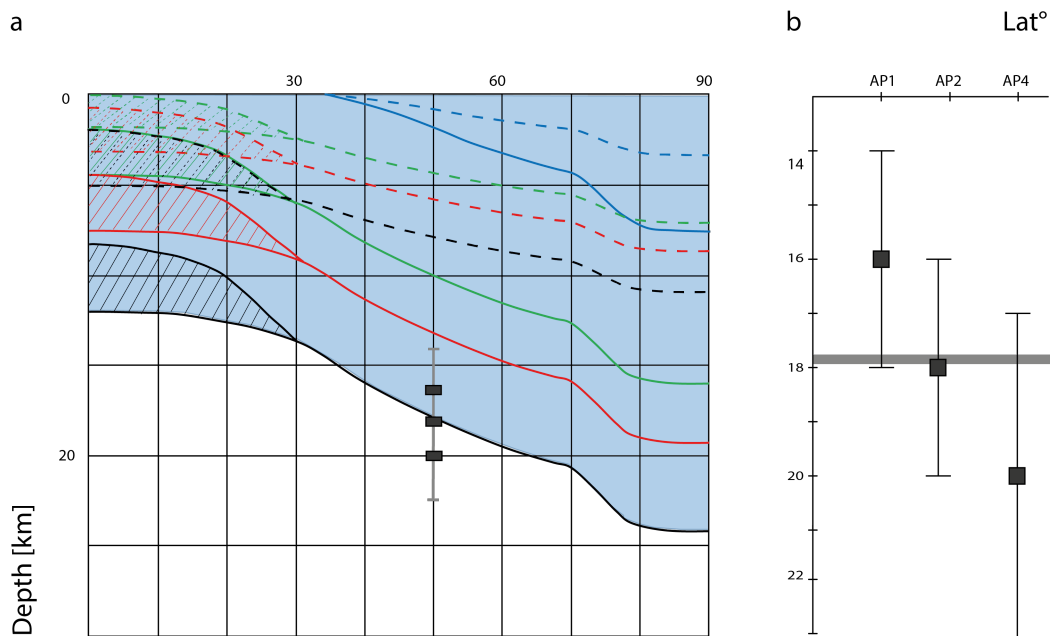


Fig.6. Latitudinal variation in depth of a hydrate-rich cryosphere for three different groundwater freezing temperatures: 203°K: sulfate-rich and $\text{Mg}(\text{ClO}_4)_2$ brine (blue line); 252°K: NaCl brine (green line); 273°K: pure groundwater (red line); 303°K: base of the gas hydrate stability zone (black line); assumed heat flow is 15 mW m^{-2} for solid lines and 30 mW m^{-2} for dashed lines. Below 30° latitude, high and low regolith porosity can influence the isotherms distribution as displayed by the divergent pattern (modified after Clifford et al., 2010). Maximum extensions of fracture systems inferred beneath the mound population is plotted as three boxes aligned in correspondence of the Arcadia location latitude (a). Break down for each deep single cluster maximum extension value (b). Grey line in graph b displays the gas hydrate stability zone base level.

The great majority of the mound-like features herein observed appear then to have been fed from portions of a fractured medium that acted as reservoir and pipeline system that reach the base of the gas hydrate stability zone. This produces a meaningful relation between gas hydrate potential distribution in the subsurface and the occurrence of such surface expressions. This linkage leads to suppose that the involvement of water, ostensibly as a result of gas hydrate dissociation, plays a role in the subsurface processes that potentially worked as triggers of venting, corroborating the hypothesis of sediment mobilisation and eruption as the more likely formation process.

AP4 cluster displays a double plateau, the shallower one (Uco ~3 km) has been discarded due to its very narrow size range leading to high statistical uncertainties (e.g. Darcel et al., 2003). Whether an interpretation would be hypothesized, such shallow plateau could be the product of an earlier stage of pulses of the same phenomenon and preserved without being obliterated by newer inputs, or it could be the result of the circulation of brines with either different composition, or higher temperatures, or a combination of the two, which can be found nestled in shallower reservoirs.

6. Conclusions

According to the observations and analyses herein collected, we recognized evidence of fluid circulation in the Martian upper crust involving large areas in the northern lowlands thanks to its well-recognisable surface expression. We interpreted such features, LLF and so TT, as subsurface sediment mobilization and resurgence matching together: (i) geomorphological traits that belong to chains of eruption vents; (ii) thermal inertia behaviour that resembles what is to be expected from fine grained loose materials; (iii) the relationship with network of percolating fractures that probably functioned as pipelines for the fluid flow from the subsurface toward the surface and (iv) the extent of such fracture systems that reaches up to the depth where it is supposed to lie the base of the gas-hydrate rich cryosphere (on present heat-flow Mars estimates) so drawing a connection between mound-like features and the dissociation of such clathrates deposits. Clathrates can indeed firstly act as massive storage of gasses in the subsurface (Max et al., 2013; Mousis et al., 2012), which could be released through their destabilization; secondly, clathrates can insulate the subsurface efficiently enough to produce thermal anomalies beneath that could facilitate the local cryosphere melting, so stimulating the presence of shallow

groundwater, and possible paroxysmal resurgence events (Prieto-Ballestreros et al., 2006; Chastain & Chevrier, 2007; Kargel et al 2007). Additional tapering and destabilization of the cryosphere layer could be induced at the hypothetical ice-water contact due to combination of freezing point depressing through high salinity fluid circulation and low temperature convection of groundwater (Travis, 2003; Clifford et al.,2010; Travis et al. 2013).

The implication of such outcomes is that thumbprint terrains could therefore be good gas emission centres candidates for geologically recent degassing pulses. Even if no relationship between these observed features and any biological contribution can be drawn from this new data load, such environments need to be taken into account for astrobiological exploration purposes. In fact, one of the large-scale astrobiological questions concerns the investigation of the possibility that life arose on other planets beyond Earth (for a complete review refer to Cockell, 2015) and we approach this task by widening and improving the knowledge of environments where life could find niches to survive on planet Mars by finding long-lasting fluid activity even in geologically recent times.

This study likewise suggests that LLFs and so TT should be taken into account for further geological and astrobiological investigations since they appear to be products of subsurface material mobilization and therefore likely linked to water, in the form of gas hydrates dissociation, that seems to lie at the origin of this phenomenon. Furthermore, the erupted materials would accordingly come from depths that are still not reachable by our present-day instrumentations making them a unique chance to study what is stored several kilometres beneath the surface.

Acknowledgments

This Paper is part of a project supported from the European Union's Horizon 2020 research and innovation programme under grant agreement N°776276 (PLANMAP)

References

- Atreya, S.K., Mahaffy, P.R., Wong, A.-S., 2007. Methane and related trace species on Mars: Origin, loss, implications for life, and habitability. *Planet. Space Sci.* 55, 358–369. doi:10.1016/j.pss.2006.02.005
- Bernhardt, H., Hiesinger, H., Ivanov, M.A., Ruesch, O., Erkeling, G., Reiss, D., 2016. Photogeologic mapping and the geologic history of the Hellas basin floor, Mars. *Icarus* 264, 407–442. doi:10.1016/j.icarus.2015.09.031
- Bridges, J.C., Seabrook, A.M., Rothery, D.A., Kim, J.R., Pillinger, C.T., Sims, M.R., Golombek, M.P., Duxbury, T., Head, J.W., Haldemann, A.F.C., Mitchell, K.L., Muller, J.-P., Lewis, S.R., Moncrieff, C., Wright, I.P., Grady, M.M., Morley, J.G., 2003. Selection of the landing site in Isidis Planitia of Mars probe Beagle 2. *J. Geophys. Res.* 108, 5001. doi:10.1029/2001JE001820
- Bruno, B.C., Fagents, S.A., Thordarson, T., Baloga, S.M., Pilger, E., 2004. Clustering within rootless cone groups on Iceland and Mars: Effect of nonrandom processes. *J. Geophys. Res. E Planets* 109, 1–11. doi:10.1029/2004JE002273
- Chastain, B.K., Chevrier, V., 2007. Methane clathrate hydrates as a potential source for martian atmospheric methane. *Planet. Space Sci.* 55, 1246–1256. doi:10.1016/j.pss.2007.02.003
- Clifford, S.M., Parker, T.J., 2001. The evolution of the Martian hydrosphere: Implications for the fate of a primordial ocean and the current state of the Northern Plains. *Icarus* 154, 40–79. doi:10.1006/icar.2001.6671
- Clifford, S.M., 1993. A model for the hydrologic and climatic behavior of water on Mars. *J. Geophys. Res.* 98, 10973–11016. doi:10.1029/93JE00225
- Clifford, S.M., Lasue, J., Heggy, E., Boisson, J., McGovern, P., Max, M.D., 2010. Depth of the Martian cryosphere: Revised estimates and implications for the existence and detection of subpermafrost groundwater. *J. Geophys. Res.* 115, E07001. doi:10.1029/2009JE003462
- Cockell, C.S., 2015. *Astrobiology*. John Wiley & Sons Ltd, 472 pp.
- Costard, F., Séjourné, A., Kelfoun, K., Clifford, S., Lavigne, F., Di Pietro, I., Bouley, S., 2017. Modeling tsunami propagation and the emplacement of thumbprint terrain in an early Mars ocean. *J. Geophys. Res. Planets* 1–17. doi:10.1002/2016JE005230
- Darcel, C., Bour, O., Davy, P., and de Dreuzy, J.R., 2003. Connectivity properties of two-dimensional fracture networks with stochastic fractal correlation: *Water Resources Research*, v. 39, p. 1272, doi: 10.1029/2002WR001628.
- De Toffoli, B., Pozzobon, R., Mazzarini, F., Orgel, C., Massironi, M., Giacomini, L., Mangold, N., Cremonese, G., 2018. Estimate of depths of source fluids related to mound fields on Mars. *Planet. Space Sci.* 164–173. <https://doi.org/10.1016/j.pss.2018.07.005>
- Farrand, W.H., Gaddis, L.R., Keszthlyi, L., 2005. Pitted cones and domes on Mars: Observations in Acidalia Planitia and Cydonia Mensae using MOC, THEMIS, and TES data. *J. Geophys. Res.* 110. doi:10.1029/2004JE002297
- Formisano, V., Atreya, S., Encrenaz, T., Ignatiev, N., Giuranna, M., 2004. Detection of methane in the atmosphere of Mars. *Science* 306, 1758–1761
- Geminale, A., Formisano, V., Giuranna, M., 2008. Methane in Martian atmosphere: Average spatial, diurnal, and seasonal behaviour. *Planet. Space Sci.* 56, 1194–1203. doi:10.1016/j.pss.2008.03.004
- Ghent, R.R., Anderson, S.W., Pithawala, T.M., 2012. The formation of small cones in Isidis Planitia, Mars, through mobilization of pyroclastic surge deposits. *Icarus* 217, 169–183
- Grizzaffi, P., Schultz, P.H., 1989. Isidis Basin: Site of ancient volatile-rich debris layer. *Icarus* 77, 358–381
- Guidat, T., Pochat, S., Bourgeois, O., Souček, O., 2015. Landform assemblage in Isidis Planitia, Mars: Evidence for a 3 Ga old polythermal ice sheet. *Earth Planet. Sci. Lett.* 411, 253–267. doi:10.1016/j.epsl.2014.12.002
- Hartmann, W.K., Daubar, I.J., 2017. Martian cratering 11. Utilizing decameter scale crater populations to study Martian history. *Meteorit. Planet. Sci.* 52, 493–510. <https://doi.org/10.1111/maps.12807>
- Hartmann, W.K., Neukum, G., 2001. Cratering chronology and the evolution of Mars. *Space Science Reviews* 96, 165–194.
- Hiesinger, H., Rohkamp, D., Sturm, S., Thiessen, F., Reiss, D., 2009. Thumbprint Terrain in Isidis Planitia, Mars: Geology, Ages, Morphology. *Geophys. Res. Abstr.*, EGU General Assembly 11, EGU2009-781Kargel, J.S. et al., 1995. Evidence of ancient continental glaciation in the martian northern plains. *J. Geophys. Res.* 100, 5351–5368.
- Hovland, M., Hill, A., Stokes, D., 1997. The structure and geomorphology of the Dashgil mud volcano, Azerbaijan. *Geomorphology* 21, 1–15. doi:10.1016/S0169-555X(97)00034-2
- Ivanov, M.A., Hiesinger, H., Erkeling, G., Hielscher, F.J., Reiss, D., 2012. Major episodes of geologic history of Isidis Planitia on Mars. *Icarus* 218, 24–46.
- Judd, A.G., Hovland, M., 2007. Seabed Fluid Flow: The Impact on Geology, Biology and the Marine

- Environment. University Press, Cambridge. 475 pp.
- Kargel, J.S., Furfaro, R., Prieto-Ballesteros, O., Rodriguez, J.A.P., Montgomery, D.R., Gillespie, A.R., Marion, G.M., Wood, S.E., 2007. Martian hydrogeology sustained by thermally insulating gas and salt hydrates. *Geology* 35, 975–978. doi:10.1130/G23783A.1
- Kneissl, T., Van Gasselt, S., Neukum, G., 2011. Map-projection-independent crater size-frequency determination in GIS environments - New software tool for ArcGIS. *Planet. Space Sci.* 59, 1243–1254. <https://doi.org/10.1016/j.pss.2010.03.015>
- Kopf, A.J., 2002. Significance of mud volcanism. *Rev. Geophys.* 40, 1005. doi:10.1029/2000RG000093
- Kreslavsky, M. a., Head, J.W., 2002. Fate of outflow channel effluents in the northern lowlands of Mars: The Vastitas Borealis Formation as a sublimation residue from frozen ponded bodies of water. *J. Geophys. Res.* 107, 5121. doi:10.1029/2001JE001831
- Lockwood, J.F., Kargel, J.S., Strom, R.B., 1992. Thumbprint terrain on the northern plains: A glacial hypothesis. *Lunar Planet. Sci.* 23, 795–796
- Lucchitta, B.K., 1981. Mars and Earth: Comparison of cold-climate features. *Icarus* 45, 264–303.
- Mazzarini, F., 2007. Vent distribution and crustal thickness in stretched continental crust: The case of the Afar Depression (Ethiopia). *Geosphere* 3, 152–162. <https://doi.org/10.1130/GES00070.1>
- Mazzarini, F., Isola, I., 2010. Monogenetic vent self-similar clustering in extending continental crust: Examples from the East African Rift System. *Geosphere* 6, 567–582. <https://doi.org/10.1130/GES00569>.
- Mazzarini, F., Keir, D., Isola, I., 2013. Spatial relationship between earthquakes and volcanic vents in the central-northern Main Ethiopian Rift. *Journal of Volcanology and Geothermal Research* 262 (2013) 123–133. <http://dx.doi.org/10.1016/j.jvolgeores.2013.05.007>.
- Max, M.D., Clifford, S.M., and Johnson, A.H. (2013) Hydro- carbon system analysis for methane hydrate exploration on Mars. In *Energy Resources for Human Settlement in the Solar System and Earth’s Future in Space*, AAPG Memoir 101, edited by W.A. Ambrose, J.F. Reilly II, and D.C. Peters, American Association of Petroleum Geologists, Tulsa, OK, pp 99–114
- Mellon, M., Jackosky, B.M., Kieffer, H.H., Christensen, P.R., 2000. High-Resolution Thermal Inertia Mapping from the Mars Global Surveyor Thermal Emission Spectrometer. *Icarus* 148, 437–455. <https://doi.org/10.1006/icar.2000.650>
- Milkov, a. V., 2000. Worldwide distribution of submarine mud volcanoes and associated gas hydrates. *Mar. Geol.* 167, 29–42. doi:10.1016/S0025-3227(00)00022-0
- Mousis, O., Lunine, J.I., Chassefière, E., Montmessin, F., Lakhliif, A., Picaud, S., Petit, J.M., Cordier, D., 2012. Mars cryosphere: A potential reservoir for heavy noble gases? *Icarus* 218, 80–87. doi:10.1016/j.icarus.2011.12.007
- Mumma, M.J., Villanueva, G.L., Novak, R.E., Hewagama, T., Bonev, B.P., Disanti, M. a, Mandell, A.M., Smith, M.D., 2009. Strong release of methane on Mars in northern summer 2003. *Science* 323, 1041–1045. doi:10.1126/science.1165243
- Oehler, D.Z., Allen, C.C., 2010. Evidence for pervasive mud volcanism in Acidalia Planitia, Mars. *Icarus* 208, 636–657. doi:10.1016/j.icarus.2010.03.031
- Okubo, C.H., 2016. Morphologic evidence of subsurface sediment mobilization and mud volcanism in Candor and Coprates Chasmata, Valles Marineris, Mars. *Icarus* 269, 23–37. doi:10.1016/j.icarus.2015.12.051
- Orgel, C., Hauber, E., Skinner, J.A., Gasselt, S. Van, Ramsdale, J., Balme, M., Survey, U.S.G., Keynes, M., 2015. Distribution, origin and evolution of hypothesized mud volcanoes, thumbprint terrain and giant polygons in Acidalia, Utopia and Arcadia Planitiae: Implications for sedimentary processes in the northern lowlands of Mars, in: *Lunar and Planetary Science Conference*. <https://doi.org/10.1002/2014JE004682>
- Pomerantz, W.J., Head, J.W., 2003. Thumbprint Terrain and Sinuous Troughs with Medial Ridges in the Northern Lowlands of Mars: Assessment of the Glacial Hypothesis Using New Spacecraft. *Lunar Planet. Sci. Conf.* 34, 1277.
- Prieto-Ballesteros, O., Kargel, J.S., Fairén, A.G., Fernández-Remolar, D.C., Dohm, J.M., Amils, R., 2006. Interglacial clathrate destabilization on Mars: Possible contributing source of its atmospheric methane. *Geology* 34, 149. doi:10.1130/G22311.1
- Rodriguez, J.A.P., Tanaka, K.L., Berman, D.C., Kargel, J.S., 2010. Late Hesperian plains formation and degradation in a low sedimentation zone of the northern lowlands of Mars. *Icarus* 210, 116–134. doi:10.1016/j.icarus.2010.04.025
- Rodriguez, J.A.P., Fairén, A.G., Tanaka, K.L., Zarroca, M., Linares, R., Platz, T., Komatsu, G., Miyamoto, H., Kargel, J.S., Yan, J., Gulick, V., Higuchi, K., Baker, V.R., Glines, N., 2016. Tsunami waves extensively resurfaced the shorelines of an early Martian ocean. *Sci. Rep.* 6, 25106. <https://doi.org/10.1038/srep25106>

- Scott, D.H., and Underwood, J.R., Jr., 1991. Mottled terrain: A continuing Martian enigma, in Ryder, G., and Sharpton, V.L., eds., *Proceedings of the 21st Lunar and Planetary Science Conference*: Houston, Texas, Lunar and Planetary Institute, p. 627-634.
- Skinner, J.A., Tanaka, K.L., 2007. Evidence for and implications of sedimentary diapirism and mud volcanism in the southern Utopia highland–lowland boundary plain, Mars. *Icarus* 186, 41–59. doi:10.1016/j.icarus.2006.08.013
- Skinner Jr., J.A., Mazzini, A., 2009. Martian mud volcanism: Terrestrial analogs and implications for formational scenarios. *Marine Petrol. Geol.* doi:10.1016/j.marpetgeo.2009.02.006.
- Tanaka, K.L., Robbins, S.J., Fortezzo, C.M., Skinner, J.A., Hare, T.M., 2014. The digital global geologic map of Mars: Chronostratigraphic ages, topographic and crater morphologic characteristics, and updated resurfacing history. *Planet. Space Sci.* 95, 11–24. <https://doi.org/10.1016/j.pss.2013.03.006>
- Travis, B.J., 2003. On the role of widespread subsurface convection in bringing liquid water close to Mars' surface. *J. Geophys. Res.* 108, 8040. doi:10.1029/2002JE001877
- Travis, B.J., Feldman, W.C., Maurice, S., 2013. A mechanism for bringing ice and brines to the near surface of Mars. *J. Geophys. Res. E Planets* 118, 877–890. doi:10.1002/jgre.20074

Paper in Preparation

EVIDENCE OF MUD VOLCANISM RELATED TO GAS HYDRATE-RICH CRYOSPHERE ON MARS

Barbara De Toffoli ^{a,b}, Riccardo Pozzobon ^{a,b}, Francesco Mazzarini ^c,
Matteo Massironi ^{a,b}, Gabriele Cremonese ^b

^a Department of Geosciences, University of Padova, Via Gradenigo 6, Padova 35131, Italy

^b INAF, Osservatorio Astronomico di Padova, Vicolo dell'Osservatorio 3, Padova I-35122, Italy

^c Istituto Nazionale di Geofisica e Vulcanologia, Via Della Faggiola 32, Pisa 56100, Italy

Abstract

This study provides new evidence of the presence of mud volcanic processes on Martian lowlands according to new insights on their origin. In particular, this work is focused on Hellas basin, Utopia basin and a portion of the Northern Plains lying north of Arabia Terra, and it is based on a population of ~6000 mounds that span over ~90.000 km² area in each region. Context Camera (CTX) on Mars Reconnaissance Orbiter (MRO) images show circular to elliptical mounds with central and/or distal pits and lobate flow-like features, such as apron-like extensions and concentric circular lobes around the source pits. To support the geomorphological observations we performed height-to-diameter morphometric analysis on stereo-derived CTX DTMs on two samples of mounds of ~30 specimens each. In addition, sediment and fluid reservoirs that fed the mounds were inferred by means of cluster and fractal analyses. A good correlation seems to occur between the locations of the reservoirs and the gas hydrate rich cryosphere-hydrosphere contact hypothesized by Clifford et al. (2010) in the Martian subsurface. Thus, the fields were fed, at least partially, by reservoirs located at the base of gas hydrate stability zone, suggesting that a common trigger factor linked to a specific deep environment could exist. This supports the interpretation that the mounds are actually mud volcanoes and makes these structures an intriguing target for astrobiology.

1. Introduction

Mud volcanism is a well-known phenomenon involving the expulsion of gases, water and sediments from the subsurface. These resurgences occur when the buoyancy forces that push the mixtures exceed the confining lithostatic pressure (Kopf, 2002). To allow the mud effusion, unconsolidated or poorly consolidated materials need to be stored and confined in the subsurface in correspondence of a source of fluids; the up-flow can be then triggered by new fluid supply, increasing of pore pressures and a decrease of viscosity (e.g. Dimitrov, 2002; Kopf, 2002; Skinner & Tanaka, 2007). Within these conditions, hydrocarbon generation can produce suitable context to unleash mud resurgences, in this case products of organic matter deterioration (i.e. liquid and gaseous components, like methane) can be brought to the surface along with mud and water (e.g. Milkov, 2000). Morphological features interpreted as mud volcanoes in the northern Martian lowlands has been widely discussed among the scientific community (e.g. Davis & Tanaka, 1995; Tanaka et al., 2000, 2003, 2008; Rodríguez et al., 2007; Skinner & Tanaka, 2007; Allen et al., 2009; Oehler & Allen, 2009, 2010; Skinner & Mazzini, 2009; McGowan, 2009; McGowan & McGill, 2010; McGowan, 2011; Komatsu et al., 2016). Indeed, the clear identification is hard to endorse given the morphological affinity which mud volcanoes have with other geomorphological features of different origin such as cinder cones, tuff cones, rootless cones or pingos (Tanaka, 1997; Tanaka et al., 2005; Farrand et al., 2005; Burr et al., 2009). Nevertheless the analysis of these features, observed in a wide number of locations on the Martian surface (e.g. Oehler & Allen, 2010; McGowan 2011; Pondrelli et al., 2011; Okubo, 2016), remain a crucial step to improving the understanding of the subsurface, which they are strictly connected to, where life could find water, nutrients and a niche shielded from the inhospitable conditions that affect the surficial environment (e.g. Cockell et al., 2012; Nixon et al., 2013; Parnell & McMahon 2016). The expansion of astrobiological exploration to mud volcanoes could, therefore, be one of the few chances to infer what was hosted, at the moment of the eruption, in the deep subsurface, until new drilling techniques will be provided.

2. Geologic setting

In this work, we focused on three different regions on the Martian surface located in areas attributed to different impact basins. The case study regions are (1) the northwestern part of the Hellas basin floor, (2) the southwestern area of Utopia basin, and (3) a portion of the Northern Plains laying north of Arabia Terra, between Acidalia and Utopia Planitiae (Fig.1).

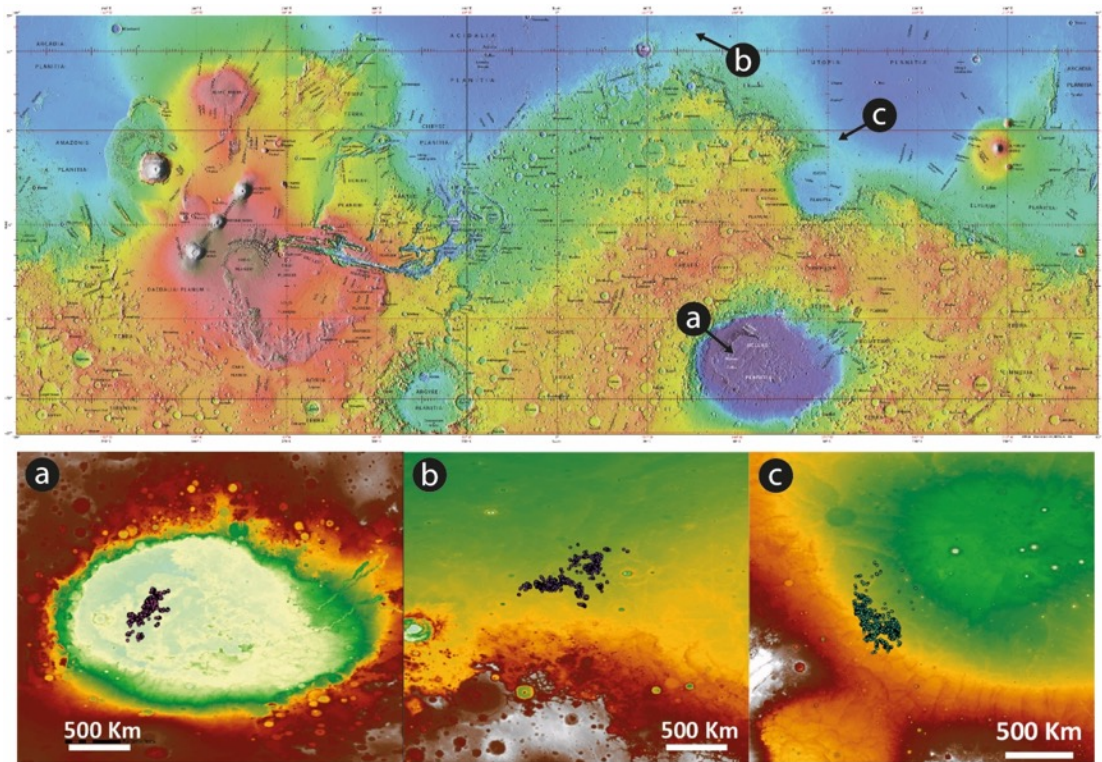


FIG 1. USGS MOLA-based topographic map of Mars; black arrows indicate the location of target areas. Dot groups overlaid to the magnification of the study regions, in (a) Hellas basin (60°E 40°S), (b) the Northern Plain region (50°E 57°N) and (c) Utopia Planitia (95°E 31°N), show the exact position of the mapped mound examined in the present work

In these regions, among the lowlands in general, mound-like topographically positive features have been already recorded in literature and reported as mounds or, on larger scale, as knobby fields and terrains or thumbprint terrains based on the detail of the description and the aims of the investigation (e.g. Tanaka, 1997; Pomerantz and Head, 2003; Rodriguez et al., 2010; Guidat et al., 2015; Bernhardt et al., 2016). Specifically we chose to investigate wide areas where mounds are visible at the Context Camera (CTX) resolution (6 m/pixel). All these three regions belong to areas of low elevation located in both the hemispheres and in different great basins.

Hellas basin is one of the largest impact structures in the Solar System and it is the largest topographic depression of the southern Martian hemisphere with diameters of $\sim 1700 \times \sim 1300$ km, showing an approximate average elevation of -6.5 km. The basin covers an area of $\sim 5.6 \times 10^6$ km²; it is elliptically shaped elongated in east-west direction and centered at 68°E and 41°S (Bernhardt et al., 2016). In this area, volcanic activity started after the Hellas impact $\sim 3.6\text{-}3.9$ Ga, probably associated with the ring fractures linked to the basin impact structures and triggered by massively wetter conditions, when the atmosphere was denser and volatiles were more abundant and closer to the surface, that could have likely enabled large explosive eruptions (Williams et al., 2008; Williams et al., 2009). The presence of two volcanic edifices on the northeastern flank, Tyrreheha and Hadriatica Paterae, and four on the southwestern side, Amphitrites, Peneus, Malea and Pityusa Paterae (whose interpretation is still uncertain) characterize the so called Circum-Hellas province (Williams et al., 2009) that had a significant impact on the asset of the region, putatively also in relation to the hotter conditions resulting from the rise of magmas. Resurfacing due to volcanic activity together with fluvial and aeolian processes lasted until ~ 0.8 Ga (Williams et al., 2008). Likewise, water played a role in the Hellas basin evolution, in fact, it has been suggested that during the geological past Hellas could have been a water-filled basin (Andrews-Hanna et al., 2010). Even if there is a lack of evidence of outflows within Hellas, the intense cratering that took place over the entire Noachian period, mainly registered on the highlands, could have significantly fractured the crust contributing to the formation of a globally interconnected aquifer system (Andrews-Hanna et al., 2010). Information about the present-day Hellas is provided by Bernhardt et al., 2016 geological map (scale 1:2.000.000) where a detailed description of units and morphologies can be found.

Utopia basin is another extremely large depressed area produced by a pre-Noachian impact (e.g. Skinner & Tanaka, 2007; e.g., McGill, 1989; Tanaka et al., 2005; Carr & Head, 2010 from Broz & Hauber 2013) centered at 40°N and 105°E that is ~ 3200 km in diameter (Carr, 2006; McGowan, 2011). It is located in the northern Martian hemisphere, it is larger than 9×10^6 Km² and characterized by an average elevation of ~ -4 Km (e.g. Skinner & Tanaka, 2007; Thomson & Head, 2001). Utopia is mainly surrounded by the Northern Plains of Vastitas Borealis on its northern

portion. Tanaka et al., 2005 provide a complete geologic map (scale 1:15.000.000) of the Northern Plains that describes the portion analyzed in this work and Utopia region.

The third region of study is in the Northern Plains, located at the boundary between Utopia basin and Acidalia Planitia (centered at 338°E and 55°N) and is confined by Arabia Terra on the south. Similar to the above mentioned basins, Acidalia is supposed to be the product of large impacts that took place during the early history of the planet and it is centered at about 55°N, 338°E and is ~3000 km wide (Oehler & Allen, 2010). As well as Hellas basin, water could have influenced the evolution of northern lowlands where, in fact, was suggested the presence of a standing ocean that covered a significant part of the northern Martian hemisphere during wetter conditions (e.g. Clifford & Parker, 2001 and references therein; Fairén et al., 2003, Carr, 2006; Oehler & Allen, 2012; Ivanov et al., 2014; Wordsworth et al., 2015; Costard et al., 2017) or alternatively the presence of short-lasting (e.g. thousands of years) water bodies as a consequence of paroxysmal outflows (Kreslavsky & Head, 2002; Head & Marchant, 2014).

3. Methods

We performed (i) geomorphological observations, implemented with morphometric analyses where applicable (see Table 1), and (ii) cluster and fractal analyses. We aimed to produce an exhaustive investigation on mound morphologies and distributions estimating if the phenomena involved are shallow or cover significant depths, in order to step ahead in the understanding of the link between the observed surface expressions and the potential deep processes.

3.1 Geomorphological observations and morphometric analysis

The geomorphological observations were performed only on CTX (MRO) images in order to produce a comparable mapping on the three areas. In this respect, we designated as features of interest topographically positive mound-shaped features that showed circular or elliptical base (coalescent mounds-like features included) above 100 m of diameter. Mosaics of a hundred CTX images were produced by means of Pilot software (pilot.wr.usgs.gov). HiRISE (High Resolution Imaging Science

Experiment on board the Mars Reconnaissance Orbiter mission, resolution 0,25 m/pixel) images were consulted, when available, to enhance the observation of the mounds' morphological details, although, HiRISE images were never used to map the mounds. Analyses of the CTX image mosaics were performed within ArcGIS® software using sinusoidal projections centered in each area in order to minimize spatial distortions. CTX images may show enough overlap to allow the generation of stereo-derived DTMs.

Suitable images were identified only in the regions of Utopia and Hellas basins, respectively: B19_017128_2108_XI_30N262W (5.79 m/pixel resolution), B19_017062_2108_XI_30N262W (5.93 m/pixel resolution) with 21.1° of convergence and D19_034654_1451_XI_34S299W (5.88 m/pixel resolution), G21_026439_1435_XI_36S299W (5.40 m/pixel resolution) with 10.8° of convergence. ISIS 3 (Torson & Becker; 1997) software suite and Ames Stereo Pipeline (Shean et al., 2016; Moratto et al., 2010) were used for image processing, calibration and stereo matching and DTM generation. All raw CTX images underwent a pre-process that included radiometric calibration, destriping and spice kernels attachment in order to correctly locate them onto the Martian surface. Bundle adjustment of each stereo couple was a key procedure before stereo matching. All the potential errors on the DTM that could affect the internal consistency of features and slopes due to mistaken camera pointing and satellite position are iteratively minimized by analyzing the shift of the retro-projection of the pixels constituting the surface (Moratto et al., 2010). The 3D point cloud then obtained by the stereo matching is then aligned onto MOLA PEDR shots to correct possible shifts in height and displacements. The point cloud was then sampled in a raster DTM with 18 meters post spacing and the height values adjusted according to the Martian areoid. Height-to-Diameter ratios are then extrapolated from DTMs. CTX images allow the identification of the maximum and minimum axes of the ellipses that describe the mound bases. Two profiles for each mound were produced on DTMs, in ArcGIS® environment, along the principal axes; height and base diameter were therefore measured twice on each mound and averaged before the ratio calculation (see Table 1).

Utopia			Hellas		
Ellipse ratio	Description	Mean H-to-D	Ellipse ratio	Description	Mean H-to-D
1,18	circular	0,061	1,35	slightly elongate	0,058
1,23	slightly elongate	0,057	1,46	elongate	0,043
1,12	circular	0,049	1,00	circular	0,015
1,00	circular	0,039	1,00	circular	0,013
1,22	slightly elongate	0,052	1,28	slightly elongate	0,027
1,47	elongate	0,026	1,00	circular	0,008
1,20	circular	0,025	1,71	very elongate	0,023
1,50	elongate	0,060	1,58	elongate	0,025
1,17	circular	0,029	1,56	elongate	0,029
1,89	cleft/coalescent cone	0,042	1,30	slightly elongate	0,024
1,42	elongate	0,037	1,98	very elongate	0,026
1,42	elongate	0,043	1,92	very elongate	0,026
1,21	slightly elongate	0,043	1,00	circular	0,017
1,33	slightly elongate	0,057	1,80	cleft/coalescent cone	0,032
1,60	elongate	0,045	1,35	slightly elongate	0,040
1,00	circular	0,058	1,39	slightly elongate	0,014
1,00	circular	0,041	1,29	slightly elongate	0,027
1,00	circular	0,066	1,00	circular	0,016
1,71	very elongate	0,054	1,41	elongate	0,013
1,11	circular	0,066	1,43	elongate	0,045
1,55	elongate	0,026	1,10	circular	0,029
1,38	slightly elongate	0,043	1,59	elongate	0,037
1,36	slightly elongate	0,052	1,04	circular	0,033
1,00	circular	0,055	1,68	very elongate	0,049
1,33	slightly elongate	0,042	1,47	elongate	0,018
1,43	elongate	0,038	1,45	elongate	0,035
1,66	very elongate	0,026	1,40	elongate	0,014
1,00	circular	0,048	1,00	circular	0,034
1,25	slightly elongate	0,010	1,00	circular	0,031
1,10	circular	0,039	1,52	elongate	0,029
1,03	circular	0,040	1,00	circular	0,029
1,37	slightly elongate	0,043	1,00	circular	0,017
1,69	very elongate	0,050			
1,38	slightly elongate	0,041			
1,16	circular	0,047			
1,55	elongate	0,058			
1,42	elongate	0,051			
1,05	circular	0,043			
1,27	slightly elongate	0,064			

Table 1. Ellipse ratio, associate description and mean Height-to-Diameter measured for each mound in the samples

3.2 Clustering and Fractal Analyses

The analysis of spatial distribution of vents and/or fractures on rocky and icy planetary surfaces is crucial to infer the distribution of the parent network of connected fractures in the subsurface and the possible linkage with the fluid source (Mazzarini, 2004; Mazzarini & Isola, 2010; Le Corvec et al., 2013; Pozzobon et al., 2015; De Toffoli et al., 2018). Indeed, fracture length and distribution control the overall permeability of the system. The percolation theory quantifies a critical fracture density threshold that

defines the limit above which the fracture network is connected (Mazzarini & Isola, 2010 and references therein). When the fracture system is actually percolating, as it seems to be in the case of this study, then the network shows self-similarity in a specific length range, i.e. the network is scale-invariant and, accordingly, it shows similar characteristics at any magnification degree within the specific range of existence that will be following discussed (Mazzarini & Isola, 2010). Fractal analysis is already recognized as a valid technique to be applied to mud volcanoes on Earth (see Bonini & Mazzarini, 2010 where mud-prone source layers depths have been correctly identified in the Azerbaijan province) and on volcanoes vents on Mars (Pozzobon et al., 2015 provides insights on the application of the method to estimate the depths of the magmatic reservoirs). Such analysis evaluates the scaling properties of the fracture systems following two steps: (i) investigation of mound distribution and (ii) spatial properties. The fractal analysis allows thus the identification of clusters of fracture networks that show scale-invariance.

Step 1. Clustering of mounds was detected computing the coordinates of all the vents in MINITAB® software and applying an agglomerative hierarchical clustering method (Mazzarini, 2004). The coordinates used for the analysis were extrapolated by sinusoidal projections of the surface of Mars centered on the observed area, for this reason the procedure was separately repeated for each area.

Step 2. The spatial properties (i.e. how fractures or vents fill the space) of fractures in the subsurface beneath the mound fields is derived by applying self-similar clustering analysis. The fractal behaviour of fracture networks is defined over a range of lengths whose thresholds span between a lower (Lower cutoff, L_{co}) and an upper (Upper cutoff, U_{co}) limits (Bonnet et al., 2001; Mazzarini & Isola, 2010). U_{co} is the high interest parameter that has to be investigated herein, because it scales as the maximum thickness of the fractured medium (Mazzarini & Isola, 2010). The size range is bound within the lower and upper cutoffs, as mentioned above, and it is detectable as a linear fit (a plateau) comprised between the L_{co} and U_{co} in a local slope ($\Delta \log(C(l))/\Delta \log(l)$) vs. $\log(l)$ diagram (Fig. 2; Walsh & Watterson 1993).

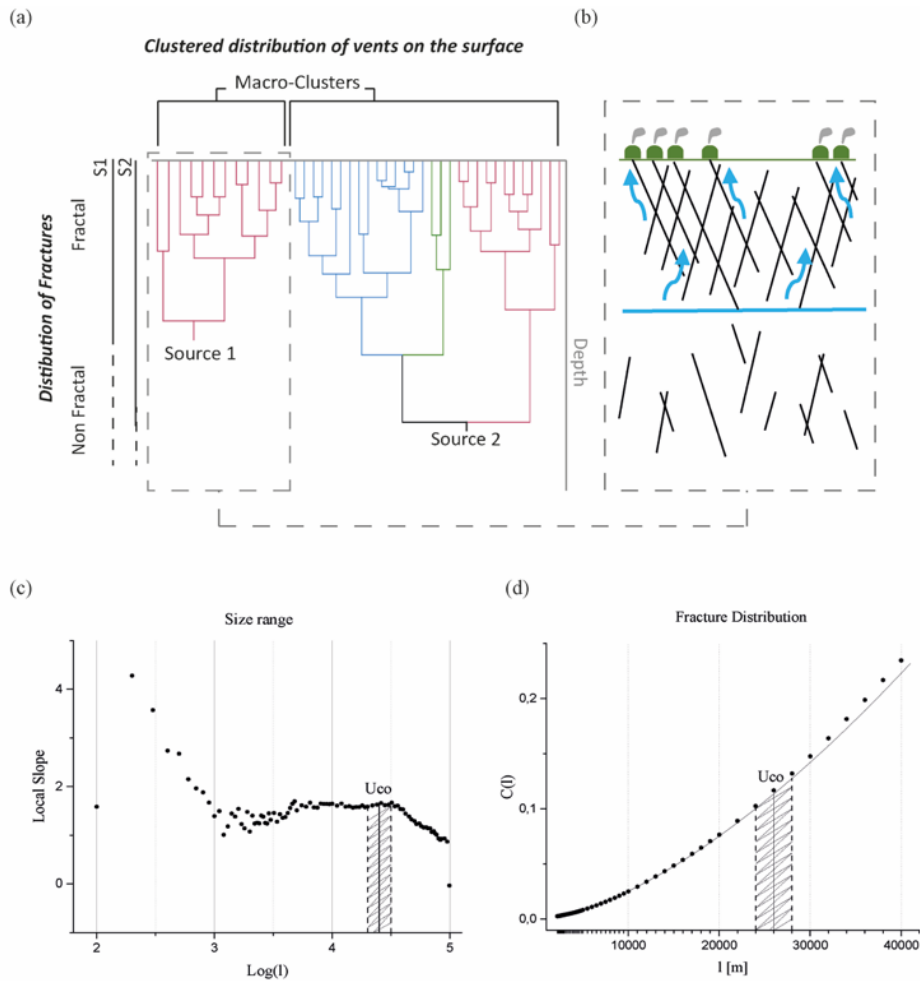


FIG 2. Sketches (a) and (b) schematically represent how the cluster distribution of vents on the surface develops with depth. (a): Natural systems show clustered distribution of vents at all scales; macro-clusters are clusters big enough to allow the reservoir depth estimate. (b): Fluid accumulations in the subsurface (blue line) could be pushed to the surface by buoyance forces; the resurgence process can crack the medium generating a network of connected fractures, thus showing fractal distribution, up to the surface where seepage vents (green mounds) can be observed. Graph (c) displays the size range of interconnected fractures represented by the plateau stage of the curve.

Where the slope breaks the fractures distribution stops to be fractal. The corresponding $\log(l)$ value

coincides to a specific maximum thickness of the fractured medium that connects the surface to the subsurface (U_{co}). Graph (d) shows the variation of fractures distribution compared to the Power Law (solid line). Here the goodness of the U_{co} picking in the previous graph is tested. Fractal distribution follows the Power Law, where data matches the solid line the distribution of fractures/vents is fractal. In the displayed case, for values shallower than the detected maximum length the data matches the Power Law, for higher values the data trend detaches. [l : fractures length; $C(l)$: correlation integral defines the correlation between point at a distance lower to l ; *Local Slope*: represents the $\Delta \text{Log}(C(l))/\Delta \text{Log}(l)$ ratio]

The Uco (upper cutoff) is thus defined by the maximum value of the size range, defining the hypothetical maximum fracture length in the system that directly connects the deep fluid reservoirs to the surface; i.e. Uco (the highest plateau breaking point) value represents the maximum extension of the pipeline, that is the depth of the fluids source (Mazzarini & Isola 2010; Pozzobon et al., 2015 and references therein). The goodness of the Lco and Uco picking was estimated on the determination coefficient (R^2) maximum values, defined as the proportion of data variability in the Lco-Uco interval. R^2 is defined as shown in equation (1)

$$R^2 = 1 - \frac{SS_{res}}{SS_{tot}} \quad (1)$$

where SS_{res} represents the residuals sum of squares, which is meant to be minimized in proportion to the normalization coefficient SS_{tot} (total sum of squares) in accordance to the order of magnitude involved in the calculation. We detected the depth range corresponding to the higher values of R^2 , thus describing the values of best-fit for the Upper cutoff selection. The error of the measure was estimated calculating the half-difference between the maximum and the minimum depths where the R^2 shows the best-fit value.

In the specificity of the case studies herein, mounds have been mapped since intrinsically representative of resurgences through fractures of migrating fluids. They are indeed recognizable as localized venting spots and not diffused homogenous seeping areas (Fig.3 and Fig.6). Accordingly, this means that: (i) those areas have surely experienced some kind of fluid flow that delivered materials across the fractured medium and (ii) relying on the vent distribution is equivalent to relying on the parent fractures’.

In order to produce meaningful estimates, the sample size effect needed to be taken into account. As a rule of thumb, at least 50 samples are required to extract robust parameter estimates (Clauset et al., 2009) and, in accordance, in our study the number of observed mounds spans between a minimum of 62 to a maximum of 1383 per single cluster. Indeed, a number of observations greater than this threshold, endure a robust estimate of the fractal distribution parameters. Mazzarini and Isola (2010) showed that removing a random sample of 20% of the vents from large (i.e. > 200 vents) datasets does not affect the estimation of the fractal exponent (less than 0.01% of variation) and the error introduced into the estimation of the cut-offs is less than 1%–2%.

In Mazzarini et al. (2013) the effect of uncertainties in point (mound) locations has been tested by adding random errors (in the 0–100 m, 0–300 m and 0–500 m ranges) to the sampled points. In this test, the added errors were as high as five to twenty-five times that of the coarsest image resolution used to locate vents. The 0–100 m errors generate fractal exponent and cut off value identical to those computed for the original dataset.

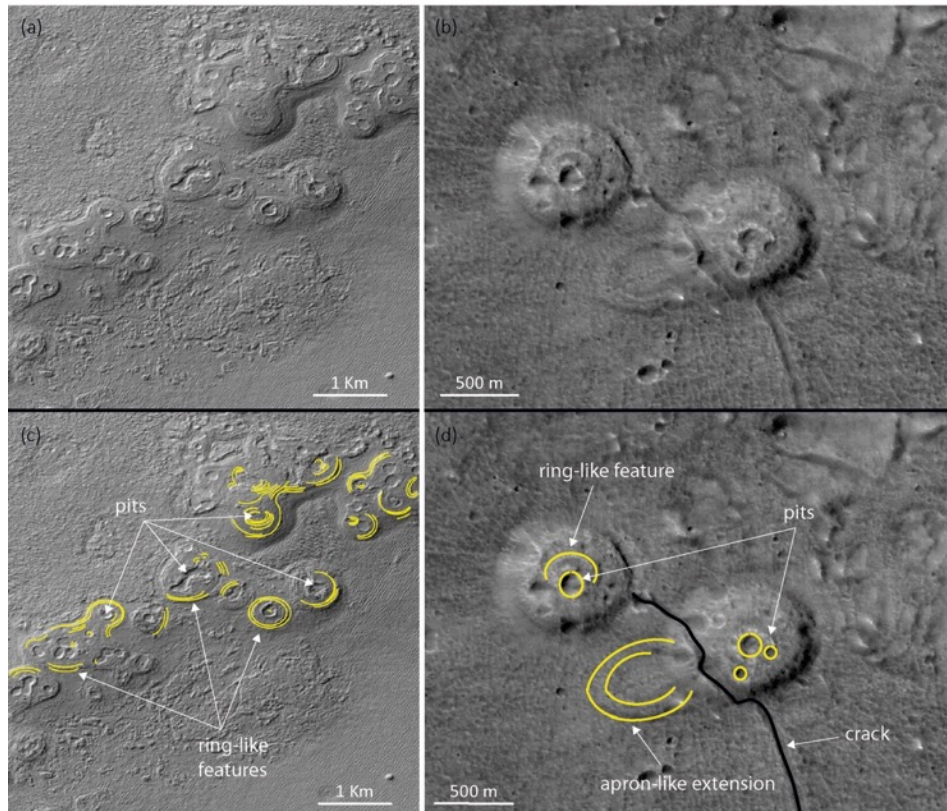


FIG 3. Original (a, b) and interpreted (c, d) CTX images of Martian mounds. The mounds in captures (a) and (c), from Hellas basin (61°38' E 42°9' S; 19_008295_1387_XI_41S298W), well display ring-like features spreading concentrically around the central pits. The mounds in captures (b) and (d), from Utopia region (96°16' E 31°41' N; D02_028165_2120_XI_32N263W), are in relationship with a well-visible crack; in addition, the mound on the right has an apron-like flow extending over the mound and the surrounding plain morphologically similar to the ones reported in Fig.5

In the case of 0–500 m random errors, the resulting fractal exponent is 3% higher than that computed for the original dataset, and the cut offs are very similar to those computed for the original dataset. Accordingly, we performed analyses on clusters exceeding the precautionary value of 60 units where the accuracy of the method is

guarantee for datasets larger than 50 units to keep the error on the scaling parameter smaller than 1%.

The combined application of these methods of image analysis and interpretation and spatial distribution allowed us to obtain the following results.

4. Results

4.1 Geomorphological observations and morphometry

The mounds mapped herein amount to a total of 1745 in Hellas basin, 2094 in Utopia Planitia and 2196 in the Northern Plains region (Fig.4). The mounds are circular to elliptical structures with base diameters ranging from hundreds of meters to a few kilometres. Base shape is described through axes ratios of the basal ellipse (that were measured on 2D CTX images) according to Paulsen & Wilson, (2010) and are classified as follows: <1.2 circular, ≥ 1.2 and <1.4 slightly elongate, ≥ 1.4 and <1.6 elongate, ≥ 1.6 and <1.8 very elongate, and ≥ 1.8 cleft or coalescent mounds. Mounds in the study areas can occur as single well-defined structures; often clusters of coalescent mounds or short alignments of mounds are observed, both patterns can occur associated with fractures or swarms of impact craters.

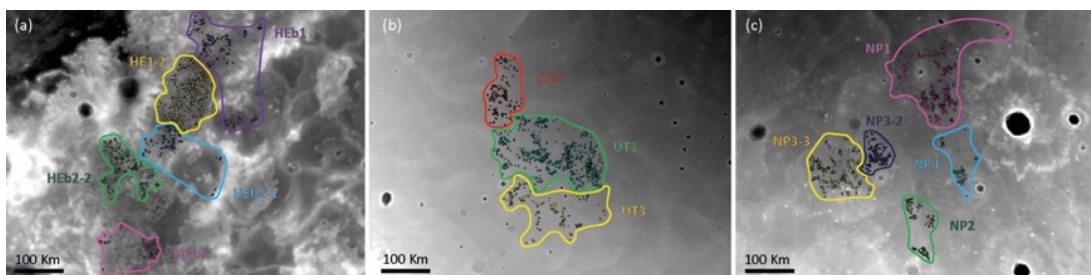


FIG 4. Distribution of mounds and clusters in (a) Hellas basin, (b) Utopia basin and (c) Northern Plains region (USGS MOLA-based topography in the background)

The majority of the mounds have well recognizable central pits and, especially in the Utopia Planitia field, mounds may show multiple distal pits. Many mounds have well visible concentric ring-like features (Oehler & Allen, 2010) on their topmost part proximal to the central pit, and, less commonly, along the base. In Hellas basin, ring-like features are pervasively common to almost all the detected mounds, while in Utopia and the Northern Plains they may appear blurred or not present. Other detected

flow-like features are aprons extending from the mounds tops to the surrounding plain (Fig.3 and Fig5). Surface albedo is a good discerning trait in the Northern Plain region where mound albedo is clearly higher compared to the surrounding area, making the mounds brighter than the plain. In the other study areas, high albedo mounds are less common and albedo is generally equal for mounds and plains (Fig.6).

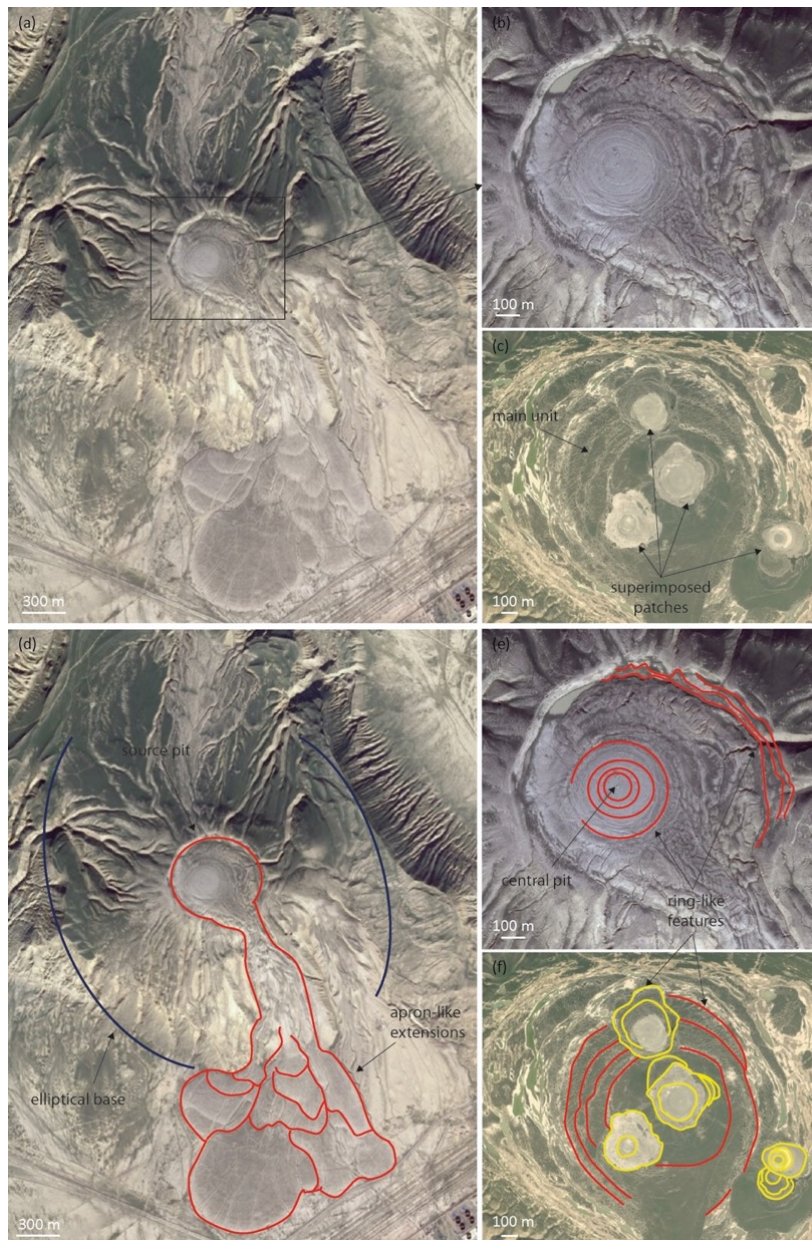


FIG 5. Original (a, b, c) and interpreted (d, e, f) images of terrestrial mud volcanoes from the Azerbaijan region. Qaraqus Dagi mud volcano (a, d) shows apron-like mud flows extending over the mound and the surrounding plain; in the magnification (b, e) of its source portion concentric ring-like flow features mark different mud eruption inputs. In captures (c) and (f) is displayed a flat top mud volcano with concentric structures both on the overall feature and on the superimposed patches (Oehler and Allen, 2009)

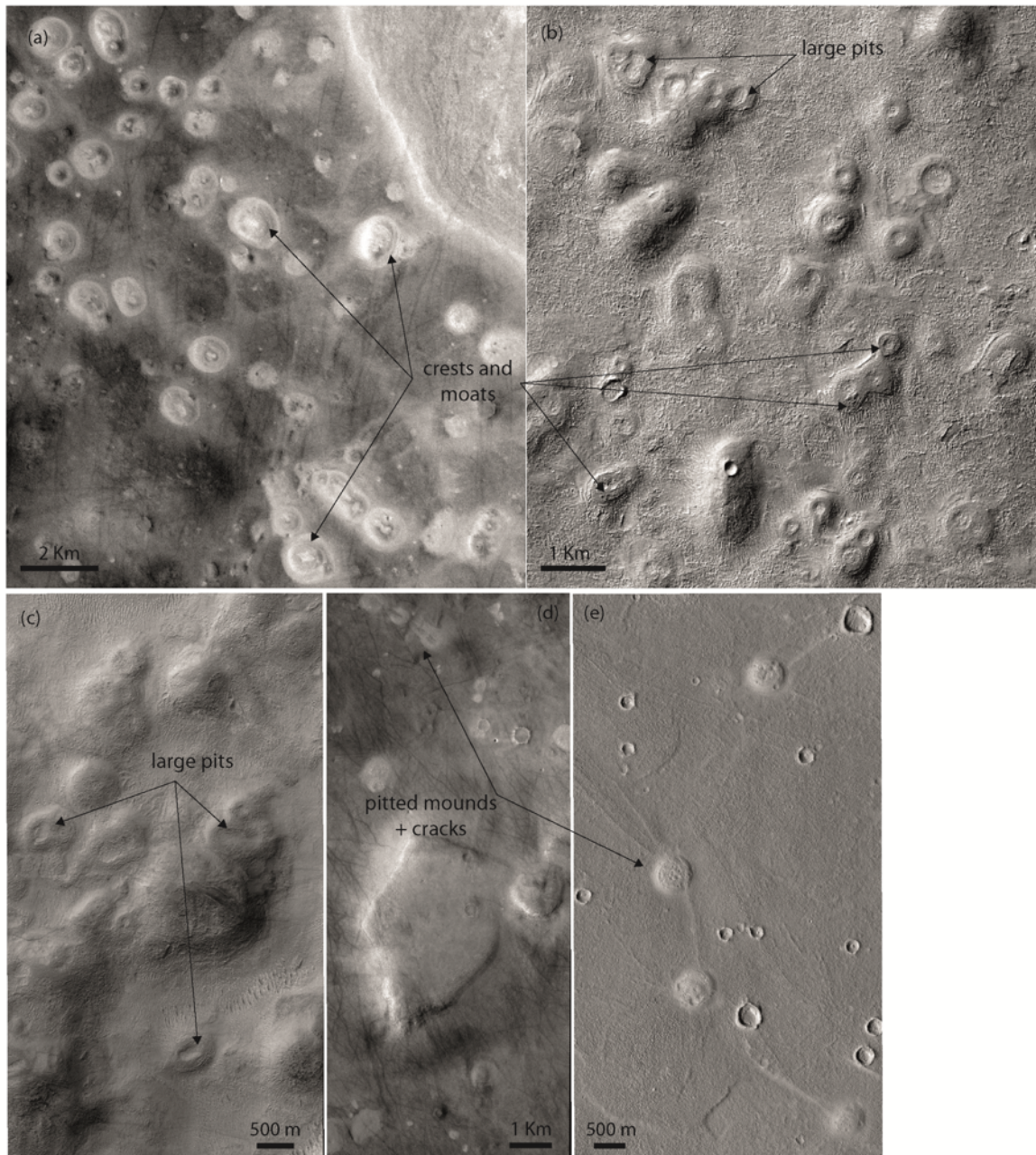


FIG 6. CTX medium resolution images of mounds from the (a) Northern Plains ($54^{\circ}32' \text{ E } 58^{\circ}42' \text{ N}$; B19_016892_2400_XN_60N305W) and (b) Hellas ($61^{\circ}7' \text{ E } 39^{\circ}22' \text{ S}$; P19_008295_1387_XI_41S298W) and HiRISE high resolution images from (c) Hellas (ESP_025740_1370), (d) the Northern Plains (PSP_009086_2360) and (e) Utopia (ESP_042723_2165) regions. Widely recognizable key characteristics are round shape of the base, summit pits, crests and moats concentrically distributed around the pits. Additionally, in image (a) brighter albedo compared to the surrounding plain is well recognizable; in images (b) and (c) some mounds are characterized by large pits that appear like central apical concave depressions; in images (d) and (e) pitted mounds are associated to cracks

Mounds show flat shapes that may appear like flat-topped or domes, depending on the flattening grade estimated on slope angles (a mound is defined as flat-topped when slope angles do not exceed 5°) according to Kopf, (2002), alternatively with summit pits of variable dimensions, not always recognizable in the topographic profiles, or rarely with summit wide concave depressions (Fig.6b and 6c).

Morphometric measures were performed on available samples of mounds included in the areas covered by the DTMs, that is to say 31 mounds in Hellas region and 39 in Utopia Planitia. After Komatsu et al. (2016), three different morphometric classes have been subdivided according to Height-to-Diameter ratios and morphological traits:

(i) type 1

morphologically distinct by cone shape, smooth or hummocky surface and circum-pit layers; 0.071-0.100 H-to-D ratios, which correspond to diameter range spanning between 2100 – 3000 m and height range of 150 – 300 m

(ii) type 2

characterized by “shield-like” shape, lobate flow-like features, single or multiple pits with perimetral concentric layering; 0.003-0.044 H-to-D ratios, which correspond to a diameter range of 900 – 2900 m and height range of 10 – 40 m.

(iii) type 3

defined as circular, steep sided mounds with flat top area; 0.075-0.143 H-to-D ratios which correspond to diameter range spanning between 420 – 800 m and height range of 40 – 60 m.

Measured averaged Height-to-Diameter ratios of our samples span between 0.008 and 0.058 with a mean value of 0.027 in Hellas (raw measures: diameter range between 120 – 2000 m, height range between 5 – 65 m) basin and between 0.010 and 0.066 with a mean value of 0.045 in Utopia (raw measures: diameter range between 250 – 1150 m, height range between 5 – 45 m). Very slight differences are detectable in non-averaged ratios, which values span between 0.007 and 0.071 and between 0.009 and 0.075 respectively in Hellas and Utopia basins (Fig.7 and Table1). Hence, measured and state-of-art ratios belong to the same order of magnitude, particularly close to the shield-like shape of type 2 and are independent from the flattening of the base shape.

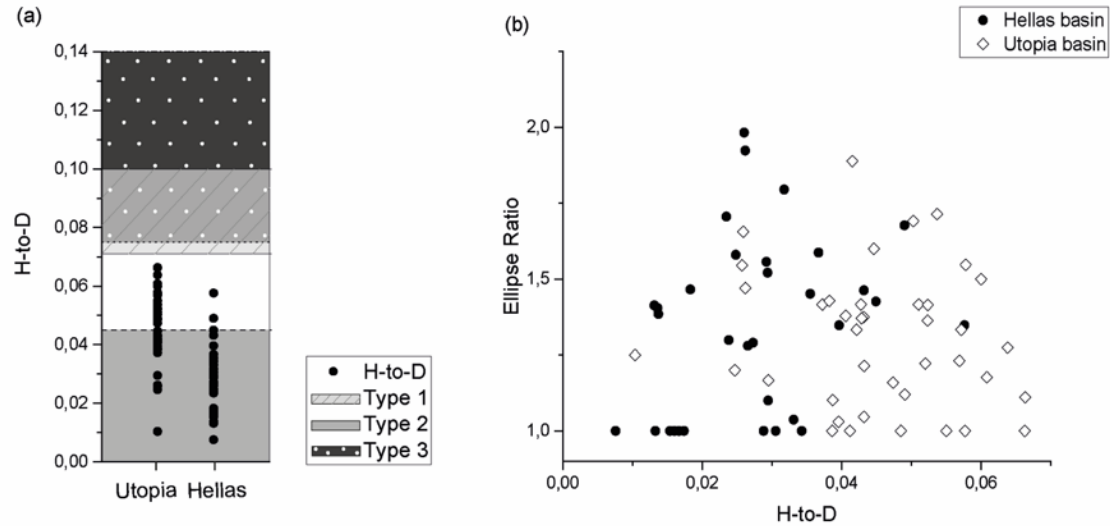


FIG 7. (a) Sample mounds' Height-to-Diameter ratios are plotted on a background displaying the ratio ranges for the three different types described by Komatsu et al. (2016). (b) H-to-D are plotted against ellipse ratios and no visible correlation occurs between base shape and mound profile

4.2 Clustering and Fractal analyses

Clustering was performed on the mapped mounds to delimitate groups of vents that could more likely be linked to the same fracture system. To avoid excessive clustering, that might lead to a non-representative cluster analysis, we chose four clusters for each field. To optimise the analyses, this procedure needed to be coupled with further sub-clustering steps in some of the areas. The Upper cutoff identification for each cluster was derived from *local slope* *v.* $\log(l)$ and $C(l)$ *vs.* $l(m)$ diagrams used for both Lco and Uco picking (Fig.2). The correct selection of the cutoffs was performed identifying the wider size range with the highest correlation between $\log(l)$ and the *local slope* values (Mazzarini, 2004). Accordingly, results of the picking procedure for the Utopia basin mound clusters are 14 ± 2 km (cluster Ut1), 10 ± 1 km (cluster Ut2) and 18 ± 5 km (cluster Ut3). The Northern Plains mound field analysis produced clusters Np1, Np2, Np4 and sub-clusters Np3-2 and Np3-3 that gave back values of the fractured medium thickness between 4 and 20 km. Hellas basin mounds clustering allowed the identification of one outlier cluster (He1-2) located at an extremely large depth (35 ± 3 km) compared to all the others. Beside it, four meaningful clusters were detected: He-b1 with a maximum fractured medium thickness of 15 ± 3 km; He-b2, that was split into two different sub-clusters, output He-b2/1 with 17 ± 1 km depth and He-b2/2 with 24 ± 4 km; and He-b3 with fractured

medium thickness of 16 ± 4 km. Fractal analysis outputs of the other clusters, belonging to Utopia and the Northern Plains study cases, were too noisy making it impossible to perceive any distribution pattern. For this reason, no further deductions can be made out of this group of data. The summary of the obtained results is reported in Fig.8 (aqueous solution cryosphere data are reported after Clifford et al. (2010)).

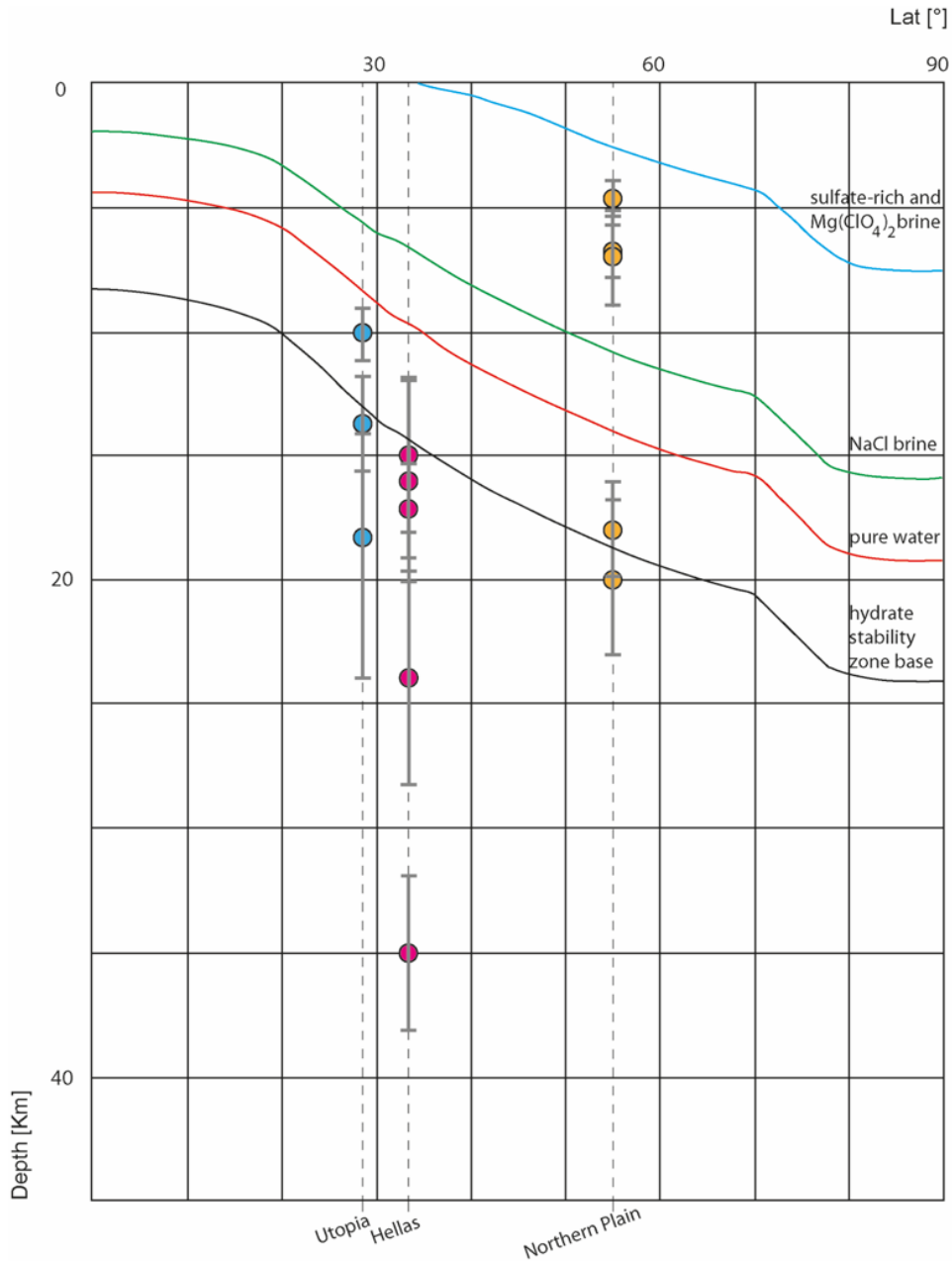


FIG 8. Latitudinal variation in depth of a hydrate-rich cryosphere for three different groundwater freezing temperatures: 203°K: sulfate-rich and Mg(ClO₄)₂ brine (blue line); 252°K: NaCl brine (green line); 273°K: pure groundwater (red line); 303°K: base of the gas hydrate stability zone (black line); assumed heat flow is 15 mW m⁻² (from Clifford et al., 2010). Colored marks represent calculated maximum thicknesses of the reservoirs for Hellas (pink), Utopia (blue) and the Northern Plains (yellow) region

5. Discussions

In order to understand the mechanisms that originated these mound fields, it is necessary to undertake a comparison between the Martian features to the closest terrestrial counterparts. In the case of this work, we tested morphologically similar features such as mud volcanoes, pingos and magmatic volcanoes analogues aiming to settle agreement on the three major interpretations of the mounds (e.g. Lanagan et al., 2001; Balme & Gallagher, 2009; Burr et al., 2009; Brož & Hauber, 2013).

5.1 *Testing mud volcano analogue hypothesis*

The mud volcanism hypothesis is crucial to be tested, in fact the identification of such kind of features would be relevant to astrobiological purposes due to their close relationship with liquid water and the degassing phenomenon, specifically concerning the methane release (see the introduction chapter). Mud volcanoes can present different appearance, shapes and dimensions depending on the properties of the erupted material, the conduits dimensions and abundance (Kopf, 2002), the amount of involved material and gravity, that on Mars is around one third ($3,711 \text{ ms}^{-2}$) of the Earth. Therefore, a certain variability among mud volcano populations is reasonable to be detected depending on the geologic, tectonic and environmental context of the hosting region and planet. In this study we focused on Martian areas that display comparable characteristics and potentially underwent similar processes throughout the geological time (i.e. large impact basins that could have hosted large bodies of water during wetter periods) in order to have a uniform context and minimize the natural differences within our samples of mounds.

Firstly, the analogue hypothesis testing was carried out comparing the morphological distinctive traits of terrestrial and Martian mud-volcano-like mounds that have been exhaustively investigated by several authors in the regions of Acidalia and Chryse Planitiae (e.g. Oehler & Allen, 2010; Komatsu et al., 2016; Oehler & Etiope, 2017). Accordingly, many of the morphological traits detected in the Hellas, Utopia and Northern Plains fields point to mud volcanoes as best terrestrial analogue (Fig.3 and Fig.5). The considered characteristics are listed below moving from the descriptive ones to the quantitatively measurable ones:

(i) *Surface morphologies*

The majority of the mounds we observed showed summit pits and, in some cases, peripheral pits or craters although some rare cases of non-pitted mounds were also detected. We identified several flow-like features, such as apron-like extensions, and concentric annular structures that are widely present among the mound populations. All these traits, especially if combined together, suggest an eruptive activity that generate typical observable morphologies of mud volcanoes edifices in both terrestrial and Martian settings (e.g. Hovland et al., 1997; Oehler & Allen, 2010; Okubo, 2016).

(ii) *Albedo*

Albedo depends on the nature of the extruded materials and in the cases of our regions albedo are equal or higher than the surrounding plains. This trait matches previous collected data on other proposed mud volcanoes described by Skinner & Tanaka, (2007) and Oehler & Allen, (2010).

(iii) *Base shape*

Majority of the mounds displayed sub-circular shapes, but we also detected elliptical mounds. Many coalescent mounds were observed in all the regions (Paulsen & Wilson, 2010).

(iv) *Diameter of the mounds*

Mound diameter averages ~600 m but it can vary by up to few hundreds of meters. This is fully comparable with terrestrial and other Martian mud-volcanoes-like mounds which are typically few hundred of meters in diameter with minimum and maximum sizes that can span a few meters to kilometers, depending on the eruption rates and speeds, properties of conduits and erupted materials and the subaerial or subaqueous environment of formation (e.g. Kopf, 2002; Martinelli & Judd, 2004; Judd & Hovland, 2007; Oehler & Allen, 2010; Fryer, 2012).

(v) *Height of the mounds*

Heights were measured on the samples of mounds included in the areas covered by DTMs. Collected data display heights typically around 20-30 m, but never exceeding few tens of meters in agreement with other studies of similar mounds on Mars (e.g. Kopf, 2002; Farrand et al., 2005; Oehler & Allen, 2010; Komatsu et al., 2016).

(vi) *Height-to-Diameter ratios*

Morphometric analysis revealed similar ratios between Chryse mud volcanoes and the studied mounds. Mounds in Hellas and Utopia show aspect ratios converging with

type 2 H-to-D ranges along with coinciding associate key morphologies (Komatsu et al., 2016). Part of the mound population (around 50% of the sample in Utopia and less than the 10% in Hellas) whereas displays H-to-D ratios that slightly exceed that type 2 maximum limit (Komatsu et al., 2016), anyway they do not reach the minimum values recorded for the other two types (sharing very similar minimum limit value).

We then tested the mud volcano hypothesis by implementing the results derived from the fractal analyses that allowed us to overcome the issue derived from morphological convergence with other features. The three study areas we herein describe are large enough (~90.000 km² each) to be considered reasonably unaffected by significant local variations that can influence the putative subsurface ice and water distribution such as exposure to the sun or thermal and hydraulic properties of the crust (Clifford et al., 2010). Ice and water distribution is indeed a crucial aspect to be taken into account while testing the mud volcanism hypothesis. In fact the cryosphere is a natural water trap in the subsurface and groundwater persists as liquid phase when its inventory exceed the actual pore volume of the cryosphere leading to an accumulation of water in the lower portion of the crust. Alternatively, groundwater could be just transiently produced by thermal alterations of the crust (Clifford, 1993; Clifford et al., 2010). In our case study, the considered regions are as well representative of different latitudes and hemispheres, all situated in low topographic areas where an actual physical contact between the cryosphere base and the groundwater reservoir is likely to be present in the subsurface, whether the H₂O inventory is sufficient (e.g. Clifford, 1993; Clifford & Parker, 2001; Clifford et al., 2010). An additional tapering of the cryosphere layer could be induced by such a contact due to combination of freezing point depressing through high salinity fluid circulation and low temperature convection of groundwater (Travis, 2003; Travis & Feldman, 2009; Clifford et al., 2010; Travis et al. 2013). Hence, we undertake a meaningful comparison between our calculated extensions of fracture networks and the depths of isotherms describing the behavior of putative different brines in the Martian subsurface, hypothesized on global scale by Clifford et al., (2010), and we find a correlation between our resulting thicknesses of fractured medium involved beneath the mound fields and the hydrate-rich cryosphere stability zone (Fig.8 and Table 2). The basal limits of the cryosphere, displayed in Figure 8 by different lines in function of brines salinity, are representative of the best-insulated scenario modelled by Clifford et al., (2010), i.e. describing the shallowest calculated position of the isotherms marking the transition from solid to

liquid phase of the brines. In fact, the authors assumed the maximum realistic porosity ($\Phi = 0.35$ at the surface and follows the exponential decay relationship of Clifford, (1993) in the subsurface), a low thermal conductivity value ($0.5 \text{ W m}^{-1} \text{ K}^{-1}$) of the crust and a cryosphere fully saturated of gas-hydrates instead of water-ice. Astronomically induced variations are also described in Clifford et al., (2010) but, since they are estimated to have affected the cryosphere depth just of few hundred of meters in equatorial and polar positions, these parameters are neglected in this work. Accordingly, the comparison between these data and the new insights provided by this work shows that a relationship exists between the maximum depths (U_{co}) we calculated and the depths of the putative cryosphere-hydrosphere transition.

Cluster ID	n° vents	Lco [Km]	Uco [Km]	D
Hellas				
1-2	842	2 ± 0.5	35 ± 3	1.6345
b1	308	1.2 ± 0.1	15 ± 3	1.2503
b2-1	260	3.2 ± 0.2	17 ± 1	0.9095
b2-2	275	2.2 ± 1.5	24 ± 4	1.3091
b3	62	3.3 ± 0.1	16 ± 4	1.2784
Utopia				
1	1383	1.1 ± 0.1	14 ± 2	1.3148
2	436	1.2 ± 0.1	10 ± 1	0.9429
3	272	2.1 ± 0.1	18 ± 5	1.1005
Northern Plains				
1	676	1.5 ± 0.1	6.5 ± 2	1.4944
2	214	0.8 ± 0.1	4.5 ± 0.5	1.2383
3-2	323	1.6 ± 0.1	18 ± 2	1.5793
3-3	592	0.8 ± 0.1	6.5 ± 1	1.2222
4	143	1.8 ± 0.1	20 ± 3	1.0104

Table 2. Details of the meaningful clusters plotted in Figure 8

Specifically, it is to be noticed a strict correlation between the U_{co} of clusters Ut1, He-b1, He-b-3, Np3-2, Np4 and the gas hydrate stability zone base hypothesized for an average present-day Martian heat flow. In the regions of Utopia and Hellas the U_{co} of clusters Ut3, He-b2/1, He-b2/2 and He1-2 are estimated to be located below the gas hydrate stability zone base meaning that the fracture systems connected with the surface are spreading underneath that limit. Nevertheless, in Figure 8 is displayed the shallowest cryosphere base estimate and if variations of porosity and/or thermal conductivity and/or ice/clathrate content occur it is reasonable to be forecasted a shift of the isotherms of a few kilometers (Clifford et al., 2010). Accordingly, Ut3, He-b2/1 and Heb-2/2 U_{co} locations can be legitimately considered sitting at depth where the cryosphere base can actually be present. Nevertheless, the correlation might be evaluated weaker than the previously mentioned clusters. In the case of He1-2 U_{co} a

different interpretation is to be considered because its location spans between 33 and 43 km below the surface, an exceptionally greater depth compared to all the other Uco detected in the three areas and far below the cryosphere stability zone base estimate. Vents belonging to cluster He1-2 do not show any significant morphological difference with the other mounds, leading us to suppose that no substantial differences occur in the formation process of the mounds, but they are clearly the expression of a different conformation of the subsurface fracture systems, possibly involving ancient extensively distributed fractures related to the original impact that generated the Hellas multi-ring basin structure. Depths of excavation for such large basins are estimated from the inner diameter of the rugged annulus. Since Hellas show an average diameter of 1500 km, this rough estimate suggest that this basin may have excavated from ~38 to 150 km according to the different hypothesized models (Schultz & Frey, 1990 and references therein; McGowan & McGill, 2010; McGowan, 2011). Hence, the fracture system extension observed underneath cluster He1-2, that is to say the fracture systems that fluids exploited during the up-flow, could be assimilated to a pre-existing damaged zones linked to the initial excavation of the basin. In Utopia and Northern Plains regions we detected Uco shallower than the gas hydrate stability zone base. For the interpretation of the Ut2 cluster Uco we refer to the same argumentation carried out for clusters Ut3, He-b2/1 and He-b2/2. Differently, Np1, Np2 and Np3-3 Uco are sitting at significantly shallower locations. Two possible, not mutually exclusive, explanations can be suggested to explain the involvement of very shallow fracture systems. Firstly, since the morphology of the mounds does not appear recognizably different from the others, it can be hypothesized that these vents are the result of an older pulse of water activity beneath the surface (i.e. older enough to have happened in a “hotter” planet condition) whereas the cryosphere-hydrosphere contact is estimated to be at shallower depths due to higher heat flow. Hence in the context of this hypothesis, data would suggest that the majority of the mud volcanism (except Np1, Np2 and Np3-3, as stated above) could has been a geologically recent event in terms of planetary thermal evolution because of a stronger bound to the cryosphere-hydrosphere contact estimated for a present-day heat flow. Nevertheless, all the mounds could be coeval and such shallow systems of fractures could be representative of the path of high salinity fluid resurgences, which appear to be possibly stable in liquid phase at those depths.

Summarizing, we observed a trend of Uco locations that identify multiple clusters on the surface that have been fed from portions of a fractured medium that acted as reservoir and pipeline system located at the base of the gas hydrate stability zone. This produces a meaningful relation between gas hydrate potential distribution in the subsurface and the occurrence of mounds. This linkage leads us to suppose that the involvement of water, ostensibly as a result of gas hydrate dissociation, plays a role in the subsurface processes that potentially worked as triggers of venting, corroborating the hypothesis of mud volcanism.

In addition, we can find confirmation of the likelihood of the involvement of gas hydrate destabilization in the mounds' morphologies. As previously discussed, the morphometric analyses showed that the large majority of the mounds in our samples belong to type 2 mud volcanoes, characterized by the lowest Height-to-Diameter ratios so describing short and large top-flatted shaped mounds (i.e. flat very low elevated shape; Lance et al., 1998 and references therein). During the study of mud volcanoes located at the ocean floor offshore Barbados Island, where gas-hydrates are present, (Lance et al., 1998) this kind of flat and poorly elevated shapes were observed. The mound morphologies were related to the presence of clathrates, in fact, the porosity of the erupted material was found to have an influence on the mound shapes and different porosities were attributed to the percentage of gases extruded along with water and sediments. Specifically, high porosity was linked to top-flatted shaped mounds and low porosity was linked to a more dome shaped kind. The elevated concentration of gases in the pie shaped mud volcanoes was ascribed to the dissociation of hydrates that, due to their peculiar structure, can bear and release higher amounts of gasses compared to the melting of water ice. Hence, clathrates need to be considered also on Mars as part of the process that originated the mud eruptions since both the reservoir locations and mounds morphologies highlight a relationship between mounds and gas hydrate (for more insights on the suggested processes involved in the Barbados offshore systems refer to Godon et al. (2004) and Deville et al., (2006)).

5.2 *Testing other morphological analogues*

Mound-like morphologies alone can lead to diverse interpretations due to many factors, such as quality and quantity of the data sample or the performed investigation. Thus different interpretations have been suggested for such kind of Martian mounds

and, in accordance to these hypotheses, we tested other analogue features bringing into the appraisal the new insights we have collected by H-to-D ratio measurements, clustering and fractal analyses.

5.2.1 *Pingo analogue*

Pingos are periglacial landforms produced by the upwelling of freezing water that results in transient hill shaped morphologies. Such appearance is, indeed, due to the volume increase during the transition from liquid water, capillary up-flowing, to solid state ice close to the surface and are usually subjected to apex collapse due to the subaerial exposition and destabilization of the ice core. In our mound population typical pingo distinctive morphologies are completely missing, in fact, there is no evidence of (i) top clefts, whether single or multiple intersected clefts, instead of pits, (ii) collapse structures and (iii) irregular lobate base shape (e.g. Dundas & McEwen, 2010; Page & Murray, 2006). Moreover, the results obtained by clustering let us discard the pingo hypothesis as well. Pingos do not have a direct dependence with faults and fractures extending in the crust since they are the products of the expansion of freezing water, so a random or regular distribution of these features is to be expected. The presence of coalescent and aligned mounds, association of mounds and cracks and clustered distribution of the populations reflecting deep fracture systems cannot be reconciled with such interpretation. Due to these reasons, the pingo analogue interpretation seems improbable.

5.2.2 *Magmatic feature analogue*

Similarly, interpreting the landforms as volcanoes is to be considered unlikely. Reservoir locations singularly considered, especially the extra deep Hellas cluster case, are compatible with locations where magma chambers could be expected (e.g. Pozzobon et al., 2015), but the dataset in its entirety additionally provides evidence of the relationship with the ice-water contact that weakens the magmatic volcanism hypothesis (see Fig.8, distribution of maximum depths associated to Utopia, Northern Plains Np3-2 and NP4 clusters and Hellas clusters, excluding cluster He1-2). Based on the outcomes of the fractal analysis, an argument can be conducted against the rootless cones hypothesis as well. Rootless cones (or pseudocraters) are the products

of the interaction between water-rich substrates and lava flows which leads to an explosive interplay that generates pyroclastic cones (Thorarisson, 1953). These features are called “rootless” since they are superficial phenomena characterized by the absence of magma chambers. Distribution of rootless cones on the surface can be clustered, but their non-random arrangement is ascribed to lava pathways (Bruno et al., 2004) so fractal distribution, proven to be expressed in the study areas, is not to be expected and significantly weakens the reliability of this hypothesis. Additionally, observed morphologies do not match with pyroclastic cones. Indeed, flow features would be unfitting in this genetic context since these cones are the products of a fully explosive interaction, so no effusions are to be expected, moreover rootless cones are steep sided mounds (Noguchi et al., 2016) and, even if a certain variability has been found, the pie shapes of the herein observed mounds are distinctly different. Our work then does not provide support for magmatic volcano analogues interpretation due to the above mentioned poor reconciliation of all the collected observations and results with this group of features.

6. Conclusions and astrobiological implications

On the basis of this study we state that: (i) mud volcanoes are the best terrestrial features to consider for a comparative study with the analyzed Martian mounds and that (ii) the base of the gas hydrate-rich cryosphere stability zone is the recurrent specific subsurface environment where the phenomenon seems to be triggered and fed.

One of the *large-scale questions* that astrobiology wants to answer concerns the investigation of the possibility that life arose on other planets beyond Earth (for a complete review refer to Cockell, 2015). We approach this task by widening and improving the knowledge of environments where life could find niches to survive on planet Mars. We claim that mud volcanoes are pivotal features of interest for astrobiological investigations since they appear to be strictly linked to the two key life detection proxies, water and methane (e.g. Formisano et al., 2004; Atreya et al., 2007; Geminale et al., 2008; Mumma et al., 2004, 2009). Mud volcanoes are indeed water-related features, since during their formation liquid water is involved in the upwelling process. Secondly, these features are widely associated to the degassing phenomenon where methane, along with CO₂, is one of the most common and abundant released gasses (e.g. Kopf et al., 2002). Additionally, the detected amount of methane outgassed

on Mars (according to Atreya et al. (2007), $\sim 12,6 \times 10^1$ tons/year of CH₄ emission are needed to maintain the 10 ppb atmospheric methane reported by Krasnopolsky et al. (2004), Mumma et al. (2004) and Formisano et al. (2004) is comparable with methane expulsion estimated for terrestrial provinces rich in seep and mud volcano activity qualifying such features as good preferential degassing pathways to connect the subsurface reservoirs with the atmosphere (Etiope et al., 2004, 2011). Methane origin and nature of the reservoirs are still unclear but we suggest, by means of the presented investigation and analyses, a large scale involvement of gas hydrates in the outgassing process. Clathrates can indeed firstly act as massive storage of gasses in the subsurface (Max et al., 2011, 2013; Mousis et al., 2012, 2013), which could be released through their destabilization; secondly, clathrates can insulate the subsurface efficiently enough to produce thermal anomalies beneath that could facilitate the local cryosphere melting, so stimulating the presence of shallow groundwater, and possible paroxysmal resurgence events (Prieto-Ballestreros et al., 2006; Chastain & Chevrier, 2007; Kargel et al 2007). For these reasons, mud volcanoes are matching the interests of the ExoMars mission (<http://exploration.esa.int/mars/>) objectives linked to methane emission centers in the search for life prospective. The CaSSIS camera might indeed provide new pivotal insight on such features delivering stereo-pairs and colored images (Thomas et al., 2017) enhancing both the information on structures and morphologies of the mounds and on putative alteration zones due to effusion of deep water and materials.

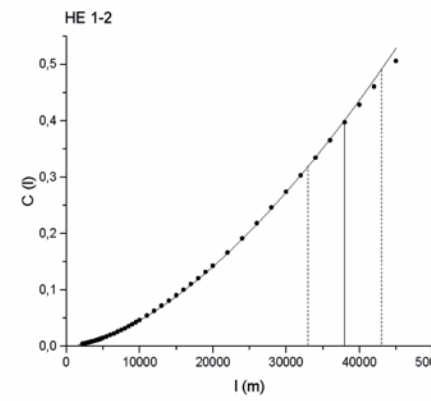
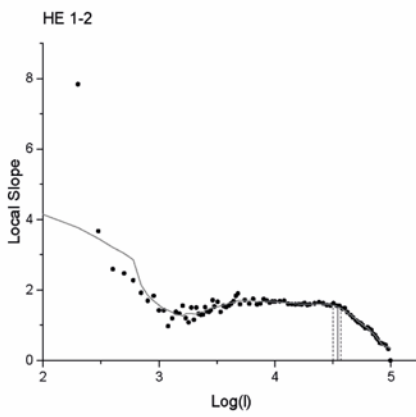
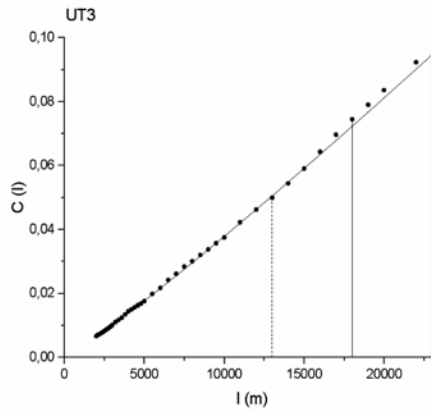
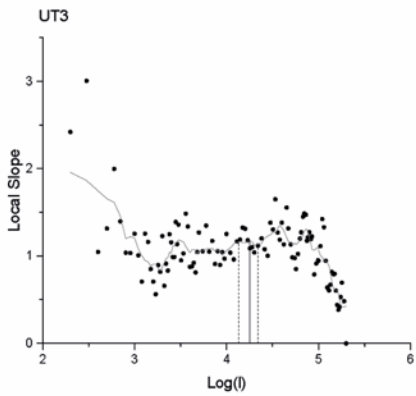
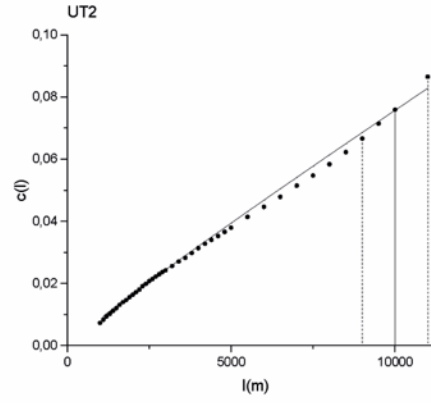
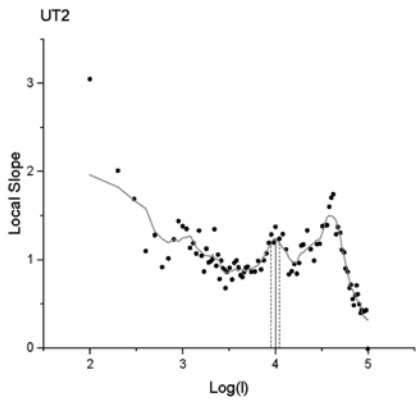
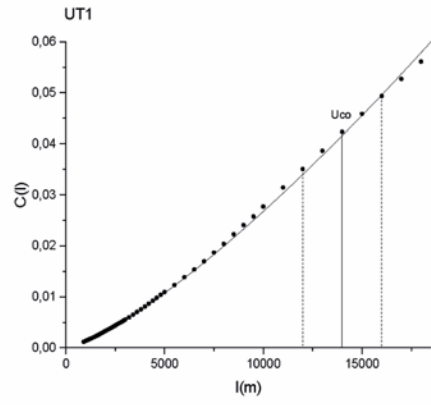
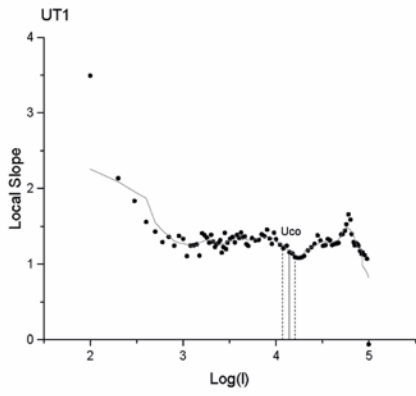
This study likewise suggests that mud volcanoes should be taken into account for further astrobiological investigations due to their observed relationship with water, in the form of gas hydrates-water interface, that seems to lie at the origin of this phenomenon. Furthermore, these mud volcanoes erupted material from depths that are still not reachable by our present-day instrumentations making them a unique chance to study what is stored several kilometers beneath the surface. Mud volcanoes eruptions could have thus sampled and brought to the surface, along with the sediment and fluid mixtures, clues of a putative extinct or extant deep biosphere. Indeed, on Earth, a large variety of colonies of microorganisms, widely recognized and studied in terms of Martian habitability, live in the deep subsurface and extreme environments (for an overview see Atreya et al., 2007; Gainey & Elwood Madden, 2012; Cockell, 2014; Cockell et al., 2012; McMahon & Parnell, 2014; Preston & Dartnell, 2014) and

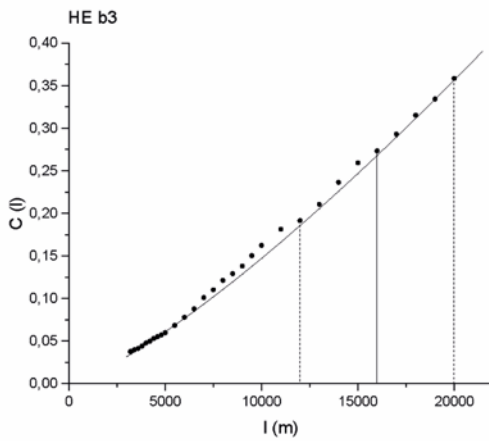
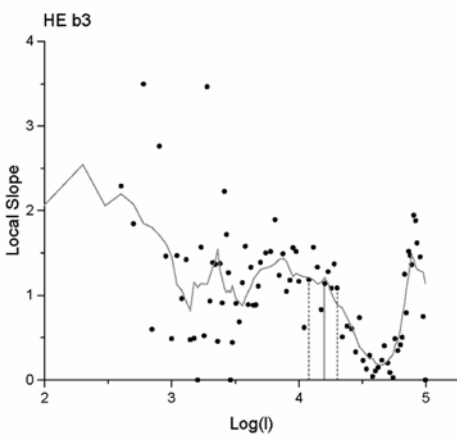
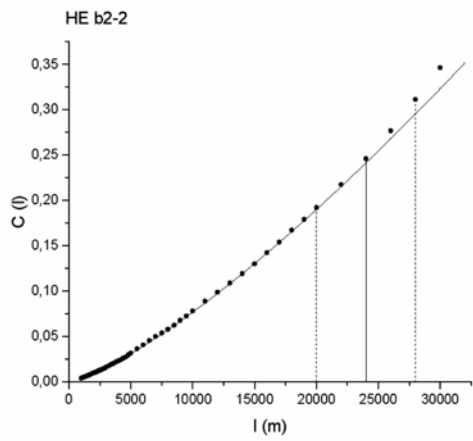
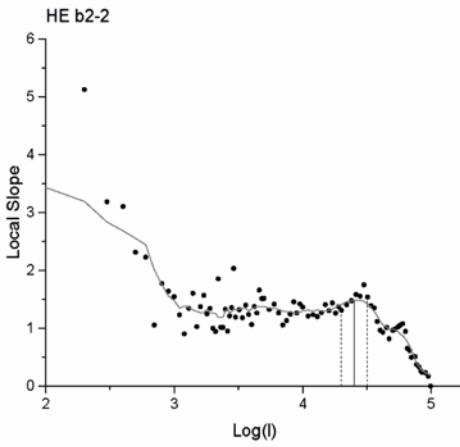
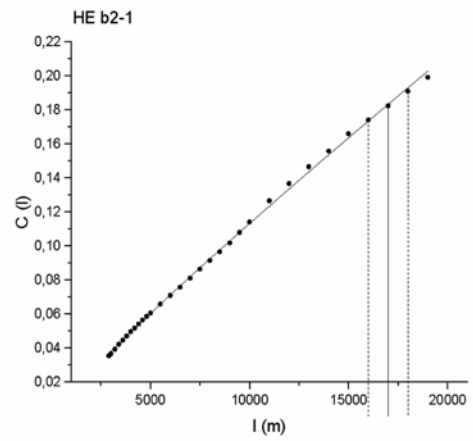
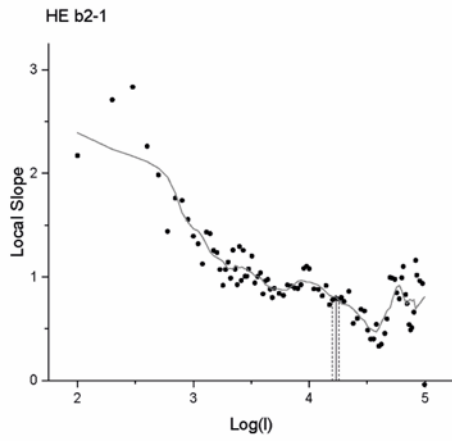
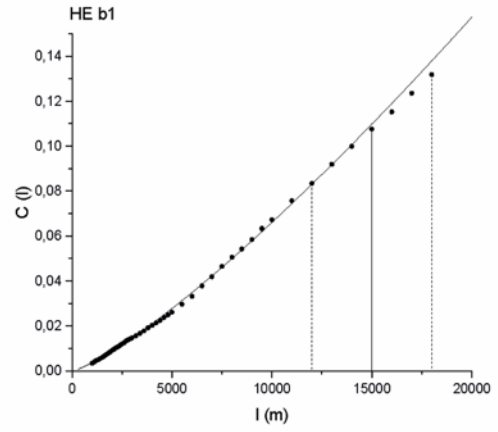
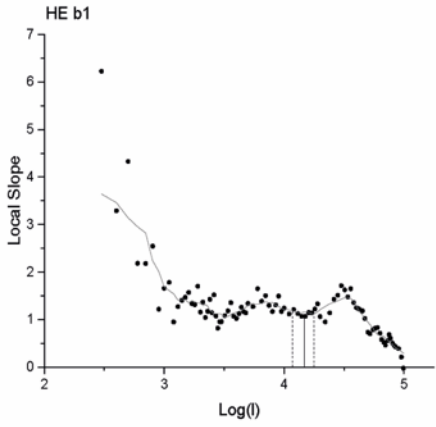
analogously these kind of colonies could have appeared in similar niches on Mars due to its inhospitable surficial environment (e.g. Wadsworth & Cockell, 2017).

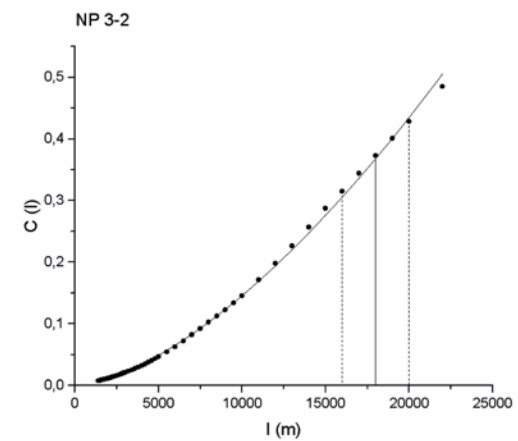
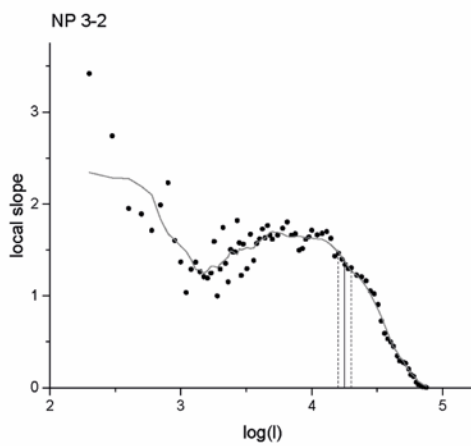
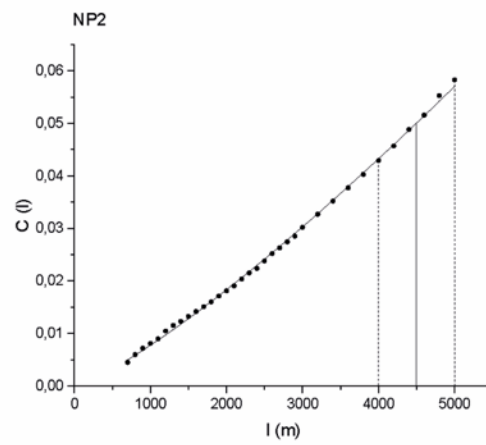
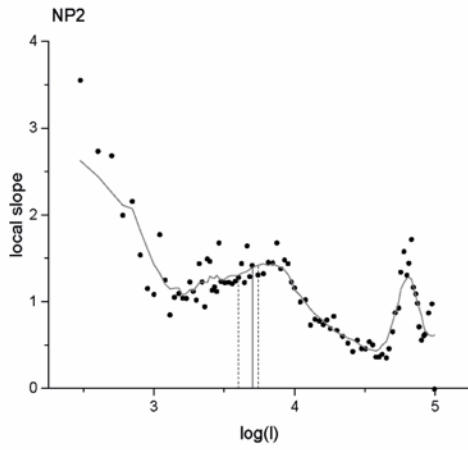
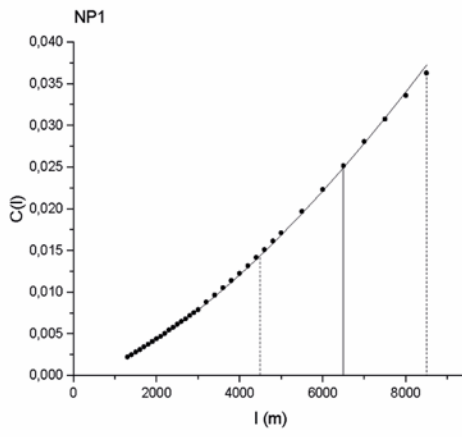
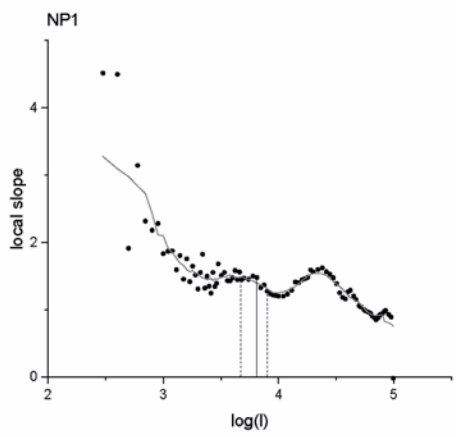
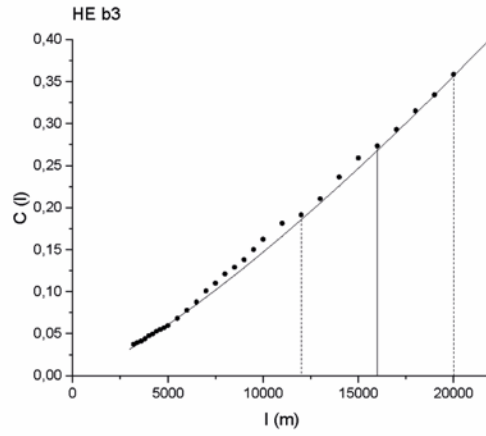
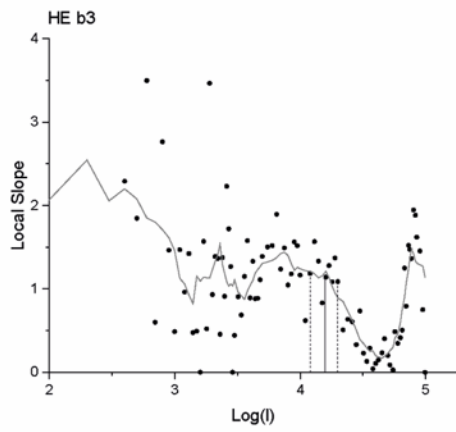
Concluding, these findings provide new insights on Martian habitability constituting evidence of presumable water and gas release through mud volcanism-like phenomena rooted in gas-hydrates. This let us link the deep environment and its surface expression, put new constraining conditions to the phenomenon, at least in the study areas, and shrink the number of mechanisms that can be involved in the process opening up a new broad spectrum of astrobiological questions that need to be addressed with further studies.

Appendix A

In Fig A.1. the complete record of plots obtained by the fractal analysis is displayed and two graphs are associated to each cluster as described in Fig.2. The U_{co} values have been highlighted in all the plots by a solid black dropline while the error range has been displayed by dashed black droplines according to the values reported in Table 2.







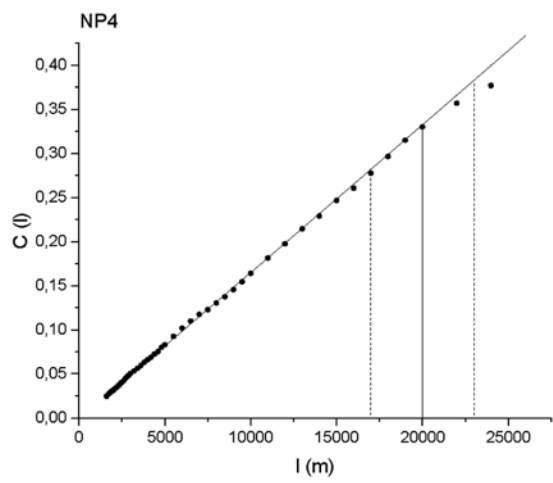
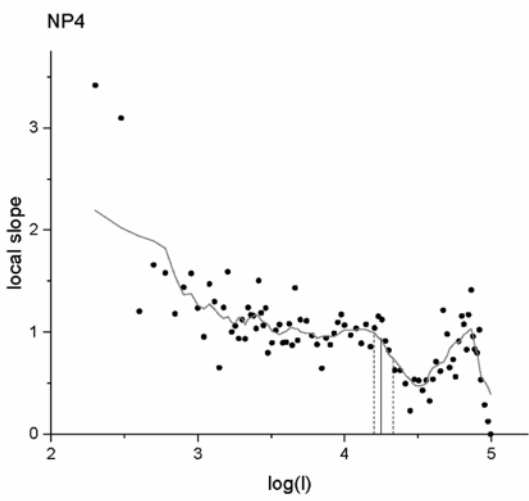
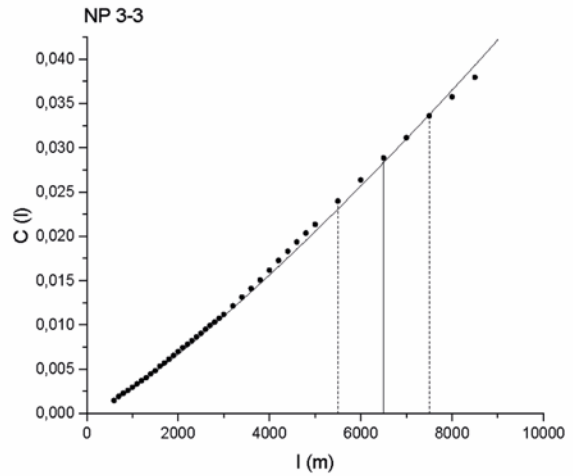
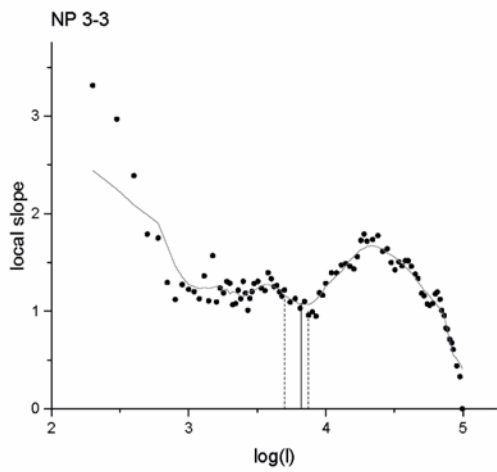


FIG A.1. Size range plots are displayed on the left column and fracture distribution plots are displayed on the right column for all the cluster dataset (refer to Fig.5 and Table.2)

References

- Allen, C.C., Oehler, D.Z., Baker, D.M., 2009. Mud volcanoes – A new class of sites for geological and astrobiological exploration of Mars. *Lunar Planet. Sci.* XXXX. Abstract 1749.
- Andrews-Hanna, J.C., Zuber, M.T., Arvidson, R.E., Wiseman, S.M., 2010. Early Mars hydrology: Meridiani playa deposits and the sedimentary record of Arabia Terra. *J. Geophys. Res. E Planets* 115, 1–22. doi:10.1029/2009JE003485
- Atreya, S.K., Mahaffy, P.R., Wong, A.-S., 2007. Methane and related trace species on Mars: Origin, loss, implications for life, and habitability. *Planet. Space Sci.* 55, 358–369. doi:10.1016/j.pss.2006.02.005
- Balme, M.R., Gallagher, C., 2009. An equatorial periglacial landscape on Mars. *Earth Planet. Sci. Lett.* 285, 1–15. doi:10.1016/j.epsl.2009.05.031
- Bernhardt, H., Hiesinger, H., Ivanov, M.A., Ruesch, O., Erkeling, G., Reiss, D., 2016. Photogeologic mapping and the geologic history of the Hellas basin floor, Mars. *Icarus* 264, 407–442. doi:10.1016/j.icarus.2015.09.031
- Bonini, M., Mazzarini, F., 2010. Mud volcanoes as potential indicators of regional stress and pressurized layer depth. *Tectonophysics* 494, 32–47. doi:10.1016/j.tecto.2010.08.006
- Bonnet, E., Bour, O., Odling, N.E., Davy, P., Main, I., Cowie, P., Berkowitz, B., 2001. Scaling of Fracture System in Geological Media. *Rev. Geophys.* 39, 347–383.
- Brož, P., Hauber, E., 2013. Hydrovolcanic tuff rings and cones as indicators for phreatomagmatic explosive eruptions on Mars. *J. Geophys. Res. E Planets* 118, 1656–1675. doi:10.1002/jgre.20120
- Bruno, B.C., Fagents, S.A., Thordarson, T., Baloga, S.M., Pilger, E., 2004. Clustering within rootless cone groups on Iceland and Mars: Effect of nonrandom processes. *J. Geophys. Res. E Planets* 109, 1–11. doi:10.1029/2004JE002273
- Burr, D.M., Tanaka, K.L., Yoshikawa, K., 2009. Pingos on Earth and Mars. *Planet. Space Sci.* 57, 541–555. doi:10.1016/j.pss.2008.11.003
- Carr, M.H., 2006. *The Surface of Mars*, Cambridge Planetary Science Series. doi:10.1086/518077
- Chastain, B.K., Chevrier, V., 2007. Methane clathrate hydrates as a potential source for martian atmospheric methane. *Planet. Space Sci.* 55, 1246–1256. doi:10.1016/j.pss.2007.02.003
- Clauset, A., Shalizi C. R., and Newman M. E. J., 2009. Power-law distributions in empirical data, *SIAM Rev.*, 51, 661–703. doi:10.1137/070710111.
- Clifford, S.M., 1993. A model for the hydrologic and climatic behavior of water on Mars. *J. Geophys. Res.* 98, 10973–11016. doi:10.1029/93JE00225
- Clifford, S.M., Lasue, J., Heggy, E., Boisson, J., McGovern, P., Max, M.D., 2010. Depth of the Martian cryosphere: Revised estimates and implications for the existence and detection of subpermafrost groundwater. *J. Geophys. Res.* 115, E07001. doi:10.1029/2009JE003462
- Clifford, S.M., Parker, T.J., 2001. The evolution of the Martian hydrosphere: Implications for the fate of a primordial ocean and the current state of the Northern Plains. *Icarus* 154, 40–79. doi:10.1006/icar.2001.6671
- Cockell, C.S., 2014. Trajectories of Martian Habitability. *Astrobiology* 14, 182–203. doi:10.1089/ast.2013.1106
- Cockell, C.S., 2015. *Astrobiology*. John Wiley & Sons Ltd, 472 pp.
- Cockell, C.S., Balme, M., Bridges, J.C., Davila, A., Schwenzer, S.P., 2012. Uninhabited habitats on Mars. *Icarus* 217, 184–193. doi:10.1016/j.icarus.2011.10.025
- Costard, F., Séjourné, A., Kelfoun, K., Clifford, S., Lavigne, F., Di Pietro, I., Bouley, S., 2017. Modeling tsunami propagation and the emplacement of thumbprint terrain in an early Mars ocean. *J. Geophys. Res. Planets* 1–17. doi:10.1002/2016JE005230
- Davis, P.A., Tanaka, K.L., 1995. Curvilinear ridges in Isidis Planitia, Mars - the result of mud volcanism? *Lunar Planet. Sci.* doi:10.1017/CBO9781107415324.004
- De Toffoli, B., Pozzobon, R., Mazzarini, F., Orgel, C., Massironi, M., Giacomini, L., Mangold, N., Cremonese, G., 2018. Estimate of depths of source fluids related to mound fields on Mars. *Planet. Space Sci.* 164–173. <https://doi.org/10.1016/j.pss.2018.07.005>
- Deville, E., Guerlais, S.H., Callec, Y., Griboulard, R., Huyghe, P., Lallemand, S., Mascle, A., Noble, M., Schmitz, J., 2006. Liquefied vs stratified sediment mobilization processes: Insight from the South of the Barbados accretionary prism. *Tectonophysics* 428, 33–47. doi:10.1016/j.tecto.2006.08.011
- Dimitrov, L., 2002. Mud volcanoes – the most important pathways for degassing deeply buried sediments. *Earth Sci. Rev.* 59, 49–76. doi:10.1016/S0012-8252(02)00069-7
- Dundas, C.M., McEwen, A.S., 2010. An assessment of evidence for pingos on Mars using HiRISE.

- Icarus 205, 244–258. doi:10.1016/j.icarus.2009.02.020
- Etioppe, G., Oehler, D.Z., Allen, C.C., 2011. Methane emissions from Earths degassing: Implications for Mars. *Planet. Space Sci.* 59, 182–195. doi:10.1016/j.pss.2010.06.003
- Etioppe, G., Feyzullayev, A., Baciú, C.L., Milkov, A.V., 2004. Methane emission from mud volcanoes in eastern Azerbaijan. *Geology* 32 (6), 465–468.
- Fairén, A.G., Dohm, J.M., Baker, V.R., de Pablo, M.A., Ruiz, J., Ferris, J.C., Anderson, R.C., 2003. Episodic flood inundations of the northern plains of Mars. *Icarus* 165, 53–67. doi:10.1016/S0019-1035(03)00144-1
- Farrand, W.H., Gaddis, L.R., Keszthlyi, L., 2005. Pitted cones and domes on Mars: Observations in Acidalia Planitia and Cydonia Mensae using MOC, THEMIS, and TES data. *J. Geophys. Res.* 110. doi:10.1029/2004JE002297.
- Formisano, V., Atreya, S., Encrenaz, T., Ignatiev, N., Giuranna, M., 2004. Detection of methane in the atmosphere of Mars. *Science* 306, 1758–1761.
- Fryer, P., 2012. Serpentinite Mud Volcanism: Observations, Processes, and Implications. *Ann. Rev. Mar. Sci.* 4, 345–373. doi:10.1146/annurev-marine-120710-100922
- Gainey, S.R., Elwood Madden, M.E., 2012. Kinetics of methane clathrate formation and dissociation under Mars relevant conditions. *Icarus* 218, 513–524. doi:10.1016/j.icarus.2011.12.019
- Geminale, A., Formisano, V., Giuranna, M., 2008. Methane in Martian atmosphere: Average spatial, diurnal, and seasonal behaviour. *Planet. Space Sci.* 56, 1194–1203. doi:10.1016/j.pss.2008.03.004
- Godon, A., Jendrzewski, N., Castrec-Rouelle, M., Dia, A., Pineau, F., Boulégué, J., Javoy, M., 2004. Origin and evolution of fluids from mud volcanoes in the Barbados accretionary complex. *Geochim. Cosmochim. Acta* 68, 2153–2165. doi:10.1016/j.gca.2003.08.021
- Guidat, T., Pochat, S., Bourgeois, O., Souček, O., 2015. Landform assemblage in Isidis Planitia, Mars: Evidence for a 3 Ga old polythermal ice sheet. *Earth Planet. Sci. Lett.* 411, 253–267. doi:10.1016/j.epsl.2014.12.002
- Head, J.W., Marchant, D.R., 2014. The climate history of early Mars: insights from the Antarctic McMurdo Dry Valleys hydrologic system. *Antarct. Sci.* 26, 774–800. dx.doi.org/10.1017/S0954102014000686.
- Hovland, M., Hill, A., Stokes, D., 1997. The structure and geomorphology of the Dashgil mud volcano, Azerbaijan. *Geomorphology* 21, 1–15. doi:10.1016/S0169-555X(97)00034-2
- Ivanov, M. a., Hiesinger, H., Erkeling, G., Reiss, D., 2014. Mud volcanism and morphology of impact craters in Utopia Planitia on Mars: Evidence for the ancient ocean. *Icarus* 228, 121–140. doi:10.1016/j.icarus.2013.09.018
- Judd, A.G., Hovland, M., 2007. *Seabed Fluid Flow: The Impact on Geology, Biology and the Marine Environment*. University Press, Cambridge. 475 pp.
- Kargel, J.S., Furfaro, R., Prieto-Ballesteros, O., Rodriguez, J.A.P., Montgomery, D.R., Gillespie, A.R., Marion, G.M., Wood, S.E., 2007. Martian hydrogeology sustained by thermally insulating gas and salt hydrates. *Geology* 35, 975–978. doi:10.1130/G23783A.1
- Komatsu, G., Okubo, C.H., Wray, J.J., Ojha, L., Cardinale, M., Murana, A., Orosei, R., Chan, M.A., Ormö, J., Gallagher, R., 2016. Small edifice features in Chryse Planitia, Mars: Assessment of a mud volcano hypothesis. *Icarus*. doi:10.1016/j.icarus.2015.12.032
- Kopf, A.J., 2002. Significance of mud volcanism. *Rev. Geophys.* 40, 1005. doi:10.1029/2000RG000093
- Krasnopolsky, V.A., Maillard, J.P., Owen, T.C., 2004. Detection of methane in the Martian atmosphere: evidence for life? *Icarus* 172 537–547.
- Kreslavsky, M. a., Head, J.W., 2002. Fate of outflow channel effluents in the northern lowlands of Mars: The Vastitas Borealis Formation as a sublimation residue from frozen ponded bodies of water. *J. Geophys. Res.* 107, 5121. doi:10.1029/2001JE001831
- Lanagan, P.D., McEwen, A.S., Keszthelyi, L.P., Thordarson, T., 2001. Rootless cones on Mars indicating the presence of shallow equatorial ground ice in recent times. *Geophys. Res. Lett.* 28, 2365–2367. doi:10.1029/2001GL012932
- Lance, S., Henry, P., Le Pichon, X., Lallemand, S., Chamley, H., Rostek, F., Faugères, J.C., Gonthier, E., Olu, K., 1998. Submersible study of mud volcanoes seaward of the Barbados accretionary wedge: Sedimentology, structure and rheology. *Mar. Geol.* 145, 255–292. doi:10.1016/S0025-3227(97)00117-5
- Le Corvec, N., Spörl, K.B., Rowland, J., Lindsay, J., 2013. Spatial distribution and alignments of volcanic centers: Clues to the formation of monogenetic volcanic fields. *Earth-Science Rev.* 124, 96–114. doi:10.1016/j.earscirev.2013.05.005
- Martinelli, G., Judd, A.G., 2004. Mud volcanoes of Italy. *Geol. J.* 39, 49–61. doi:10.1002/gj.943
- Max, M., Johnson, A., and Clifford, S. (2011) Methane hydrate on Mars: a resource-rich stepping

- stone to the outer planets? In Proceedings of the 7th International Conference on Gas Hydrates (ICGH 2011), Edinburgh, Scotland
- Max, M.D., Clifford, S.M., and Johnson, A.H. (2013) Hydro- carbon system analysis for methane hydrate exploration on Mars. In Energy Resources for Human Settlement in the Solar System and Earth's Future in Space, AAPG Memoir 101, edited by W.A. Ambrose, J.F. Reilly II, and D.C. Peters, American Association of Petroleum Geologists, Tulsa, OK, pp 99–114
- Mazzarini, F., 2004. Volcanic vent self-similar clustering and crustal thickness in the northern Main Ethiopian Rift. *Geophys. Res. Lett.* 31, 1–4. doi:10.1029/2003GL018574
- Mazzarini, F., Isola, I., 2010. Monogenetic vent self-similar clustering in extending continental crust: Examples from the East African Rift System. *Geosphere* 6, 567–582. doi:10.1130/GES00569.1
- Mazzarini F., Keir D., Isola I., 2013. Spatial relationship between earthquakes and volcanic vents in the central-northern Main Ethiopian Rift. *Journal of Volcanology and Geothermal Research*, 262, 123–133.
- McGowan, E., 2009. Spatial distribution of putative water related features in southern Acidalia/Cydonia Mensae, Mars. *Icarus* 202, 78–89.
- McGowan, E.M., McGill, G.E., 2010. The Utopia/Isidis overlap: Possible conduit for mud volcanism. *Lunar Planet. Sci.* 41. Abstract 1070.
- McGowan, E.M., 2011. The Utopia/Isidis overlap: Possible conduit for mud volcanism on Mars. *Icarus* 212, 622–628. doi:10.1016/j.icarus.2011.01.025
- Mcmahon, S., Parnell, J., 2014. Weighing the deep continental biosphere. *FEMS Microbiol. Ecol.* 87, 113–120. doi:10.1111/1574-6941.12196
- Milkov, a. V., 2000. Worldwide distribution of submarine mud volcanoes and associated gas hydrates. *Mar. Geol.* 167, 29–42. doi:10.1016/S0025-3227(00)00022-0
- Moratto, Z.M., Broxton, M.J., Beyer, R.A., Lundy, M., Husmann, K., 2010. Ames Stereo Pipeline, 707NASAs Open Source Automated Stereogrammetry Software. In: Proceedings of the 41st Lunar and Planetary Institute Science Conference. Houston, Texas, [2364].
- Mosis, O., Lunine, J.I., Chassefière, E., Montmessin, F., Lakhli, A., Picaud, S., Petit, J.M., Cordier, D., 2012. Mars cryosphere: A potential reservoir for heavy noble gases? *Icarus* 218, 80–87. doi:10.1016/j.icarus.2011.12.007
- Mosis, O., Chassefière, E., Lasue, J., Chevrier, V., Elwood Madden, M.E., Lakhli, A., Lunine, J.I., Montmessin, F., Picaud, S., Schmidt, F., Swindle, T.D., 2013. Volatile trapping in martian clathrates. *Space Sci. Rev.* 174, 213–250. doi:10.1007/s11214-012-9942-9
- Mumma, M.J., Novak, R.E., DiSanti, M.A., Bonev, B.P., Dello Russo, N., 2004. Detection and mapping of methane and water on Mars. American Astronomical Society, 36th Division of Planetary Science Meeting, 8–12 November, 2004, Louisville. *Bull. American Astronomical Society* 36 (4), Abstract No. 26.02.
- Mumma, M.J., Villanueva, G.L., Novak, R.E., Hewagama, T., Bonev, B.P., Disanti, M. a, Mandell, A.M., Smith, M.D., 2009. Strong release of methane on Mars in northern summer 2003. *Science* 323, 1041–1045. doi:10.1126/science.1165243
- Nixon, S.L., Cousins, C.R., Cockell, C.S., 2013. Plausible microbial metabolisms on Mars. *Astron. Geophys.* 54, 13–16. doi:10.1093/astrogeo/ats034
- Noguchi, R., Höskuldsson, Á., Kurita, K., 2016. Detailed topographical, distributional, and material analyses of rootless cones in Myvatn, Iceland. *J. Volcanol. Geotherm. Res.* 318, 89–102. doi:10.1016/j.jvolgeores.2016.03.020
- Oehler, D.Z., Allen, C.C., 2009. Mud volcanoes in the martian lowlands: Potential windows to fluid-rich samples from depth. *Lunar Planet. Sci.* XXXX. Abstract 1034.
- Oehler, D.Z., Allen, C.C., 2010. Evidence for pervasive mud volcanism in Acidalia Planitia, Mars. *Icarus* 208, 636–657. doi:10.1016/j.icarus.2010.03.031
- Oehler, D.Z., Allen, C.C., 2012. Giant Polygons and Mounds in the Lowlands of Mars: Signatures of an Ancient Ocean? *Astrobiology* 12, 601–615. doi:10.1089/ast.2011.0803
- Oehler, D.Z., Etiopie, G., 2017. Methane Seepage on Mars: Where to Look and Why. *Astrobiology* 17, ast.2017.1657. doi:10.1089/ast.2017.1657
- Okubo, C.H., 2016. Morphologic evidence of subsurface sediment mobilization and mud volcanism in Candor and Coprates Chasmata, Valles Marineris, Mars. *Icarus* 269, 23–37. doi:10.1016/j.icarus.2015.12.051
- Page, D.P., Murray, J.B., 2006. Stratigraphical and morphological evidence for pingo genesis in the Cerberus plains. *Icarus* 183, 46–54. doi:10.1016/j.icarus.2006.01.017
- Parnell, J., McMahan, S., 2016. Physical and chemical controls on habitats for life in the deep subsurface beneath continents and ice. *Philos. Trans. R. Soc. A* 374, 20140293. doi:10.1098/rsta.2014.0293

- Paulsen, T.S., Wilson, T.J., 2010. New criteria for systematic mapping and reliability assessment of monogenetic volcanic vent alignments and elongate volcanic vents for crustal stress analyses. *Tectonophysics* 482, 16–28. doi:10.1016/j.tecto.2009.08.025
- Pomerantz, W.J., Head, J.W., 2003. Thumbprint Terrain and Sinuous Troughs with Medial Ridges in the Northern Lowlands of Mars: Assessment of the Glacial Hypothesis Using New Spacecraft. *Lunar Planet. Sci. Conf.* 34, 1277.
- Pondrelli, M., Rossi, a. P., Ori, G.G., van Gasselt, S., Praeg, D., Ceramicola, S., 2011. Mud volcanoes in the geologic record of Mars: The case of Firsoff crater. *Earth Planet. Sci. Lett.* 304, 511–519. doi:10.1016/j.epsl.2011.02.027
- Pozzobon, R., Mazzarini, F., Massironi, M., Marinangeli, L., 2015. Self-similar clustering distribution of structural features on Ascræus Mons (Mars): implications for magma chamber depth. *Geol. Soc. London, Spec. Publ.* doi:10.1144/SP401.12
- Prieto-Ballesteros, O., Kargel, J.S., Fairén, A.G., Fernández-Remolar, D.C., Dohm, J.M., Amils, R., 2006. Interglacial clathrate destabilization on Mars: Possible contributing source of its atmospheric methane. *Geology* 34, 149. doi:10.1130/G22311.1
- Preston, L.J., Dartnell, L.R., 2014. Planetary habitability: lessons learned from terrestrial analogues. *Int. J. Astrobiol.* 13, 81–98. doi:10.1017/S1473550413000396
- Rodríguez, J.A.P., Tanaka, K.L., Kargel, J.S., Dohm, J.M., Kuzmin, R., Fairén, A.G., Sasaki, S., Komatsu, G., Schulze-Makuch, D., Jianguo, Y., 2007. Formation and disruption of aquifers in southwestern Chryse Planitia, Mars. *Icarus* 191 (2), 545–567
- Rodríguez, J.A.P., Tanaka, K.L., Berman, D.C., Kargel, J.S., 2010. Late Hesperian plains formation and degradation in a low sedimentation zone of the northern lowlands of Mars. *Icarus* 210, 116–134. doi:10.1016/j.icarus.2010.04.025
- Shean, D. E., O. Alexandrov, Z. Moratto, B. E. Smith, I. R. Joughin, C. C. Porter, Morin, P. J. 2016. An automated, open-source pipeline for mass production of digital elevation models (DEMs) from very high-resolution commercial stereo satellite imagery. *ISPRS Journal of Photogrammetry and Remote Sensing.* 116.
- Skinner, J.A., Tanaka, K.L., 2007. Evidence for and implications of sedimentary diapirism and mud volcanism in the southern Utopia highland–lowland boundary plain, Mars. *Icarus* 186, 41–59. doi:10.1016/j.icarus.2006.08.013
- Skinner Jr., J.A., Mazzini, A., 2009. Martian mud volcanism: Terrestrial analogs and implications for formational scenarios. *Marine Petrol. Geol.* doi:10.1016/j.marpetgeo.2009.02.006.
- Tanaka, K.L., 1997. Sedimentary history and mass flow structures of Chryse and Acidalia Planitiae, Mars. *J. Geophys. Res.* 102, 4131–4149. doi:10.1029/96JE02862
- Tanaka, K.L., Banerdt, W.B., 2000. The interior lowland plains unit of Mars: Evidence for a possible mud ocean and induced tectonic deformation. *Lunar Planet. Sci.* XXXI. Abstract 2041
- Tanaka, K.L., Skinner Jr., J.A., Hare, T.M., Joyal, T., Wenker, A., 2003. Resurfacing history of the Northern Plains of Mars based on geologic mapping of Mars Global Surveyor data. *J. Geophys. Res.* 108 (E4). GDS 24-1–GDS 24-32. doi:10.1029/2002JE001908.
- Tanaka, K.L., Skinner Jr., J.A., Hare, T.M., 2005. Geologic map of the Northern Plains of Mars. *Scientific Investigations Map 2888*, U.S. Geological Survey.
- Tanaka, K.L., Rodríguez, J.A.P., Skinner Jr., J.A., Mourke, M.C., Fortezzo, C.M., Herkenhoff, K.E., Kolb, E.J., Okubo, C.H., 2008. North polar region of Mars: Advances in stratigraphy, structure, and erosional modification. *Icarus* 196 (2), 318–358.
- Thomas, N., Cremonese, G., Ziethe, R., Gerber, M., Brändli, M., Bruno, G., Erismann, M., Gambicorti, L., Gerber, T., Ghose, K., Gruber, M., Gubler, P., Mischler, H., Jost, J., Piazza, D., Pommerol, A., Rieder, M., Roloff, V., Servonet, A., Trottmann, W., Uthaicharoengpong, T., Zimmermann, C., Vernani, D., Johnson, M., Pelò, E., Weigel, T., Viertl, J., De Roux, N., Lochmatter, P., Sutter, G., Casciello, A., Hausner, T., Ficai Veltroni, I., Da Deppo, V., Orleanski, P., Nowosielski, W., Zawistowski, T., Szalai, S., Sodor, B., Tulyakov, S., Troznai, G., Banaskiewicz, M., Bridges, J.C., Byrne, S., Debei, S., El-Maarry, M.R., Hauber, E., Hansen, C.J., Ivanov, A., Keszthelyi, L., Kirk, R., Kuzmin, R., Mangold, N., Marinangeli, L., Markiewicz, W.J., Massironi, M., McEwen, A.S., Okubo, C., Tornabene, L.L., Wajer, P., Wray, J.J., 2017b. The Colour and Stereo Surface Imaging System (CaSSIS) for the ExoMars Trace Gas Orbiter. *Space Sci. Rev.* 212, 1897–1944. <https://doi.org/10.1007/s11214-017-0421-1>
- Thomson, B., Head, J., 2001. Utopia Basin, Mars: Characterization of topography and morphology and assessment of the origin and evolution of basin internal structure. *J. Geophys. Res.* 106, 23209–23230. doi:10.1029/2000JE001355
- Thorarinsson, S. (1953), The crater groups in Iceland, *Bull. Volcanol.*, 14, 3–44.
- Torson, J.M., Becker, K.J., 1997. ISIS - A Software Architecture for Processing Planetary Images,

- 1036 Lunar Planet. Sci. XXVIII, Houston, Texas, Abstract [1219].
- Travis, B.J., 2003. On the role of widespread subsurface convection in bringing liquid water close to Mars' surface. *J. Geophys. Res.* 108, 8040. doi:10.1029/2002JE001877
- Travis, B.J., Feldman, W.C., 2009. Salt deposits, ice lenses and convective brine aquifers on Mars. 40th Lunar Planet. Sci. Conf. 1–2.
- Travis, B.J., Feldman, W.C., Maurice, S., 2013. A mechanism for bringing ice and brines to the near surface of Mars. *J. Geophys. Res. E Planets* 118, 877–890. doi:10.1002/jgre.20074
- Wadsworth, J., Cockell, C.S., 2017. Perchlorates on Mars enhance the bacteriocidal effects of UV light. *Sci. Rep.* 7, 4662. doi:10.1038/s41598-017-04910-3
- Walsh, J.J. & Watterson, J. 1993. Fractal analysis of fracture pattern using the standard box-counting technique: valid and invalid methodologies. *Journal of Structural Geology*, 15, 1509–1512, [http://dx.doi.org/10.1016/0191-8141\(93\)90010-8](http://dx.doi.org/10.1016/0191-8141(93)90010-8)
- Williams, D.A., Greeley, R., Ferguson, R.L., Kuzmin, R., McCord, T.B., Combe, J.P., Head, J.W., Xiao, L., Manfredi, L., Poulet, F., Pinet, P., Baratoux, D., Plaut, J.J., Raitala, J., Neukum, G., 2009. The Circum-Hellas Volcanic Province, Mars: Overview. *Planet. Space Sci.* 57, 895–916. doi:10.1016/j.pss.2008.08.010
- Williams, D.A., Greeley, R., Werner, S.C., Michael, G., Crown, D.A., Neukum, G., Raitala, J., 2008. Tyrrhena Patera: Geologic history derived from Mars Express High Resolution Stereo Camera. *J. Geophys. Res. E Planets* 113, 1–14. doi:10.1029/2008JE003104
- Wordsworth, R., Kerber, L., Pierrehumbert, R.T., Forget, F., Head, J.W., 2015. Comparison of “warm and wet” and “cold and icy” scenarios for early Mars in a 3-D climate model. *J. Geophys. Res.: Planets* 120 (6), 1201–1219. doi.org/10.1002/2015JE004787

Chapter 3: *From orbiter to field exploration*

Introduction

The formation and early evolution of Mars as a planet, the history of geological processes and the potential to have hosted life are the linchpins of the Mars exploration program that develops on the scientific question thread based on “Follow the Water”, “Explore Habitability” and “Seek Signs of Life”. To pursue such goals, *in situ* observations have been planned and realised by the exploitation of rover missions that, up to now, are the only effective tool to perform field geology on the red planet.

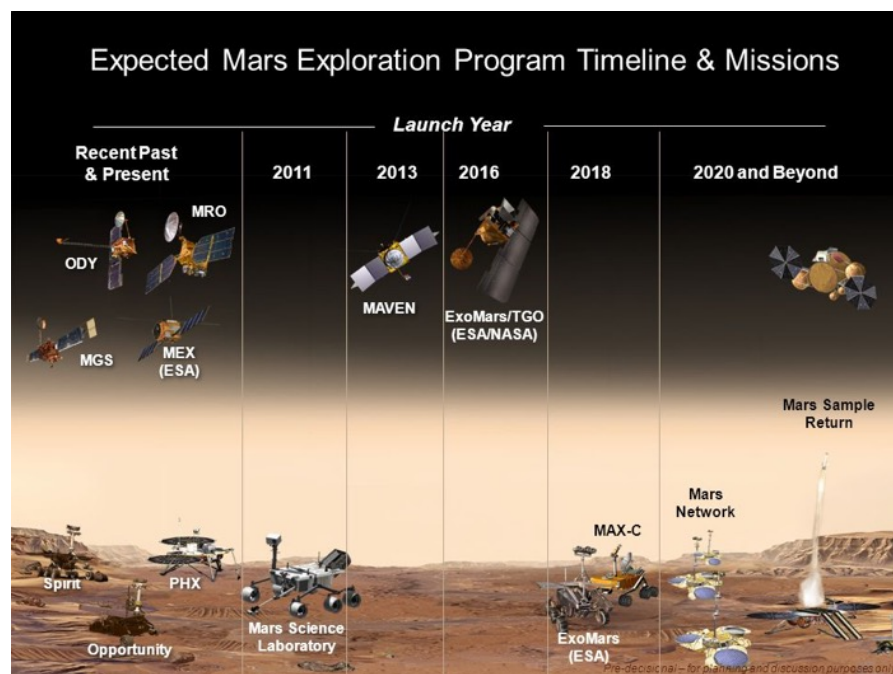


Figure 1. Main ESA and NASA Mars exploration missions.

The first rover put on the Martian surface was Pathfinder that landed successfully in 1997; after it two robotic geologists, Spirit and Opportunity, landed on Mars in 2004 with more sophisticated science instruments by means of which they sent to Earth hundreds of thousands of high-resolution, full-colour images and spectral compositional information of Martian terrains, rocks and soils. The data recovered by the twin rovers allowed the first reconstructions of an ancient wet Mars that could have possibly supported microbial life. Opportunity surveyed Eagle and Endurance craters that hosted inter-dune playa lakes that evaporated to form sulfate-rich sands. Spirit

travelled to Gusev Crater and Columbia Hills recovering clues of the early Mars evolution characterized by impacts, explosive volcanism, and subsurface water. In 2012 a new rover mission landed on Mars, Curiosity, carrying the largest and most advanced instrumentation set aimed to reach a better understanding of past and present Martian environmental conditions and their suitability to support microbial life. For the future, two separate rover missions are planned to be launched in 2020, ExoMars rover and Mars2020. ExoMars rover will be the first mission with drilling capabilities reaching up to 2 m of depth and able to produce chemistry, physical, and spectral analyses of the wall while sampling. Whereas, Mars 2020 design will be similar to Curiosity, but newer and more sophisticated payload will provide opportunities to gather knowledge and demonstrate technologies that address the challenges of future human expeditions to Mars.

References

All the above-mentioned data and images are based on open access information retrievable on ESA (<http://exploration.esa.int>) and NASA (<https://mars.nasa.gov>) official websites.

Paper in Preparation

COMPARATIVE PLANETARY STRUCTURAL ASSET ANALYSIS: INSIGHTS ON MARTIAN SULFATE VEIN NETWORKS AND THE BLETTERBACH SITE, NORTH-EASTERN ITALY

Barbara De Toffoli ^{a,b}, Nicolas Mangold ^c, Matteo Massironi ^{a,b},
Riccardo Pozzobon ^{a,b}, Jonas L'Haridon ^c, Gabriele Cremonese ^b

^a Department of Geosciences, University of Padova, Via Gradenigo 6, Padova 35131, Italy

^b INAF, Osservatorio Astronomico di Padova, Vicolo dell'Osservatorio 3, Padova I-35122, Italy

^c Laboratoire de Planetologie et Geodynamique, Universite de Nantes, Nantes, France

Abstract

The Curiosity rover's campaign in the Gale crater on Mars provides a large set of close-up images of sedimentary formations outcrops displaying a variety of diagenetic features such as light-toned veins, nodules and raised ridges. Through 2D and 3D analyses of MastCam and NavCam images we herein reconstruct the fracture distribution in a sample area, extract structural information and implement a comparative analysis with the terrestrial analogue site of the Bletterbach gorge (N-E Italy). Assessment of the spatial distribution of light-toned veins shows that the basin infillings experienced, subsequent to burial and consolidation, a sub-vertical compression and lateral extension coupled with fluid overpressure cracking. Overall, the evidence of coeval oblique and the horizontal vein networks in a confined basin scenario suggests the hypothesis that a pulse of material overload within the crater could have played a central role in rock failure and light-toned fractures formations.

1. Introduction

NASA's Mars Science Laboratory mission, Curiosity, is surveying the Gale crater since August 2012, equipped with a set of 17 cameras and 10 scientific instruments that allow rock and soil samples observation and analysis. Thanks to the *in situ* observations of the rover it has been possible to recognize fluid circulation features emplaced during diagenesis, subsequent to burial and consolidation of the sediments, specifically cross-cutting light-toned veins (L'Haridon et al., 2018;

Nachon et al., 2014), nodules (Stack et al., 2014) and raised ridges (Siebach et al., 2014; L veill  et al., 2014; McLennan et al., 2014). Light-toned veins, herein discussed, have a Ca-sulfate chemistry (Nachon et al., 2014) mainly interpreted to be bassanite ($\text{CaSO}_4 \times 0.5 \text{H}_2\text{O}$) at least on the surface exposed portions of the investigated outcrops (Rapin et al., 2016). Such veins are preferentially located below the stratigraphic unconformity with the eolian deposits (Stimson formation) topping the Murray formation and their genesis is suggested to be ascribable to complex fluid circulation events that led to dissolution and re-precipitation of hypothetical sulfate-rich materials (L'Haridon et al., 2018; Vaniman et al., 2017; Rapin et al., 2016; Schwenzer et al., 2016).

The formation of veins with mineral infilling is due to fracturing, mineral dissolution, transport and precipitation that may repeatedly and simultaneously occur to form even a single vein (Philipp, 2008). Thus fluids, a material source (with suitable T and P conditions for precipitation) and fractures providing space are the key ingredients to produce a network of mineral veins such the ones observed at Gale.

The purpose of this study is to assess the structural behaviour recorded by a well exposed crack system in a case study area along the rover traverse and the fracturing mechanism reconstruction through the comparison with terrestrial analogue sites. Contextually, this study aims to propose the Bletterbach sequence (Bolzano, north-eastern Italy) as a new analogue site for Mars concerning the sulfate veining systems herein under examination. In fact, the Bletterbach gorge shows optimal characteristics for the comparison in a structural behaviour reconstruction prospective, it is indeed characterized by well-exposed fine-grained siliciclastic host rocks with crosscutting systems of light-toned sulfate veins following geometries similar to the vein sets recorded in Gale crater.

2. Background

Gale is a complex crater located on the border of Terra Cimmeria at 5.37°S , 137.81°W (Grotzinger et al., 2014) interpreted to be filled by sedimentary deposits and showing a central mound, Aeolis Mons (informally known as Mount Sharp), for which several origins have been proposed (e.g., Wray, 2012). Gale is around 150 km in diameter and displays ~ 5 km of elevation difference between the floor and the central peak and rims (Le Deit et al., 2013; Young and Chan, 2017; Stack et al., 2016; Grotzinger et al., 2014, 2015).

The impact has been estimated to have occurred at the Noachian-Hesperian boundary (e.g. Thomson et al., 2011; Irwin et al., 2005) and since the formation the crater has experienced an intricate evolution involving the past presence of surface water indicated by the presence of rim-crossing carved channels and lacustrine deposits at the mound base (e.g. Grotzinger et al., 2014; Thomson et al., 2011; Milliken et al., 2010), this making this site invaluable for the paleoenvironment reconstruction and pivotal for the investigation of Martian habitability (e.g. Rubin et al., 2017, Caswell and Milliken, 2017). In Gale crater three formations have been identified: the Yellowknife Bay and Kimberley formations of the Bradbury group and the Murray formation of the Mount Sharp group (Grotzinger et al., 2014, 2015; Treiman et al., 2016) all representative of a fluvio-lacustrine environment recorded by laminated and cross stratified mudstones, sandstones and pebble conglomerates bearing hydrated clays and minerals (e.g. Le Deit et al., 2016; Treiman et al., 2016; Stack et al., 2015; Bristow et al., 2015; Grotzinger et al., 2014, 2015).

On Mars, fracturing mechanisms and structural behaviour are poorly constrained and a remarkable part of the collected evidence related to the light-toned veins are based on the invaluable compositional information acquired with ChemCam and its synergy with other instrument suites of Mars Science Laboratory (MSL) onboard Curiosity rover. Nevertheless, investigating possible source of fluids and minerals that interplayed in the fractures development led to a better understanding of the sulfate veins' origins (e.g. Schwenzer et al., 2016; Grotzinger et al., 2014, 2015). Sources of calcium sulfate could have been localized on higher (Nachon et al., 2015), lower (Grotzinger et al., 2014; McLennan et al., 2014; Nachon et al., 2015) or lateral (McLennan et al., 2014) units with the respect of the fractured layers, which underwent mobilization during a late diagenetic event (Young and Chan, 2017 and references therein). Recent study proposed a paleoenvironmental evolution at the entire basin scale that could lead to deposition, accumulation, burial, dissolution and reprecipitation of the sulfates that filled the light veins of Gale (Schwenzer et al., 2016). In fact, due to crater size, a long-lasting hydrothermal circulation could have been triggered by the large impact, initiating alteration and leaching processes within the deeply fractured subsurface. This possibly could have led to a mobilization of salts toward the surface where a lacustrine environment could have developed within the window of activity of the hydrothermal system (e.g. Abramov and Kring 2005; Schwenzer and Kring 2009, 2013).

On Earth, a fracturing mechanism that generates cracks morphologically and mineralogically comparable to the ones observed on Mars has been described in several locations (e.g. Cosgrove, 2001; Young and Chan, 2017), among these we chose to consider the Watchet Bay case study to carry out a comparative analysis. The Upper Triassic Mercia Mudstone Group outcrops on the Somerset Coast of SW England, Watchet Bay, and display analogue characteristics to the rocks observed in the Gale crater. The can be divided into two portions with different peculiar features, the lower part of the Group consists of several tens of meters of poorly bedded, red to reddish-brown unfossiliferous mudstones and siltstones (Whittaker and Green, 1983; Leslie et al., 1993). The upper part of the red mudstones is characterized by laterally discontinuous evaporite-rich horizons, mainly composed of white nodular gypsum (Philipp, 2008; Fig.1). The Group is interpreted to have formed in playa lake or desert plain conditions (Bennison & Wright, 1969; Simms & Ruffell, 1990). In this context, the gypsum nodules formation may be ascribed to surficial remnants of ephemeral pools or remobilization and accumulation of gypsum primarily disseminated in the sediment (Leslie et al., 1993) while the presence of an evaporite horizons in the upper part have been interpreted as the products of a floodplain environment with periodic water body drying (Schwenzer et al., 2016; Philipp, 2008; Cosgrove, 2001). The Watchet Bay outcrop shows discontinuous anastomosing networks of gypsum veins confined to portions of the hosting mudstone. The phenomenon is not pervasive to the whole mudstone group though, but it is confined to specific portions often overlain by thick grey siltstone layers weakly calcareous (Philipp, 2008), it may in fact occur that veins produced by hydrofracturing stop where mechanical contrast boundaries occur (e.g. Brenner and Gudmundsson, 2004b; Gudmundsson and Brenner, 2001; Gudmundsson et al., 2002). No clear predominant attitude was detected, vein dips show variations from horizontal to vertical and the strikes are in broad range of directions. Crosscutting relationships were investigated as well and indicated no prevalent age relationship suggesting that the veins may all have formed at the same time (Philipp, 2008).

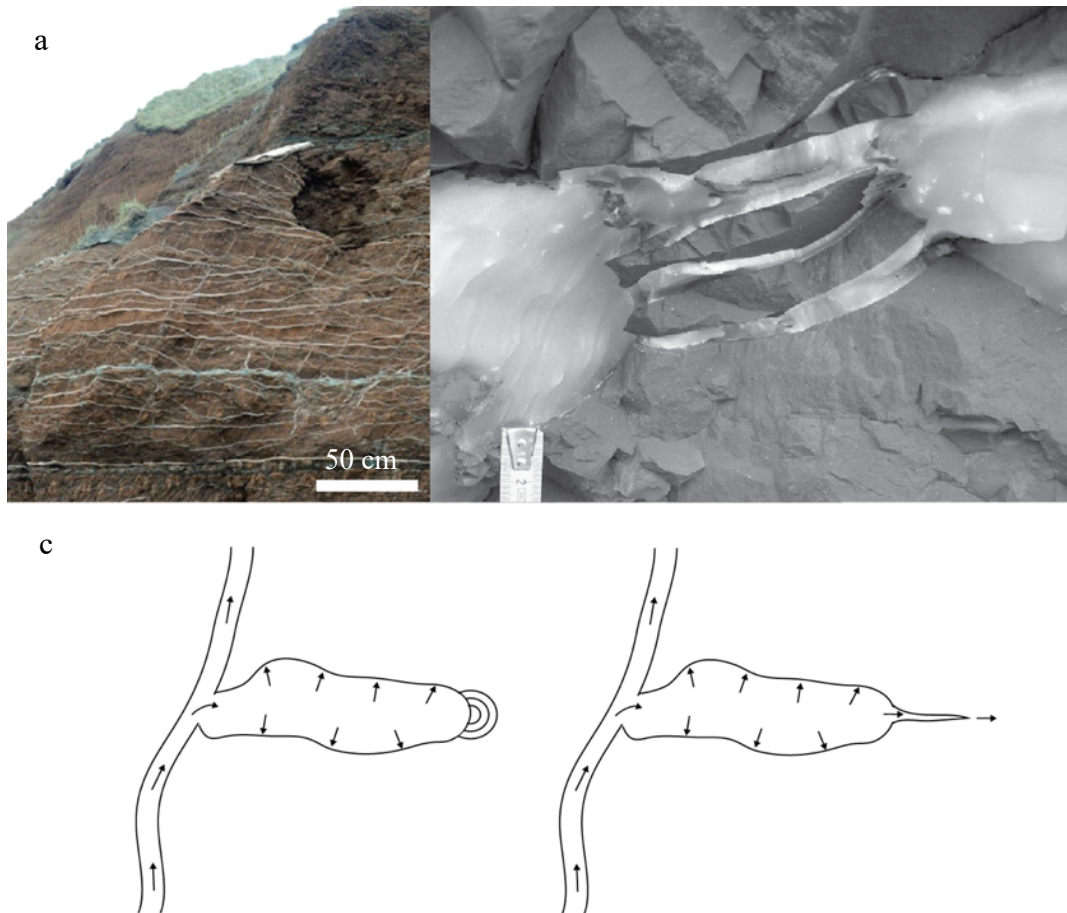


Fig.1 Sulfate vein networks on the Murcia Mudstone outcrop in England (a) and close up capture of hydrofracturing departing from the nodule's tip (b). Schematic of the hydrofracturing process involving pre-existing nodules experiencing fluid circulation (c). (Modified after Philipp, 2008 and Schwenzer, 2016)

A detailed work, made by Philipp (2008), present a paleo-hydrofracturing model for the formation of gypsum veins in the lower Mercia Mudstone Group. In Watchet Bay fluid transport took place mainly along faults and fractures since mudstones have a very low original permeability and are commonly effective barriers to fluid circulation (Philipp, 2008; Cartwright, 1997). There is no need of active slipping faults to allow fluid circulation and hydrofracturing, that are triggered when the pressure of the fluids sited within the veins exceed the lithostatic pressure; buoyancy overpressure can convey a significant contribution particularly when low density fluids are involved (e.g. geothermal fluids). Depending on the stress field, fluids can be transported along the veins, lead to hydrofracturing propagation of already existing fracture plains or generate hydrofracturing injection into the host rock (Philipp, 2008 and references therein). The fluid source for this case study is not entirely clear; fluid

flow can be triggered by very diverse physical and chemical disequilibria such as compaction due to burial, topographic gaps and buoyancy, or osmosis, chemical potential gradients, porosity and temperature changes (Neuzil, 1995; Bjørlykke, 1997; Osborne & Swarbrick, 1997). Nevertheless, these veins are not likely to have formed early in the basin history, but after compaction and consolidation; in fact a significant part of the vein population consists of extension fractures, hence the mudstone must have had some tensile strength at the time of formation excluding a young soft host rocks (Schwenzer et al., 2016; Philipp, 2008; Bell, 2000). Philipp (2008) suggests an hydrofracturing model to explain the sulfate vein network systems that cut the Mercia Mudstone Group based on low permeability of the mudstone that drove fluids, flowing from the highest to the lowest hydraulic potential (Domenico & Schwartz, 1998), to enter the rocks along faults and fractures and prevented them to penetrate intimately the host rock. In this context, fluids can penetrate pre-existing sulfate nodules present in the mudstone, that can be thus compared to overpressured elliptical fluid-filled pores, developing high concentrations of tensile stresses at their long-axis tips initiating hydraulic fracturing parallel to the maximum horizontal stress and likewise lateral propagation and sub-horizontal growth (through fracturing) of nodules into layers (Savin, 1961; Pollard & Segall, 1987; Maugis, 2000; Fig 1b, c). Where no nodules were primarily present in the mudstones fluids used existing favourably oriented weakness plans to flow. In both cases, in Watchet Bay, veins are the result of hydrofracturing injections into the host rock.

3. Methods

To investigate the light-toned veins that have been detected in Gale crater we performed 2D and 3D analyses of MastCam and NavCam images. MastCam takes colour images of 1600×1200 pixels that can be stitched together to create panoramas of the landscape around the rover; it consists of two-camera system that can acquire true RGB color images approximating what humans would perceive on Mars (Bell et al., 2012). With respect of the scientific purpose of MastCam, the NavCam systems were planned for operational use including acquisition of images for the rover's navigation, robotic planning and documentation, remote sensing science instrument pointing, but also general surface imaging (Maki et al., 2011). We coupled the observation of 2D mosaics of MastCam images and the production of a 3D model of

the same region in order to extract the structural information and reconstruct the fracture distribution in the area of interest covering around 100 m².

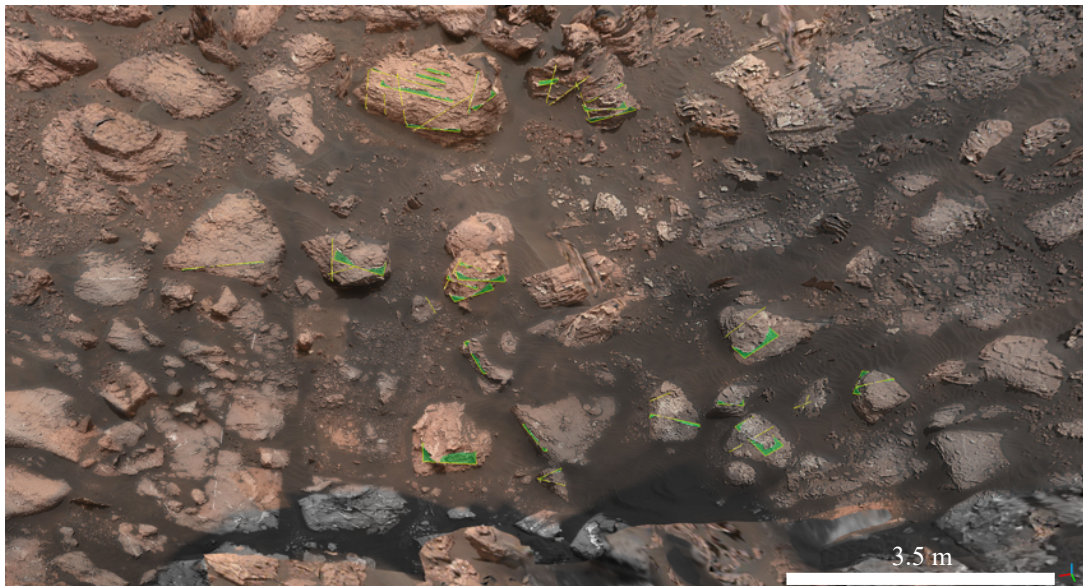


Fig.2 3D reconstruction of the Martian outcrops recorded between sols 1536-1545; some interpreted fracture planes are highlighted in green.

2D images were observed raw and stitched together, where overlapping acquisitions of neighboring areas were available, in order to exploit full resolution data for the detection of fractures' characterizing marks and local distributions in relation to other fracture sets and sediment laminations. We performed 3D reconstruction of the same investigated outcrops by means of Agisoft software (Fig.2) coupling to the 2D information the distribution of light-toned veins across the all area. We produced the three-dimensional model on the basis of spatial geometric information of the target region obtained from multiple images taken by MastCam binocular stereo vision and NavCam systems that accordingly acquired sets of overlapping photos for the reconstruction of the surface around the rover track. Agisoft PhotoScan is a 3D advanced modelling package based on image data processing and can automatically build the models without setting initial values and control points starting from images taken at any position and angle as far adjacent photos share corresponding points recognizable on the targets. The scale computed by the software was tested by comparing it with the known size objects such as rovers' wheels. Loading the images into Agisoft, the software automatically searches for the corresponding points matching and aligning the photos and finally generating a sparse point cloud. When the automatic alignment procedure failed, tie points were manually implemented in

the system to exploit the maximum number of images available. On the point cloud, that is generally denser closer to the observation point and favorably oriented surfaces (such is the case of the herein presented case study), an irregular triangle net can be built along with a dense point cloud, next the texture mapping is carried out according to the so produced triangle net. During the process of creation of the model and the stitching of images to produce its texture, data resolution is lost making impossible the details recognition. This information loss remarks the importance of coupling the 2D full resolution images analysis to the three-dimensional spatial information for a profitable interpretation. We carried out the further step of elaboration by implementing this new load of produced data into Cloud Compare environment, which is a 3D point cloud and triangular mesh processing software that allows the user to interact with 3D entities rotating, translating, drawing 2D polylines, picking points and extracting correspondent 2D and 3D information. In this context veins were marked by tracing polylines and further structural information (i.e. dip direction and dip angle, intersections angles, kinematics estimates) was developed by plane fitting and contextual data extraction through the compass plugin.

4. Results

By the analysis of the outcrop group that Curiosity rover observed between sol 1536 and 1545 we collected structural information specifically based on the distribution of light-toned veins neatly distinguishable in the area. Both in 2D images and 3D reconstruction, the presence of different sets of non-randomly distributed fractures was neatly recognizable.

The first general distinction identifiable from the raw images observation is the overall presence of one population of sub-horizontal sub-parallel light-tones veins and a second population of middle to high-angle dipping light-tones veins (Fig.3). All the fractures appear to have a better erosion resistance with respect of the host rock, thus they tend to stick out from the knobs leading to an easy identification all over the outcrops. Sub-horizontal veins do not show significant thickness variations both at the single vein scale and among the general population, although lateral continuity is unclear and a patched distribution seems to be overall the most reasonable. These layers show a well recognizable undulate, slightly wandering trend as recognizable in the measurements which display a $\sim 15^\circ$ dipping angle variation range and a broad

variability among the recorded dip directions, this recorded by veins that bend and stop on the neighbouring ones despite a consistently average sub-parallel behaviour. These veins appear to follow the rock's layer boundaries in many of the recorded outcrops and at the same time clear layers crosscuttings are also visible in the same exposed surfaces.

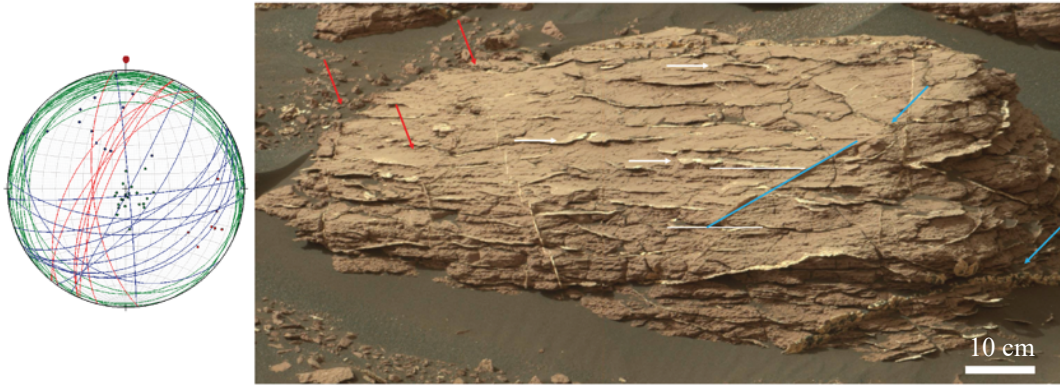


Fig.3 In the stereo plot are represented the orientation of all the fracture planes detected on the study area on Mars (a). On the Baldwin corner outcrop are visible all the vein sets recognized from the analysis of the entirety of the study area (b), these are represented in red, blue (middle to high angle sets) and white (horizontal set).

Differently from the sub-horizontal fractures, that are pervasive and very densely distributed among the whole outcrop population, the oblique ones are rarer. These veins display meaningful thickness variations in places due to clear en-echelon structures well recognizable by the distinctive arrays of sigmoidal shaped cracks (Nicholson and Pollard, 1985) that propagate from the margin of a larger parent crack, twisting out and bending as the result of mechanical interaction between tips of adjacent parallel cracks (Pollard et al. 1982). Such geometries are used to infer the state of deformation (Ramsay & Huber 1983) or the state of stress (Pollard et al. 1982, Rickard & Rixon 1983) in the surrounding rock at the time of cracking and accordingly, in the specificity of this case study, the en-echelon features display a extensional regime, that is to say that the cracking pattern recorded a vertical stress that exceeded the lateral ones producing a lowering of the hanging walls. We detected two different sets of oblique cracks based on dip/dip-direction trends: (i) one with a average value of dip direction: 290°N and dip: 67° (spanning between minimum and maximum values of: 264° - 309° dip direction and 54° - 77° dip) and a (ii) second one showing a dip direction-dip average value of 155°N - 53° (spanning between minimum and maximum values of: 126° - 184° dip direction and 31° - 71° dip). The

two population of oblique fractures are thus spaced by an angle of 60° according to the measurements, that find validation in the observation from single outcrops where fracture from both the oblique sets are visible.

Cross-cutting relationships were investigated in the light-toned veins networks and a syngenetic interplay has been inferred due to a mutual recurrent crosscutting between sub-horizontal and oblique fractures. No evidence of displacement was found and neither recurrent truncation of one set on the other were observed to determine an occurrence sequence.

5. Bletterbach analogue site

To enhance observations and understanding of the process that lay behind the veins formation, we herein implement in the comparative analysis the Bletterbach case study, where several outcrops along the gorge display fractures and light veins similar to the ones detected at Gale.

The Arenaria di Val Gardena Formation outcrops at Bletterbach, in Bolzano NE Italy, where neat sections of the arenaceous to clay terrestrial red beds are exposed along the gorge. After the interruption of volcanic activity that characterized the Early Permian period, this facies association suggest the development of extensive fluvial systems that gradually underwent a fining upward evolution. Late Permian deposits, where the Bletterbach outcrops are set, belong to fluvial, coastal sabkha and shallow marine environments (Cassinis et al., 1988). Here evidence of soils development and gypsum deposits are visible reflecting the arid climate characterized by seasonal or ephemeral fluvial activity. In the Bletterbach gorge can be found channel infillings of sandstone and red to grey mudstones displaying ripples, laminations, cracks and nodular gypsum levels (Massari et al. 1988). These facies associations have been related to the transition between the distal portion of a fluvial system and a coastal sabkha where shallow water floods were likely to happened (Conti et al., 1986; Massari et al., 1988, 1994).



Fig.4 Phase 1 represented by oblique nodular gypsum veins (a) and phase 2 characterized by mostly sub-horizontal tabular veins (b,c).

The outcrops of interest are ~5 to 10 m thick red mudstone levels sitting on top of the rhyolitic bedrock and overlain by grey sandstones. At Bletterbach, gypsum accumulations come in two different assets that we interpret to be the expression of two consecutive stages of formation: (i) gypsum nodules and nodular fractures filled with white to greyish gypsum (Fig.4a; Fig.5b), this set of veins are only present in the red mudstone levels and mostly abundant in their upper portions right below the physical contact with the overlain sandstones; (ii) neat white tabular gypsum veins (Fig.4b, c) with well recognisable antitaxially arranged crystals (i.e. gypsum fibers grow perpendicular to the fracture walls and the median zone, site of the original fracture. Typically, antitaxial veins display a mineralogy different from the hosting rock and the mineral deposition comes along with supersaturated fluid circulation during single or multiple crack-seal events (Ramsay, 1980; van der Pluijm & Marshak, 2004)) cutting both mudstones and sandstones.



Fig.5 Hydrofractured horizontal veins departing from the thicker vertical pipe (a). These set of vein shows no gypsum infilling, but a clearly recognizable green alteration. Hydrofracturing from nodules' tips (green arrows) and veins departing or crosscutting phase 1 nodules (white arrow) highlighting the two different subsequent events (b).

The first stage is represented by the nodular gypsum phase that we interpret to be the product of a percolation process that took place before the materials compaction when sediments were still loose and permeable. This phase involved sulfate-rich fluids that percolated through sandstones and stopped below their lower interface with mudstones due to a significative permeability contrast. This mechanism thus induced the accumulation of gypsum in the mudstone upper portion as a thick layer at the interface and nodules that generated under a hydrostatic isotropic drive and a plastic accommodation due to an underconsolidation of the hosting sediments.

The second stage of veining evolution took place after the consolidation of the materials and produced networks of hydrofractured veins (Fig.5) involving both mudstones and sandstones. We observed vertical to high angle ($\geq 60^\circ$ dip) pipes draining fluids in upward direction and dense systems of tabular sub-horizontal fractures with a preferential distribution along pre-existing layers. Sub-vertical veins thickness spans between 0.7 to 10 cm depending on the observed site, while sub-horizontal systems are constituted by thin veins of around 0.1 – 0.5 cm, in all the cases vertical pipes at least double the thickness of the sub-horizontal sets (Fig.6d). The subsequential timing of the events is marked by the presence of fractures and veins, displaying the characteristic traits of phase two, crosscutting nodules or nodular fractures belonging to phase one. In places nodules result to be involved in

this second stage of gypsum mobilization and typical hydrofractured cracks depart from nodule tips (Fig.5b).

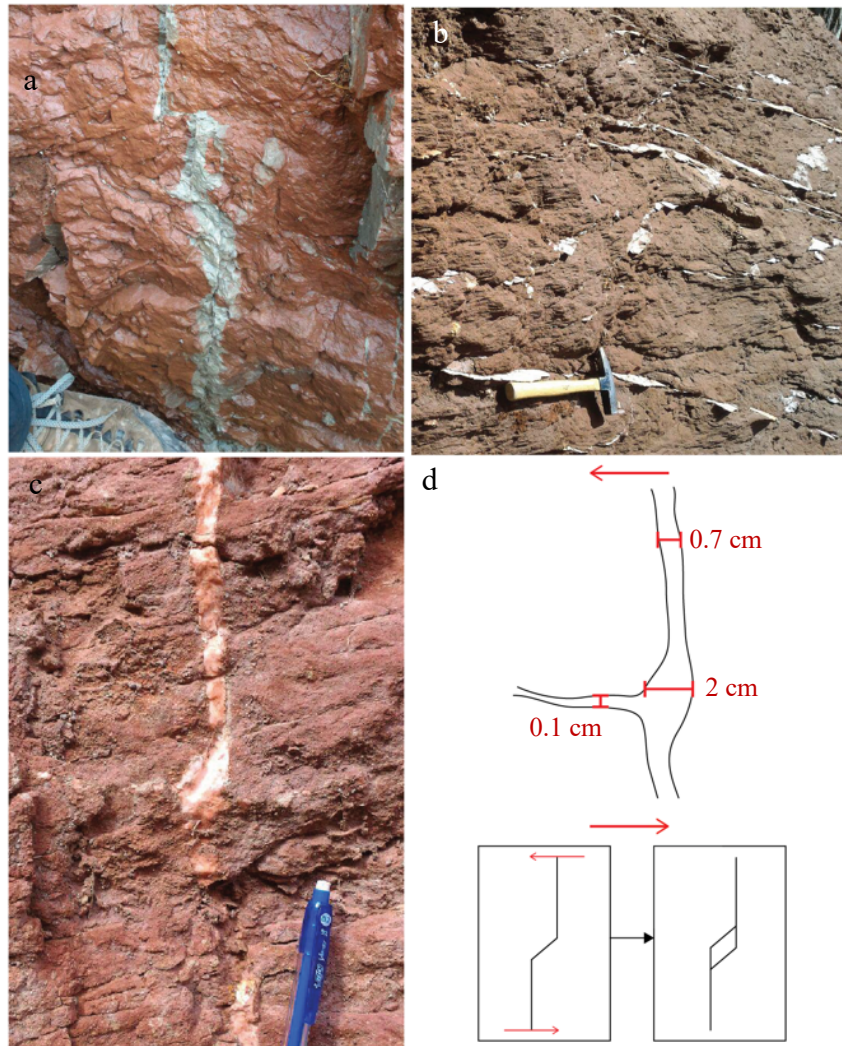


Fig.6 Step over faulting (a), bridge structures (b) and pull-apart fracture bulging (c, d) displaying shearing in an overall extensional context.

Alternatively, when nodules did not experience a secondary fluid circulation, they can act as pressure shadows spots and permeability contrast surfaces deflecting vein propagation around them. One of the outcrops shows fractures with no pervasive gypsum infilling, differently an evident green alteration testifies fluid circulation and just in places sub-millimetric thick gypsum infills can be observed within the fracture core. In both cases, with and without gypsum infilling, evidence of shearing behavior in an extensional context is recorded by bridge structures and step over faulting (Fig.6).

6. Discussions

On Mars, the combination of 2D and 3D products on the Gale crater floor with high-resolution in situ data along the rover track allows to pursue a structural interpretation of the basin at the time of cracking. Both oblique fracture sets and the horizontal one need to be taken into account, in fact both systems crosscut the host rock laminations leading to the exclusion of a depositional layering interpretation. A regime of extension seems to have been recurrently recorded by two cross-cutting sets of light-tone vein planes which intersect at angles of $\sim 60^\circ$ and show en-echelon structures displaying shear sense that led to a lowering of the hanging wall. Accordingly, the maximum principal stress is suggested to bisect the acute angle occurring between the sets, that in the specificity of this case would mean that σ_1 lays on a sub-vertical axis. The horizontal stresses σ_2 and σ_3 orientations are not equivalently well constrained because of the slightly wandering direction trend of the oblique fracture sets. Fracture strike direction can vary on a range in stress fields where σ_2 and σ_3 are equal (Caswell and Milliken, 2017; Schieber et al., 2017 and references therein) which is a reasonable scenario in a closed sedimentary basin, where the even horizontal constraint is the crater lateral confinement. Alternatively, the set of horizontal veins is well-matching disposition and morphology of failures induced by fluid overpressure recorded on Earth that happened during the fluid resurgence cracking the host rock along fresh plains or exploiting previously existing surfaces of weakness such as the mudstone layering. On Mars, Gale experienced water-rich early stages during which the crater could have been connected to both surficial and underground water reservoirs (e.g., Villanueva et al. 2015; Andrews-Hanna et al., 2010), thus implying transient flooding and drying in sabkha or ephemeral lake environments leading again to mineral accumulation in the basin. Subsequent dissolution and mobilization of these deposits by diagenetic fluids led to the formation of the sulfate veins observed on the rover traverse (L'Haridon et al., 2018; Schwenzer et al., 2016; Nachon et al., 2015, 2016; Grotzinger et al., 2014; McLennan et al., 2014).

For the reconstruction of the cracking processes on Mars a cross comparison with terrestrial environments were undertaken. The Mercia Mudstone Group outcrops in Watchet Bay, are already recognised as a valid terrestrial analogue for the Gale crater (e.g. Schwenzer, 2016; Young and Chan, 2017).

Herein we present evidence collected from the observation of several outcrops at Bletterbach that make it an efficient case study due to the multiple similarities with the Martian counterpart. Sulfate infilled fracture networks display assets and morphology closely resembling the veins recorded at Gale. On Mars, in the study area herein analysed are visible vein sets that have marked matches with the products of the second evolution phase in the Bletterbach gorge that are sub-vertical pipes surrounded by denser sub-horizontal systems of layer mostly following pre-existing layers planes and bridge structures recording shearing in an extensional regime. Additionally, at Bletterbach the mudstones are nestled between the volcanic bedrock and the roofing sandstones resembling a scenario reasonable also for its Martian counterpart where it is expectable to find the volcanic crater floor below the lacustrine sediments that are superimposed by aeolic sandstone deposits (e.g. Le Deit et al., 2016; Treiman et al., 2016; Stack et al., 2015; Bristow et al., 2015; Grotzinger et al., 2014, 2015).

Accordingly, due to the above-mentioned interpretations of previous and new analogue sites for Gale crater light-toned vein systems, we assess the relevance of both the case studies that are displaying different pivotal aspects mutually absent when considering each single scenario. New and literature observations on terrestrial environments thus function together as a comparison base for a solid interpretation of Martian structural asset.

7. Conclusions

Light-toned fracture networks have been observed repeatedly along Curiosity rover traverse (e.g. Watkins et al., 2017) and their mutual distribution reflects the stress field they have been exposed to at the moment of cracking. Within the window of ten sols (sol 1536 – sol 1545) herein analysed, Curiosity acquired a large number of images from different angles of a field of badrock knobs outcropping from the sand where many sulfate veins were neatly visible. This asset allowed the 3D reconstruction of the area and, contextually, the 3D reconstruction of the plane set where fractures lay. On Earth, similar arrangements can be observed at Watchet Bay and at Bletterbach gorge where networks of intersecting sulfate veins developed thanks to hydrofracturing regimes within reddish mudstone levels.

In Gale, the cracking process is therefore to be ascribed to two different contributions: (i) the 60° dipping fractures are to be considered the product of an extensional regime where the principal stress lays on a vertical axis and σ_2 and σ_3 are horizontal and moderately wandering (Fig.3a); (ii) the set of sub-horizontal fractures are the result of a hydrofracturing process, synchronous to the extensional deformation, where fluid overpressure was energetic enough to open new fractures just in places, but mostly used pre-existing weakness surfaces constituted by mudstone layering. This interpretation is moreover well supported by the geological context. Gale is a large crater that experienced water and sediment infilling, the vertical maximum stress is reasonably to be ascribed to such progressive overload, while the wandering nature of minimum stresses is due to the even lateral confinement produced by the crater shape. The second cracking drive, hydrofracturing, can be triggered either by the emplacement of an overburden that perturbs fluid pressure and initiates the buoyancy, or as response to an unloading event when pressurized fluids are already stored in the subsurface. The origin of fluids at Gale is still debated and overpressure cracking itself does not carry enough information to discriminate it. Nevertheless, the evidence of a coeval genesis of the oblique and the horizontal vein networks leads to the hypothesis that a pulse of material overload within the crater could have been responsible both for the extensional failure and the fluid escape from the already consolidated deposits on the crater floor.

Veins mapping and reconstruction both on Mars and Earth allowed the production of a well constrained structural context interpretation and cracking driving forces identification which are likely to have been active in the whole crater area so producing a structural context for the entirety of the fracture and vein networks that have been recorded along the rover traverse.

References

- Abramov O. and Kring D. A. 2005. Impact-induced hydrothermal activity on early Mars. *Journal of Geophysical Research* 110:E12S09. doi: 10.1029/2005JE002453.
- Andrews-Hanna, J.C., et al., 2010. Early Mars hydrology: Meridiani playa deposits and the sedimentary record of Arabia Terra. *J. Geophys. Res. E Planets* 115, 1–22. <https://doi.org/10.1029/2009JE003485>
- Bell, F. G., 2000. *Engineering Properties of Soils and Rocks*. Oxford: Blackwell.
- Bell, J. F., et al., 2012. Mastcam multispectral imaging on the Mars Science Laboratory rover: wavelength coverage and imaging strategies at the gale crater field site, *Lunar Plan. Sci. Conference*, pp 2541
- Bennison, G. M. and Wright, A. E. 1969. *The Geological History of the British Isles*. London: Edward Arnold Ltd, 406 pp.
- Bjørlykke, K. 1997. Lithological control on fluid flow in sedimentary basins. In *Fluid Flow and Transport in Rocks* (eds B. Jamtveit & B. W. D. Yardley), pp. 15–34. London: Chapman and Hall.
- Bristow, T. F., et al., 2015. The origin and implications of clay minerals from Yellowknife Bay, Gale crater, Mars, *Am. Mineral.*, 100, 824–836, doi:10.2138/am-2015-5077CCBYNCND.
- Cartwright, J. A. 1997. Polygonal extensional fault systems: a new class of structure formed during the early compaction of shales. In *Fluid Flow and Transport in Rocks* (eds B. Jamtveit & B. W. D. Yardley), pp. 35–56. London: Chapman & Hall.
- Cassinis, G., et al., 1988. The continental Permian in the Southern Alps (Italy). A review. *Zeitschrift für Geologische Wissenschaften*, 16:1117-1126.
- Caswell, T.E., Milliken, R.E., 2017. Evidence for hydraulic fracturing at Gale crater, Mars: implications for burial depth of the Yellowknife Bay formation. *Earth Planet. Sci. Lett.* 468, 72–84. doi:10.1016/j.epsl.2017.03.033.
- Conti, M.A., et al., 1986. The Bletterbach-Butterloch section (Val Gardena Sandstone and Bellerophon Formation), p. 99-119. In *Italian IGCP 203 Group (eds.)*, Field conference on Permian and Permian-Triassic boundary in the South-Alpine segment of the Western Tethys. Field Guide-Book. Società Geologica Italiana, Brescia, Italy.
- Cosgrove, J.W., 2001. Hydraulic fracturing during the formation and deformation of a basin: A factor in the dewatering of low-permeability sediments. *Am. Assoc. Pet. Geol. Bull.* 85, 737–748. <https://doi.org/10.1306/8626C997-173B-11D7-8645000102C1865D>
- Domenico, P. A. & Schwartz, F. W. 1998. *Physical and Chemical Hydrogeology*, 2nd ed. New York: Wiley, 506 pp.
- Grotzinger, J.P., et al., 2014. A habitable fluvio-lacustrine environment at Yellowknife Bay, Gale crater, Mars. *Science* (80–) 343 (6169). 1242777–1242777 doi: 10.1126/science.1242777.
- Grotzinger, J.P., et al., 2015. Deposition, exhumation, and paleoclimate of an ancient lake deposit, Gale crater, Mars. *Science* (80–) 350 (6257). aac7575-aac7575 doi: 10.1126/science.aac7575.
- Gudmundsson, A. & Brenner, S. L. 2001. How hydrofractures become arrested. *Terra Nova* 13, 456–62.
- Gudmundsson, A., et al., 2002. Propagation pathways and fluid transport of hydrofractures in jointed and layered rocks in geothermal fields. *Journal of Volcanology and Geothermal Research* 116, 257–78.
- Haridon, J.L., et al., 2018. Chemical variability in mineralized veins observed by ChemCam on the lower slopes of Mount Sharp in Gale crater, Mars. *Icarus* 311, 69–86. <https://doi.org/10.1016/j.icarus.2018.01.028>
- Le Deit, L., et al., 2016. The potassic sedimentary rocks in Gale crater, Mars, as seen by ChemCam on board Curiosity. *J. Geophys. Res. Planets* 121 (5), 784–804. doi:10.1002/2015JE004987.
- Leslie, A. B., et al., 1993. Geochemical and mineralogical variations in the upper Mercia Mudstone Group (Late Triassic), southwest Britain: correlation of outcrop sequences with borehole geophysical logs. *Journal of the Geological Society, London* 150, 67–75.
- Léveillé, R.J., et al., 2014. Chemistry of fracture-filling raised ridges in Yellowknife Bay, Gale crater: window into past aqueous activity and habitability on Mars. *J. Geophys. Res. Planets* 119 (11), 2398–2415. doi:10.1002/2014JE004620.
- Maki, J. N., et al., 2011. The Mars Science Laboratory (Msl) Navigation Cameras (Navcams), *Lunar Plan. Sci. Conference*, pp 2738
- Massari, F., et al., 1994. Sedimentology, palynostratigraphy and sequence stratigraphy of a continental to shallow-marine rift-related succession: Upper Permian of the eastern Southern Alps (Italy). *Memorie di Scienze Geologiche*, 46:119-243.

- Massari F., et al., 1988. The Val Gardena Sandstone and Bellerophon Formation in the Bletterbach Gorge (Alto Adige, Italy): biostratigraphy and sedimentology. *Memorie di Scienze Geologiche*, 40:229-273.
- McLennan, S.M., et al., 2014. Elemental geochemistry of sedimentary rocks at Yel-lowknife Bay, Gale crater, Mars. *Science* (80-) 343 (6169), 1244734. doi:10.1126/ science.1244734.
- Milliken, R.E., et al., 2010. Paleoclimate of Mars as captured by the stratigraphic record in Gale crater. *Geophys. Res. Lett.* 37 (4), 1–6. doi:10.1029/2009GL041870.
- Nachon, M., et al., 2014. Calcium sulfate veins characterized by ChemCam/Curiosity at Gale crater, Mars. *J. Geophys. Res. Planets* 119 (9), 1991–2016. doi:10.1002/ 2013JE004588.
- Nachon, M., et al., 2016. Chemistry of diagenetic features analyzed by ChemCam at Pahrump Hills, Gale crater, Mars. *Icarus* 0, 1–16. doi:10.1016/j.icarus.2016.08. 026.
- Neuzil, C. E. 1995. Abnormal pressures as hydrodynamic phenomena. *American Journal of Science* 295, 742–86.
- Nicholson, R. & Pollard, D.D. 1985. Dilation and linkage of en-echelon cracks. *Journal of Structural Geology*, 7, 583–590.
- Osborne, M. J. & Swarbrick, R. E. 1997. Mechanisms for generating overpressure in sedimentary basins: A reevaluation. *American Association of Petroleum Geologists Bulletin* 81, 1023–41.
- Phillip, S. L., 2008. Geometry and formation of gypsum veins in mudstones at Watchet, Somerset, SW England, *Geol. Mag.*, 145(6), 831–844, doi:10.1017/S0016756808005451.
- Pollard, D. D., Segall, P. & Delaney, P. T. 1982. Formation and interpretation of dilatant echelon cracks. *Bull. geol. Soc. Am.* 93, 1291-1303.
- Pollard, D. D. & Segall, P. 1987. Theoretical displacement and stresses near fractures in rocks: with application to faults, joints, veins, dikes, and solution surfaces. In *Fracture Mechanics of Rocks* (ed. B. Atkinson.), pp. 277–349. London: Academic Press
- Rapin, W., et al., 2016. Hydration state of calcium sulfates in Gale crater, Mars: identification of bassanite veins. *Earth Planet. Sci. Lett.* 452, 197–205. doi:10.1016/j. epsl.2016.07.045.
- Ramsay, J. G. 1980. The crack-seal mechanism of rock deformation. *Nature* 284, 135–9
- Ramsay, J. G. & Huber, M. I. 1983. *The Techniques of Modern Structural Geology, Volume 1, Basic Techniques--Strain Analysis.* Academic Press, London.
- Rickard, M. J. & Rixon, L. K. 1983. Stress configurations in conjugate quartz-vein arrays. *J. Struct. Geol.* 5,573-578.
- Rubin, D.M., et al., 2017. Fluidized-sediment pipes in Gale crater, Mars, and possible Earth analogs. *Geology* 45, 7–10. <https://doi.org/10.1130/G38339.1>
- Savin, G. N. 1961. *Stress Concentrations around Holes.* London: Pergamon, 430 pp.
- Schieber, J., et al., 2017. Encounters with an unearthy mudstone: Understanding the first mudstone found on Mars, *Sedimentology*. <https://doi.org/10.1111/sed.12318>
- Schwenzer, S.P., et al., 2016. Fluids during diagenesis and sulfate vein formation in sediments at Gale crater, Mars. *Meteorit. Planet. Sci.* 28. doi:10.1111/maps. 12668.
- Schwenzer S. P. and Kring D. A. 2009. Impact-generated hydrothermal systems: Capable of forming phyllosilicates on Noachian Mars. *Geology* 37:1091–1094.
- Schwenzer S. P. and Kring D. A. 2013. Alteration minerals in impact-generated hydrothermal systems—Exploring host rock variability. *Icarus* 226:487–496.
- Siebach, K.L., Grotzinger, J.P., Kah, L.C., Stack, K.M., Malin, M., L veill , R., Sumner, D.Y., 2014. Subaqueous shrinkage cracks in the Sheepbed mudstone: implications for early fluid diagenesis, Gale crater, Mars. *J. Geophys. Res. Planets* 119 (7), 1597–1613. doi:10.1002/2014JE004623.
- Simms, M. J. and Rufell, A. H. 1990. Climatic and biotic change in the late Triassic. *Journal of the Geological Society, London* 147, 321–7
- Stack, K.M., et al., 2014. Diagenetic origin of nodules in the Sheepbed member, Yel-lowknife Bay formation, Gale crater, Mars. *J. Geophys. Res. Planets* 119 (7), 1637– 1664. doi:10.1002/2014JE004617.
- Stack, K. M., et al., 2015. Sedimentology and stratigraphy of the Pahrump Hills outcrop, lower Mount Sharp, Gale Crater, Mars, 46 calcium sulfate veins as observed by the ChemCam instrument, 46 Planetary Science Conference, 2 pp.
- Stack, K. M., et al. 2016. Comparing orbiter and rover image-based mapping of an ancient sedimentary environment, Aeolis Palus, Gale crater, Mars, *Icarus*, doi:10.1016/j.icarus.2016.02.024.
- Thomson, B.J., et al., 2011. Constraints on the origin and evolution of the layered mound in Gale crater, Mars using Mars Reconnaissance Orbiter data. *Icarus* 214 (2), 413–432. doi:10.1016/j.icarus.2011.05.002

- Treiman, A.H., et al., 2016. Mineralogy, provenance, and diagenesis of a potassic basaltic sandstone on Mars: CheMin X-ray diffraction of the Windjana sample (Kimberley area, Gale crater). *J. Geophys. Res. Planets* 121 (1), 75–106. doi:10.1002/2015JE004932.
- Van Der Pluijm, B. A. & Marshak, S. 2004. *Earth Structure*, 2nd ed. New York: McGraw Hill, 656 pp.
- Vaniman, D.T., et al., 2018. Gypsum, bassanite, and anhydrite at Gale crater, Mars. *Am. Mineral.* 103, 1011–1020. <https://doi.org/10.2138/am-2018-6346>
- Villanueva G. L. et al., 2015. Strong water isotopic anomalies in the Martian atmosphere: Probing current and ancient reservoirs. *Science* 348:218–221.
- Watkins, J. A., et al., 2017. Fracture formation by compaction-related burial in Gale crater, Mars: implications for the origin of Aeolis Mons, Lunar Plan. Sci. Conference, pp 3019
- Whittaker, A. and Green, G. W. 1983. *Geology of the country around Weston-super-Mare*, memoir for 1:50,000 geological sheet 279. New series, with parts of sheet 263 and 295. Geological Survey of Great Britain, Institute of Geological Sciences. London: Her Majesty's Stationery Office, 147 pp.
- Young, B.W., Chan, M.A., 2017. Gypsum veins in Triassic Moenkopi mudrocks of southern Utah: Analogs to calcium sulfate veins on Mars. *J. Geophys. Res.* 150–171. <https://doi.org/10.1002/2016JE005118>

Appendix: *Future developments*

Introduction

On Earth, the evolution of hydrosphere and atmosphere is the result of the interplay of volcanic activity, asteroid impacts, tectonism and biological activity. Below the surface at depth, water becomes hot and saline; on Earth in such environments water may contain up to 40 wt% total dissolved solids and have temperatures greater than 100°C. These kinds of waters are also known as brines, which play a very important role in the formation of sedimentary-hosted hydrothermal mineral deposits. First organic molecules were first synthesised in aqueous solutions and the most primitive biota was likely to have flourished in proximity of hydrothermal discharges. All functioning terrestrial biological systems consist predominantly of water that is one of the fundamental requirements for life as we know it. In fact, water is an excellent solvent and the wide range of temperatures under which it maintains its liquid state makes it an ideal medium for chemical reactions to occur. Life on Earth arose in water that covers two thirds of the surface of the planet and is found in all three phases of liquid, solid and vapour. On the surface water exists in the liquid state in a variety of different environments, it also exists as vapour in the atmosphere and in volcanic emissions and as a solid in the polar ice caps, glaciers and as permafrost. This asset makes Earth a unique place for life growth and development, whereas other terrestrial planet in the Solar System are comparatively dry and water only exists in the vapour state, or as ice in the subsurface or may not be present at all. Contextually, not only water is a pivotal ingredient for life, but also hydrothermal processes may have been of critical importance in the development of early life on Earth. Today the oldest known fossil structures are putative microfossils and macroscopic stromatolites that have been interpreted to have occurred in such kind of environments.

Particularly, on Mars, as extensively discussed in the previous sections, ground ice and putative groundwater are key elements for the search for environments suitable for hosting extinct or extant biota. Martian hydrothermal processes are far less constrained with the respect of their terrestrial counterparts, but the undoubtable widespread volcanic activity that shaped the planet could have driven a fluid

circulation within the crust. Establishing if life ever existed on Mars is one of the outstanding scientific questions of our time and to reach this goal many different missions have been sent to the red planet to survey its surface and atmosphere. More than 40 missions have attempted to reach for Mars with different degrees of success since the 1960s. The latest ESA (European Space Agency) programme oriented toward the exploration of Martian habitability and the seek for signs of life is ExoMars. This is a two missions-based exploration programme: one orbiter, TGO (Trace Gas Orbiter), already orbiting the planet that entered the nominal scientific phase in April 2018, and one rover dedicated to geochemistry and exobiology, launch date planned for 2020. The main objective of the operating mission TGO is to gain a better understanding of methane (that represent less than the 1% of the Martian atmosphere) distribution since it could be evidence for possible of present-day biological or geological activity due to its short lifetime (~300 year) in the Martian atmosphere.

The following sections of this chapter represent the initial stages of research work that aims to focus on the hydrothermal nature of fluid circulation and mineral alterations, hence moving a step forward in the direction that brings from the identification of fluid circulation and the related structural asset, that has been extensively presented in the previous chapters, to the investigation of the processes that characterise such environments on Mars.

Additionally, new data load acquired by current operating missions, such as TGO and specifically the CaSSIS (Colour and Stereo Surface Imaging System) camera have been implemented in this section.

References

- Campbell, K.A., 2006. Hydrocarbon seep and hydrothermal vent paleoenvironments and paleontology: Past developments and future research directions. *Palaeogeogr. Palaeoclimatol. Palaeoecol.* 232, 362–407. doi.org/10.1016/j.palaeo.2005.06.018
- Cockell, C.S., Balme, M., Bridges, J.C., Davila, A., Schwenzer, S.P., 2012. Uninhabited habitats on Mars. *Icarus* 217, 184–193. https://doi.org/10.1016/j.icarus.2011.10.025
- F. Pirajno, Eroglu S., Toprak S., Urgan O, MD, Ozge E. Onur, MD, Arzu Denizbasi, MD, Haldun Akoglu, MD, Cigdem Ozpolat, MD, Ebru Akoglu, M., 2012. Hydrothermal Processes and Mineral Systems, *Saudi Med J.* doi.org/10.1073/pnas.0703993104
- Parnell, J., McMahon, S., 2016. Physical and chemical controls on habitats for life in the deep subsurface beneath continents and ice. *Philos. Trans. R. Soc. A* 374, 20140293. https://doi.org/10.1098/rsta.2014.0293
- Van Kranendonk, M.J., 2006. Volcanic degassing, hydrothermal circulation and the flourishing of early life on Earth: A review of the evidence from c. 3490-3240 Ma rocks of the Pilbara Supergroup, Pilbara Craton, Western Australia. *Earth-Science Rev.* 74, 197–240. doi.org/10.1016/j.earscirev.2005.09.005
- Webster, C.R., Mahaffy, P.R., Atreya, S.K., Flesch, G.J., Mischna, M.A., Meslin, P., Farley, K.A., Conrad, P.G., Christensen, L.E., Pavlov, A.A., Martín-torres, J., Zorzano, M., McConnochie, T.H., Owen, T., Eigenbrode, J.L., Glavin, D.P., Steele, A., Malespin, C.A., Jr, P.D.A., Sutter, B., Coll, P., Bridges, J.C., Navarro-gonzalez, R., Gellert, R., 2015. Mars methane detection and variability at Gale crater. *Science* (80-.). 347, 415–417. doi.org/10.1126/science.1261713
- Westall, F., Loizeau, D., Foucher, F., Bost, N., Bertrand, M., Vago, J., Kminek, G., 2013. Habitability on Mars from a microbial point of view. *Astrobiology* 13, 887–897. doi.org/10.1089/ast.2013.1000

Work in progress

LOOKING FOR WATER-RELATED ENVIRONMENTS ON MARS: ANALYSIS OF REFLECTANCE SPECTRA FOR PRESENT AND FUTURE EXPLORATION

Barbara De Toffoli ^{a,b}, Cristian Carli ^c, Alessandro Maturilli ^d, Francesco Sauro ^e,
Matteo Massironi ^{a,b}, Jörn Helbert ^d

^a Department of Geosciences, University of Padova, Italy

^b INAF, Osservatorio Astronomico di Padova, Italy

^c IAPS, Istituto Nazionale di Astrofisica, Rome, Italy

^d Institute for Planetary Research, DLR, Berlin, Germany

^e Department of Biological, Geological and Environmental Sciences, Italian Institute of Speleology, University of Bologna, Italy

Spectroscopic analyses of basalt epithermal alterations, clay minerals and samples representative of wet sedimentary environments in a broad wavelength range from the ultraviolet to the far-infrared provide new loads of information for present and future exploration of environments that could have been linked to water and gas emission. Specifically, methane emission centers on the Martian surface are high interest targets for ExoMars mission since they involve environments where life could have potentially arisen, grown and given a contribution to the degassing phenomenon.

1. Introduction

Our project aims to investigate the origin of the methane recently observed in Martian atmosphere (e.g. Geminale et al., 2008; Mumma et al., 2009) and discuss if it could be linked to biological processes. Several geological and ecological mechanisms could be supposed to contribute to methane release, such as volcanic degassing, permafrost seasonal melting and emission from subsurface traps (Oehler and Etiope, 2017; Komatsu et al., 2011; 2016). Mud and water resurgences features on Mars are primary objectives for the astrobiology and climate change studies and

investigating the nature of the unconsolidated materials that have been mobilized will lead to step forward in the understanding of the processes that lie behind. Such environments have been recognized in numerous locations on the Martian surface (see Oehler and Etiope, 2017 for an updated overview) and accordingly various scenarios need to be tackled. Indeed, during the Martian ancient past, sediments could have been deposited and trapped thanks to surficial sedimentary processes, hence hydrous alterations and possibly biomineralization or putative organic matter could be found. Differently, basalts could have experienced alteration linked to fluid circulation in the subsurface, so serpentinisation related to hydrothermal systems should be taken also into account. On Earth mud volcanoes are mainly associated to the degassing phenomenon (Skinner and Mazzini, 2009; Pondrelli et al., 2011; Okubo, 2016; Fig.1) and given recurrent observations of large fields of pitted mounds that have in place been interpreted as mud volcanoes (e.g. Oehler and Allen, 2010; McGowan, 2011), or are anyway high potential candidate for subsurface sediments and fluids mobilization (see chapter 2), mud/sedimentary volcanism has been set as primary target of such follow-up analyses that were further focused on a putative mud volcanism linked to the hydrothermal fluids and groundwater interaction, supported by evidences of a recent volcanic activity (e.g. Dohm et al., 2008).

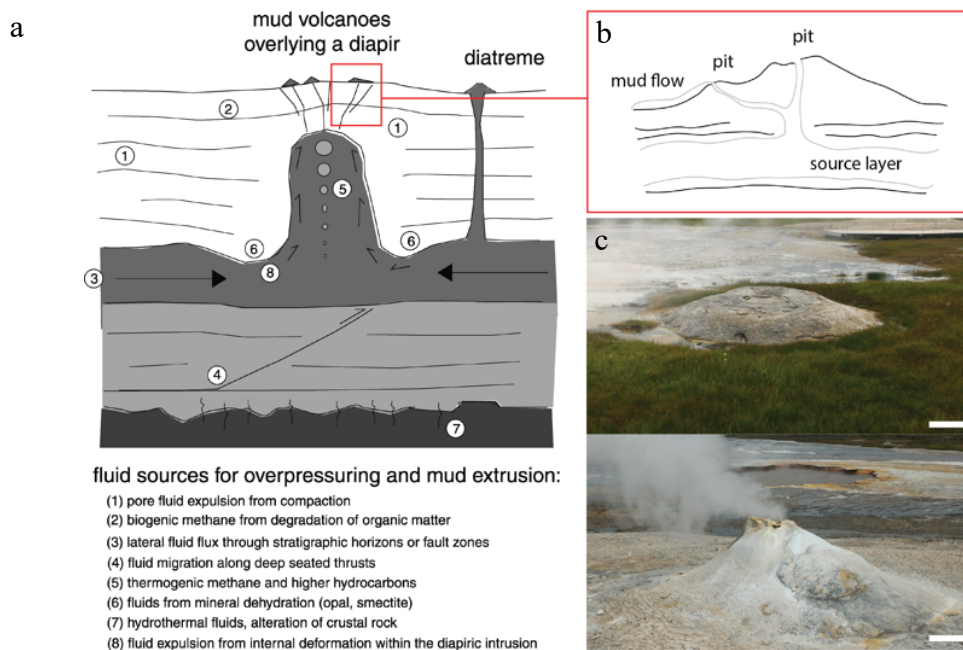


Figure 1. Schematic representation (a, b) of fluid and sediment expulsion mechanisms (modified from Kopf, 2002) and examples of Icelandic surface expressions of active epithermal systems (c).

Subsequently to geomorphological investigations of mud and water resurgence features on Mars, a compositional analysis on terrestrial analogues is to be carried out to enhance libraries for a profitable comparison with spectral images of the Martian surface (e.g. CRISM and OMEGA products). To fulfil this goal, we performed spectroscopic analyses using a wide range of wavelengths, from ultraviolet to far infrared, on powdered rocks and minerals that can be connected to fluid activity such as basalt and epithermal alterations, clay mineral family and sedimentary environments.

The epithermal mineral systems group has a high potential as terrestrial analogue type-site for such kind of environments related to sediment and water expulsion detected on Mars. These systems show key traits that are good matching with the boundary conditions observed for the pitted mound fields rooted into the gas-hydrate rich cryosphere; accordingly epithermal systems are defined by: (i) the characteristic triggering interaction between hydrothermal fluids and groundwater at shallow depth, (ii) the low temperatures ranges ($<280^{\circ}\text{C}$) for the mineral deposition, (iii) the surface expression through mud volcanoes, hot springs and pools and (iv) the connection with methane and other minor gas loss (Simmons et al., 2015, Peters et al., 1991). Overall, epithermal systems deposits show an extremely characteristic mineral association both concerning the alterations and the deposited mineralization (White et al., 1995).

2. *Methods*

Samples belonging to water related environments were investigated, specifically clays, epithermal minerals and siliceous stromatolites. Spectroscopic analyses were coupled to XRD chemical characterization to provide a complete dataset of information. We performed acquisitions on 21 powdered and dried samples under vacuum and room temperature conditions by means of reflectometric interference spectroscopy at one constant geometry of data capture. Hence, we chose 43° phase angle in a non-symmetric arrangement with illumination and emission disposition set respectively at 30° and 13° (Fig. 2b). We used the same conditions across all spectral ranges and samples preparation with few slight exceptions. All samples were ground and sieved in order to work on a constant grain size that never exceeded $100\ \mu\text{m}$, powders went then through a desiccation process by means of oven and drier. During the analyses, the acquisition spot was 4 mm in diameter, resolution was fixed at $4\ \text{cm}^{-1}$

¹ (8 cm⁻¹ in the UV field) and 500 scans were performed for each sample (250 in the far-IR field). Spectralon 99% (LabSphere ®) of reflectance and a gold-plated standard were used as reference for calibrating ultraviolet, visible and IR reflectance. A broad range of wavelengths was investigated, spanning from UV to far-IR, in order to widen and enhance spectral libraries and probe less common windows of analysis to evaluate if markers and signatures could be there recognised. Spectral analysis will be performed to evidence absorption and spectral variability and identify diagnostics parameters to be applied also to remote sensing data. Such information is aimed to enhance spectral library exploited to interpret spectral images of planetary surfaces (Clark, 1999) and to ponder if broader wavelengths windows should be considered for future instruments directed to planetary exploration.

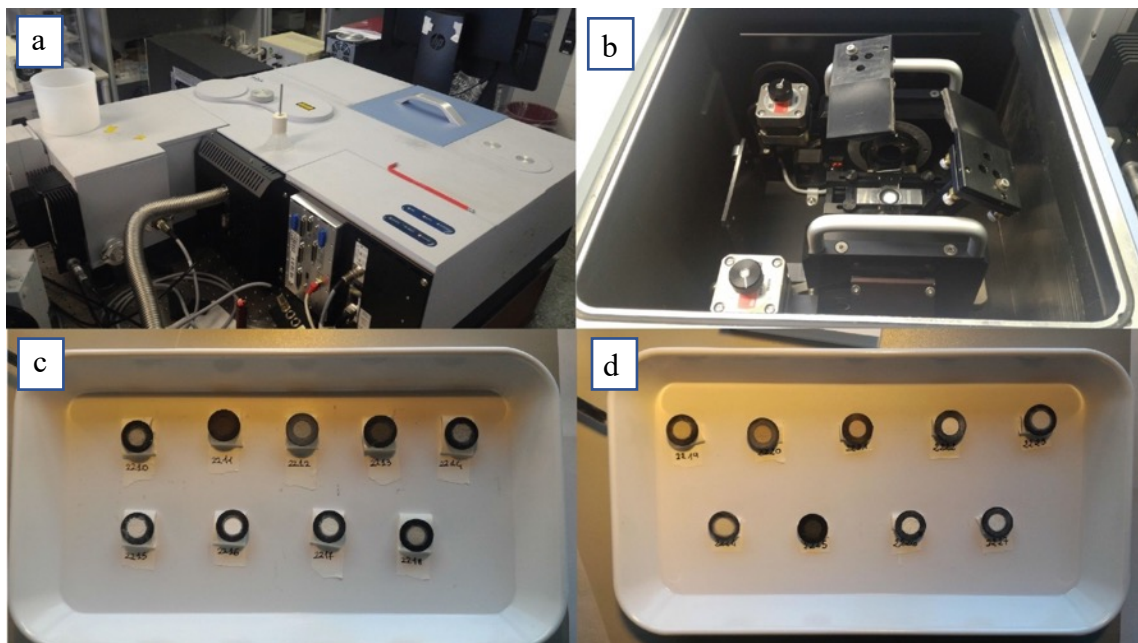


Figure 2. Spectrometer (a) and illumination asset (b) within the vacuum chamber; sample holder and mirrors positioned in analysis asset. Sample cups (c, d), ~0.3 g/sample each.

3. Preliminary results

The assignation of the absorption peaks to the relative mineral phase shows a good correspondence between the collected spectra and the library spectra used for the comparison based on the XRD data (continuum has been removed to highlight the peaks; Fig.3). Spectral signatures can thus be unequivocally assigned to specific minerals and rocks so, thanks to such reliable connection to representative mineral

phase, the expansion of peak investigation to the fringes of UV and far-IR was made possible. Accordingly, this work allowed the collection, in a very large wavelength span, of spectra belonging to materials that could be detectable on Mars at different scales.

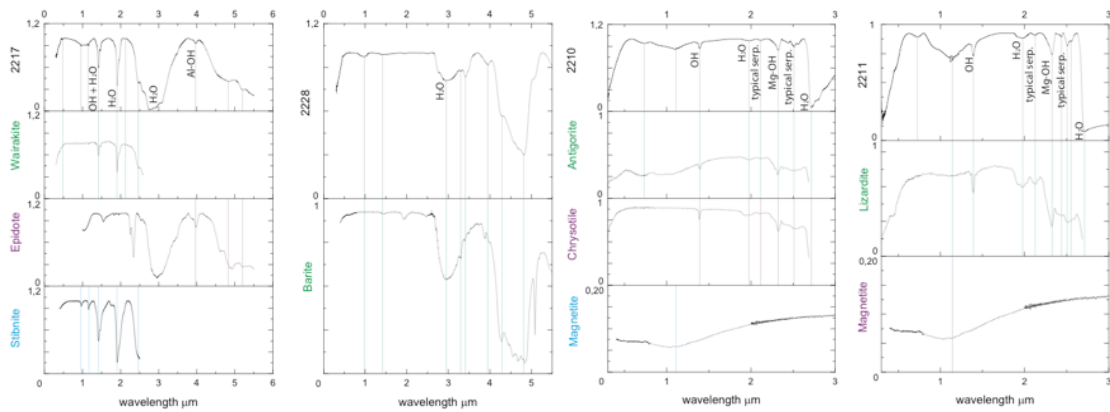


Figure 3. Spectral outcomes: samples 2217 and 2228 belong to epithermal mineral systems; samples 2210 and 2211 are representative of serpentinised rocks. In all the examples, assemblages of characterizing minerals are displayed.

Additionally, in this framework we produced a description of siliceous stromatolites that are emerging and intriguing possible analogue of past life evidence on Mars. Samples 2219 to 2222 are bio-speleothems made of porous amorphous silica which precipitation is mediated by a wide community of non-photosynthetic chemoautotrophs bacteria in the subsurface. These samples have been taken from two concretions, one more reddish and opaline (2219 inner layers, 2220 outer layers) and one white and less opaline (2221 inner layers, 2222 outer layers).

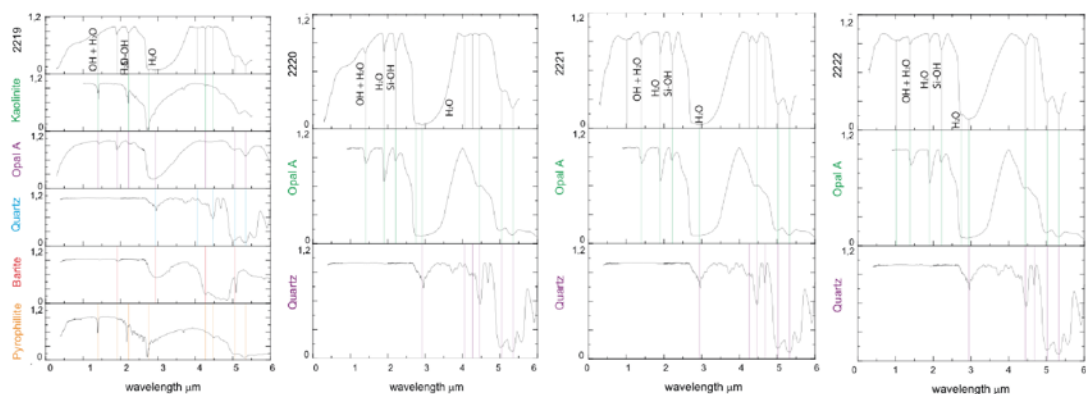


Figure 4. VIS and near-IR spectra of four investigated samples belonging to biologically mediated concretions. In the plots, assignments of the overtone absorptions are reported.

These deposits have been recently discovered in underground caves carved in quartzite rocks in the tepui table massifs of Venezuela (Aubrecht et al., 2008; Lundberg et al., 2010; Sauro, 2013; Sauro et al., 2013). These bio-speleothems are genetically different from the Chilean ones (e.g. Ruff et al., 2016), already discussed in literature, and could represent a new potential analogue of underground biologically mediated silica deposits, then exposed on the Martian surface by erosional processes. The spectroscopic information shows consistent data throughout the 4 analyses (Fig. 3, 4) producing a reliable base to look for analogue concretions elsewhere, but at the same time slight differences can be detected between the two stromatolites and the inner and outer layers (e.g. between 4 and 4.5 μm and between 8 and 12 μm , see Fig.4).

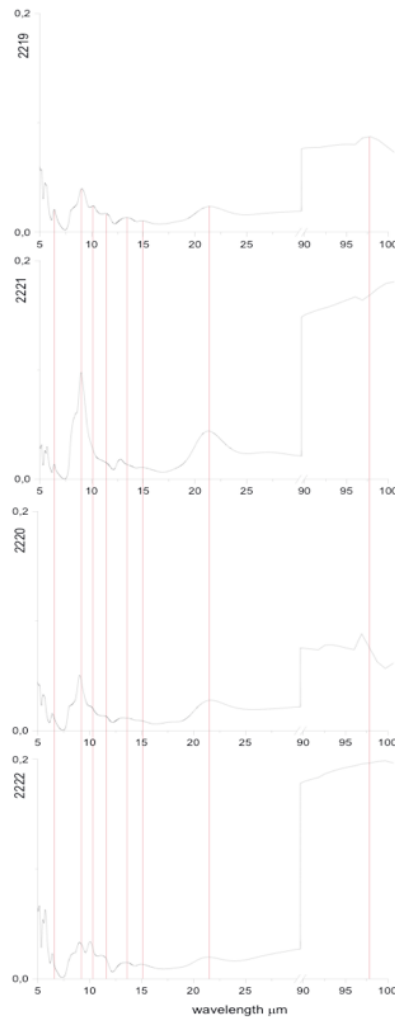


Figure 5. Far-IR spectra of inner and outer layers of the two stromatolites. Red lines are placed in correspondence of main peaks position to underscore differences and similarities.

4. Conclusions

The identification of potential hydrothermal environments in the Martian shallow subsurface will lead to a further more specific analysis of the peculiar characteristics that this kind of environment could assume on Mars. Hence, the characterization of spectral absorptions and peculiar characteristics of well described ore minerals related to epithermal environments represent a step forward toward the improvement of our knowledge about what we could expect to find within the Martian crust in correspondence of hydrothermal activity. The definition of the setting, and accordingly of a growing database on potential terrestrial analogues, could lead to the trigger processes identification and so to a better understanding of the mechanisms that lay beneath the methane release. In the end the implications that this work will have on the scientific knowledge are diverse. It could lead to the identifications of specific ancient and/or recent hydrothermal activity and eventually the detection, for the first time, of ore minerals and/or precious metals-bearing minerals. Moreover, the detection of recent hydrothermal activity linked to a specific kind of environment could improve the knowledge about the constraints to analyse a putative biological activity and other mechanisms that can lead to the methane release, such as the clathrate destabilization (Prieto-Ballestreros et al., 2006). In addition, mineralogical characterization and spectral analysis of sulphides minerals is of relevant interest also for other planetary bodies such as Mercury whose evidence of explosive activity is often related to such volatile materials (e.g. Kerber et al., 2009; Nittler et al. 2011)

References

- Aubrecht, R., Brewer-Carías, C., Šmída, B., Audy, M., Kováčik, E., 2008. Anatomy of biologically mediated opal speleothems in the World's largest sandstone cave: Cueva Charles Brewer, Chimantá Plateau, Venezuela. *Sediment. Geol.* 203, 181–195. <https://doi.org/10.1016/j.sedgeo.2007.10.005>
- Clark, R.N., 1999. Spectroscopy of Rocks and Minerals, and Principles of Spectroscopy, in: *Spectroscopy*. pp. 1–24.
- Dohm, J.M., Anderson, R.C., Barlow, N.G., Miyamoto, H., Davies, A.G., Jeffrey Taylor, G., Baker, V.R., Boynton, W. V., Keller, J., Kerry, K., Janes, D., Fairén, A.G., Schulze-Makuch, D., Glamoclija, M., Marinangeli, L., Ori, G.G., Strom, R.G., Williams, J.-P., Ferris, J.C., Rodríguez, J.A.P., de Pablo, M.A., Karunatillake, S., 2008. Recent geological and hydrological activity on Mars: The Tharsis/Elysium corridor. *Planet. Space Sci.* 56, 985–1013. <https://doi.org/10.1016/j.pss.2008.01.001>
- Geminale, A., Formisano, V., Giuranna, M., 2008. Methane in Martian atmosphere: Average spatial, diurnal, and seasonal behaviour. *Planet. Space Sci.* 56, 1194–1203. <https://doi.org/10.1016/j.pss.2008.03.004>
- Kerber, L., Head, J.W., Solomon, S.C., Murchie, S.L., Blewett, D.T., Wilson, L., 2009. Explosive volcanic eruptions on Mercury: eruption conditions, magma volatile content, and implications for mantle volatile abundances. *Earth Planet. Sci. Lett.* 285, 263–271
- Komatsu, G., Okubo, C.H., Wray, J.J., Ojha, L., Cardinale, M., Murana, A., Orosei, R., Chan, M.A., Orm, J., Gallagher, R., 2016. Small edifice features in Chryse Planitia, Mars: Assessment of a mud volcano hypothesis. *Icarus* 268, 56–75. <https://doi.org/10.1016/j.icarus.2015.12.032>
- Komatsu, G., Ori, G.G., Cardinale, M., Dohm, J.M., Baker, V.R., Vaz, D. a., Ishimaru, R., Namiki, N., Matsui, T., 2011. Roles of methane and carbon dioxide in geological processes on Mars. *Planet. Space Sci.* 59, 169–181. <https://doi.org/10.1016/j.pss.2010.07.002>
- Kopf, A.J., 2002. Significance of mud volcanism. *Rev. Geophys.* 40, 1005. <https://doi.org/10.1029/2000RG000093>
- Lundberg, J., Brewer-Carías, C., McFarlane, D.A., 2010. Preliminary results from U-Th dating of glacial-interglacial deposition cycles in a silica speleothem from Venezuela. *Quat. Res.* 74, 113–120. <https://doi.org/10.1016/j.yqres.2010.03.005>
- McGowan, E.M., 2011. The Utopia/Isidis overlap: Possible conduit for mud volcanism on Mars. *Icarus* 212, 622–628. <https://doi.org/10.1016/j.icarus.2011.01.025>
- Mumma, M.J., Villanueva, G.L., Novak, R.E., Hewagama, T., Bonev, B.P., Disanti, M. a, Mandell, A.M., Smith, M.D., 2009. Strong release of methane on Mars in northern summer 2003. *Science* 323, 1041–1045. <https://doi.org/10.1126/science.1165243>
- Nittler, L.R., Starr, R.D., Weider, S.Z., McCoy, T.J., Boynton, W.V., Ebel, D.S., Ernst, C.M., Evans, L.G., Goldsten, J.O., Hamara, D.K., Lawrence, D.J., McNutt Jr., R.L., Schlemm II, C.E., Solomon, S.C., Sprague, A.L., 2011. The major-element composition of Mercury's surface from MESSENGER X-ray spectrometry. *Science* 333, 1847–1850.
- Oehler, D.Z., Allen, C.C., 2010. Evidence for pervasive mud volcanism in Acidalia Planitia, Mars. *Icarus* 208, 636–657. <https://doi.org/10.1016/j.icarus.2010.03.031>
- Oehler, D.Z., Etiope, G., 2017. Methane Seepage on Mars: Where to Look and Why. *Astrobiology* 17, ast.2017.1657. <https://doi.org/10.1089/ast.2017.1657>
- Okubo, C.H., 2016. Morphologic evidence of subsurface sediment mobilization and mud volcanism in Candor and Coprates Chasmata, Valles Marineris, Mars. *Icarus* 269, 23–37. <https://doi.org/10.1016/j.icarus.2015.12.051>
- Peters, K., 1991. Gold bearing hot spring system of the northern coast ranges, California.
- Pondrelli, M., Rossi, a. P., Ori, G.G., van Gasselt, S., Praeg, D., Ceramicola, S., 2011. Mud volcanoes in the geologic record of Mars: The case of Firsoff crater. *Earth Planet. Sci. Lett.* 304, 511–519.
- Prieto-Ballesteros, O., Kargel, J.S., Fairén, A.G., Fernández-Remolar, D.C., Dohm, J.M., Amils, R., 2006. Interglacial clathrate destabilization on Mars: Possible contributing source of its atmospheric methane. *Geology* 34, 149. <https://doi.org/10.1130/G22311.1>
- Ruff, S.W., Farmer, J.D., 2016. Silica deposits on Mars with features resembling hot spring biosignatures at El Tatio in Chile. *Nat. Commun.* 7, 1–10. <https://doi.org/10.1038/ncomms13554>
- Sauro, F., 2013. Imawari Yeuata : a new giant cave system in the quartz-sandstones of the Auyan Tepui, Bolivar State, Venezuela.
- Sauro, F., Lundberg, J., De Waele, J., Tisato, N., Galli, E., 2013. Speleogenesis and speleothems of the Guacamaya Cave, Auyan Tepui, Venezuela. *Kars Caves Other Rocks, Pseudokarst-ICS*

- Proc. 298–304.
- Simmons, S.F., Brown, K.L., Browne, P.R.L., Rowland, J. V., 2015. Gold and silver resources in Taupo Volcanic Zone geothermal systems. *Geothermics* 2009, 205–214.
<https://doi.org/10.1016/j.geothermics.2015.07.009>
- Skinner, J. a., Mazzini, A., 2009. Martian mud volcanism: Terrestrial analogs and implications for formational scenarios. *Mar. Pet. Geol.* 26, 1866–1878.
<https://doi.org/10.1016/j.marpetgeo.2009.02.006>
- White, N.C., Hedenquist, J.W., 1995. Epithermal gold deposits: styles, characteristics and exploration. *SEG Newsl.* 23, 9–13.

Work in progress

YOUNG FLOWS PRODUCING AQUEOUS ALTERATION IN LADON BASIN, MARS, OBSERVED BY THE CASSIS IMAGING SYSTEM ON THE EXOMARS TRACE GAS ORBITER

Nicolas Thomas ^a and the CaSSIS team ^b

^a Physikalisches Institut, Sidlerstr. 5, University of Bern, Switzerland

^b http://www.cassis.unibe.ch/about_us/science_team

Authors' contribution:

This project is led by the PI of the CaSSIS camera, Nicolas Thomas, and scientific and technical contributions have been brought to the work by Co-I and science associate team members. Specifically, the geology-based Padova team, Matteo Massironi, Barbara De Toffoli and Riccardo Pozzobon, have equally contributed to: (i) the geological context, from the basin scale to the local CaSSIS scale; (ii) CTX mosaics and pan-sharpened CaSSIS-HiRISE basemaps; (iii) the geological map; (iv) surface age modelling based on crater counting.

The Colour and Stereo Surface Imaging System (CaSSIS) onboard the European Space Agency's ExoMars Trace Gas Orbiter spacecraft ^[1,2] has started observing the surface of Mars at around 4.5 m/pixel in 4 colours and in stereo. First observations have shown that, in combination with other data sets, CaSSIS will make a major contribution to studies of Mars' surface evolution. This is illustrated here with a study of the Ladon Vallis area of Mars using a four-colour image adjacent to a site known from previous observations to be rich in chloride deposits and previously suggested as a potential site for future landed missions ^[3]. The observations, in combination with previous remote sensing data sets, suggest that flows were active in the mid-Amazonian and interacted with subsurface groundwater to produce alteration products.

CaSSIS is a targeted imager and its operation has similarity to that of the HiRISE experiment on NASA's Mars Reconnaissance Orbiter but with full colour coverage and along-track stereo albeit at around a factor of 15 lower spatial resolution ^[4]. Images have been acquired regularly since 28 April 2018 at rates of up to 150 per week although from mid-June to mid-August 2018 observing was reduced because of a near-global dust storm. Despite the limited data set at this early stage of the mission, many targets have already been acquired that are provoking new assessment of processes on Mars. Here we address one example. Ladon Basin is an ancient multi-

ringed impact basin (Fig.1) located within a system of channels and basins along the Uzboi-Holdon-Ladon-Margaritifer (ULM) outflow system that extends from Argyre to the south to the Margaritifer Basin [5, 6]. This system, with its tributaries, is estimated to have provided drainage for ~9% of the Martian surface [3] and its formation is thought to have occurred in the late Noachian and/or early Hesperian [5]. The associated basins contain thick deposits of clay mineral-bearing strata and represent a large-scale sediment sink for materials derived from the surrounding Noachian terrain [7]. A geological history of the Margaritifer Basin has been proposed [8] and possible application of that chronology to Ladon Basin was noted.

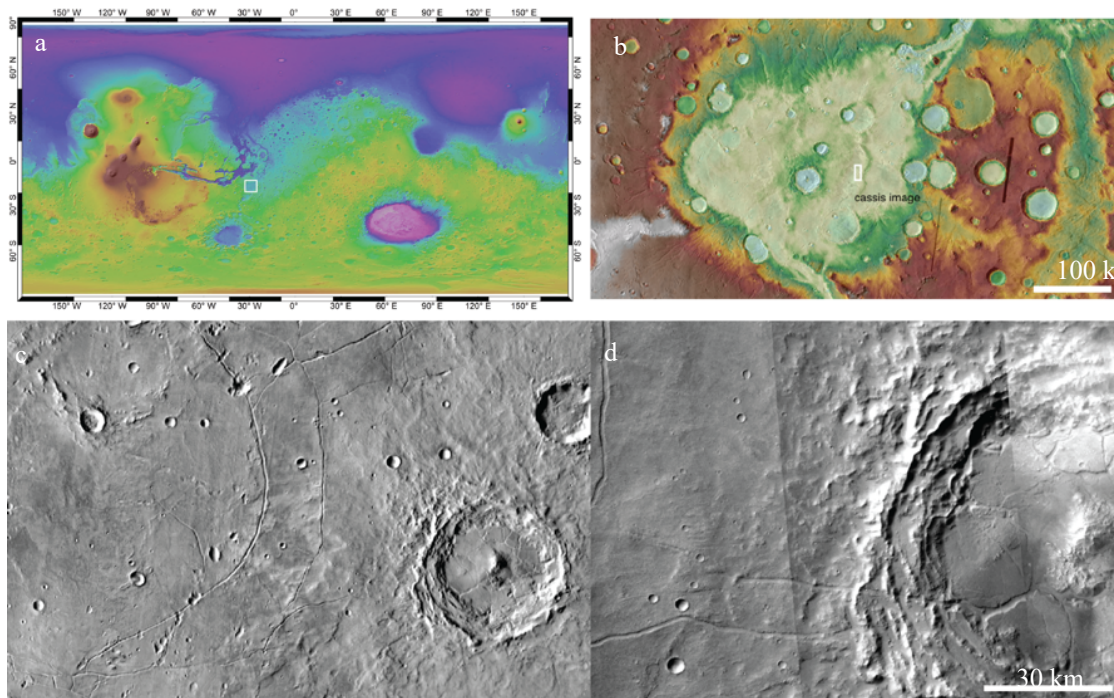


Figure 1. Location (a) and topographic map (b) of Ladon Basin showing the position of the CaSSIS image within the basin used for this study. Concentric and radial graben cutting the basin (c) and complex craters within it (d).

Figure 1 shows the location of a CaSSIS four-colour image within Ladon Basin. CaSSIS acquires data using a push-frame technique. Four colour filters have been mounted directly above the detector. The instrument acquires frames (typically 2048 x 256 pixels) roughly every 400 ms. These frames are then radiometrically calibrated [8] and geometrically rectified before being mosaicked to produce typically 9 km x 40 km swaths in one colour with subsequent combination into colour products similar to that seen in Figure 2. The registration is performed in ISIS3 [9].

The craters internal to the basin have polygonal floor materials. Graben cut the craters with polygonal floors suggesting later extensional activity (Fig.1). The CaSSIS image has been acquired at a point of coalescence of graben belonging to this system. CTX images that observed the area and the nearby regions show that the graben systems with Y or T-junctions typical of radial deformation.

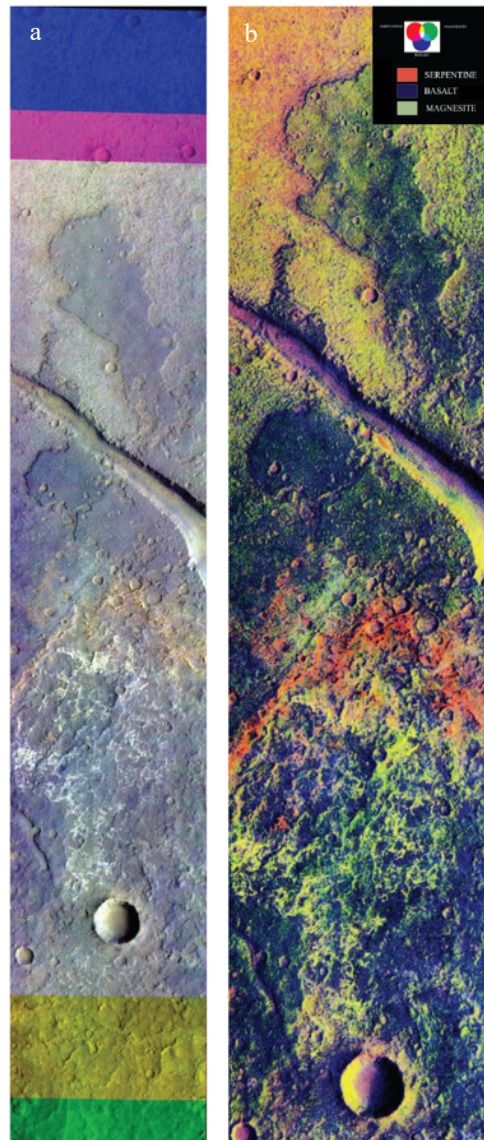
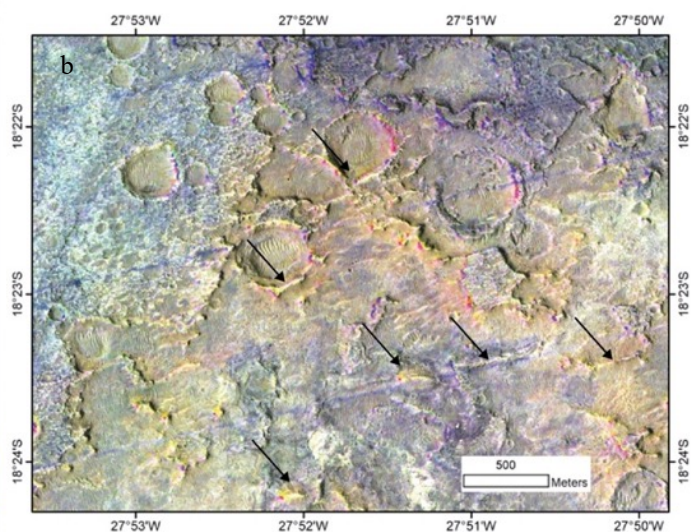
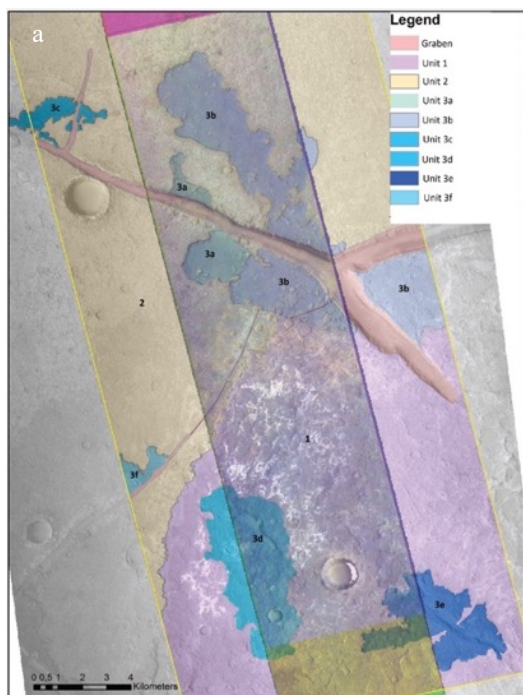


Figure 2. CaSSIS image (MY34_002009_200_0) of a graben in Ladon Basin (a). The push-frame imager generates a coaligned swath in four colours. These individual swaths can be combined to produce high quality colour products. The non-overlapping parts of the swaths can be seen at the top and bottom of the figure and have been left herein to help illustrate the technique. (b) Mineralogic or rock (i.e., basalt) compositional interpretations of CaSSIS 4-colour coverage based on multiple end-member spectral mixture analysis algorithm.

Such features are similar to those seen in Ladon are found in lunar impact basins and are generally interpreted to be graben formed as the surface was uplifted by magmatic

intrusions, in fact grabens are observed in places being the direct evolution of ridges implying that extensive dike intrusions are involved in graben production [10]. This indicates that extensional activity was (a) basin-wide, (b) not influenced significantly by stresses from outside the basin, and (c) relatively recent.

The CaSSIS image, in combination other data sets, show several provocative aspects of this area. The fracture walls show discrete bands of colour (Fig.2) that can be correlated with areally extensive materials, providing strong evidence that we are observing a sequence of near-horizontal layers of significant extent. In Figure 3, we identify three surface units and provide age modelling based on crater counting methodology. The youngest (labeled 3a and 3b) is closely associated with the fracture. The margins of this deposit appear lobate, suggesting this material was the result of the outpouring of a viscous fluid. However, when examined in detail, the margins are clearly erosional with small outliers of the deposit scattered beyond the main body. As such, the original extent and shape of the deposit cannot be determined but we assume the erosion was limited in extent and interpret this as a flow deposit. Similar materials are found across much of eastern Ladon Basin [11] so this deposit should be a significant part of the geologic history of this area. A similar young plains unit in Margaritifer basin, showing positive gravity anomalies just as Ladon, has been interpreted as lava [12] and geologic mapping of the Ladon Basin has suggested young volcanism to the south of this area [11].



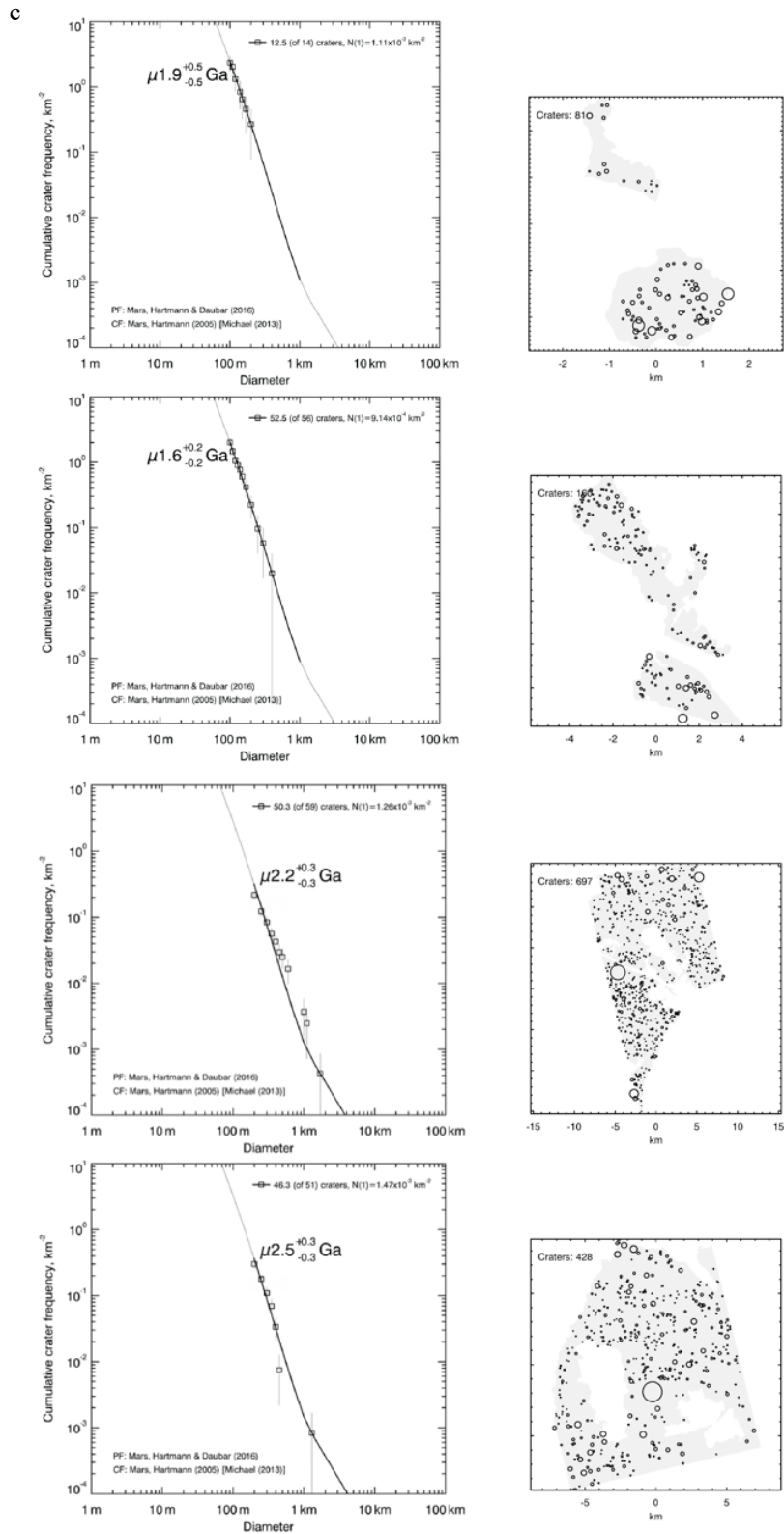


Figure 3. Preliminary geological map (a) of the surface frame covered by the CaSSIS image and the surrounding zone. Cassis 4 colour image PAN-sharpened with HiRISE to combine colour information with 0.25 m/pixel resolution of the region displaying linear light-toned alteration features (b). The main units (in order of appearance: two flow units 3a and 3b and two plain units 2 and 1) have been dated through crater counting (c).

Another interesting observation in the CaSSIS image are light toned rectilinear ridges (Fig.3; Fig.4). These are similar to ridges in other parts of Mars that have been interpreted as alteration along a percolating fracture system possibly caused by hydrothermal activity ^[13]. In addition, red/yellow colours are also observed at the unit boundaries. These deposits were exposed by erosion and ranged from 4 to 15 km in extent and were ~10 m thick. The largest and best-defined chloride deposit is cut by one of many fractures in the area and it is supported by a HiRISE IRB product in which chloride salts have a distinctive colour and texture. In Figure 3, the young ages of units 3a and 3b would support this chronology. These observations suggest that the older deposits have been hydrothermally altered into smectites and perhaps serpentine (Fig.2) possibly through contact alteration of lava units 3a and 3b. Alternatively, the older deposit may have formed independently and subsequently buried by the flows of Unit 3. The chloride salt indicates that surface or subsurface water may have been available locally during the formation of the older units. Given the crater retention ages, this would imply phyllosilicate formation well into the Amazonian period. Similar scenarios have been suggested previously. Ehlmann & Mustard (2012) ^[12] suggested that jarosite-bearing boxwork structures there could have formed from hydrothermal fluids circulating in lava flow fractures or by contact metamorphism of evaporite sediments ^[14,15,16]. In Ladon Vallis, however, the units are potentially much younger, and that may allow a better chance of distinguishing between competing hypotheses than has been possible in the much studied, much debated Syrtis/Nili region.

We suggest that the observations are consistent with a lava flow interacting with volatiles from a former shallow lake or playa that contained chloride deposits that are now observed in the oldest terrain. The subsequent alteration has led to the remarkable colour diversity seen in the CaSSIS data. The relative youth of the flows and the possible reactivation of subsurface groundwater make this a highly interesting area for further study about hydrothermal circulation and possibly biosignatures. The observations also show that the good signal to noise colour capability, combined with the high resolution and non-Sun synchronous illumination geometries accorded to CaSSIS by the TGO orbit will provide a highly useful tool for the investigation of mineralogical diversity at Mars including where trace gas species have been seen by the other instruments on TGO. This will allow to compile and prioritize a list of

observation targets needed to test specific hypotheses concerning active surface processes on Mars, specifically the detection of unusual or changing colours could function as markers of active processes, perhaps linked to water and methane circulation or release.

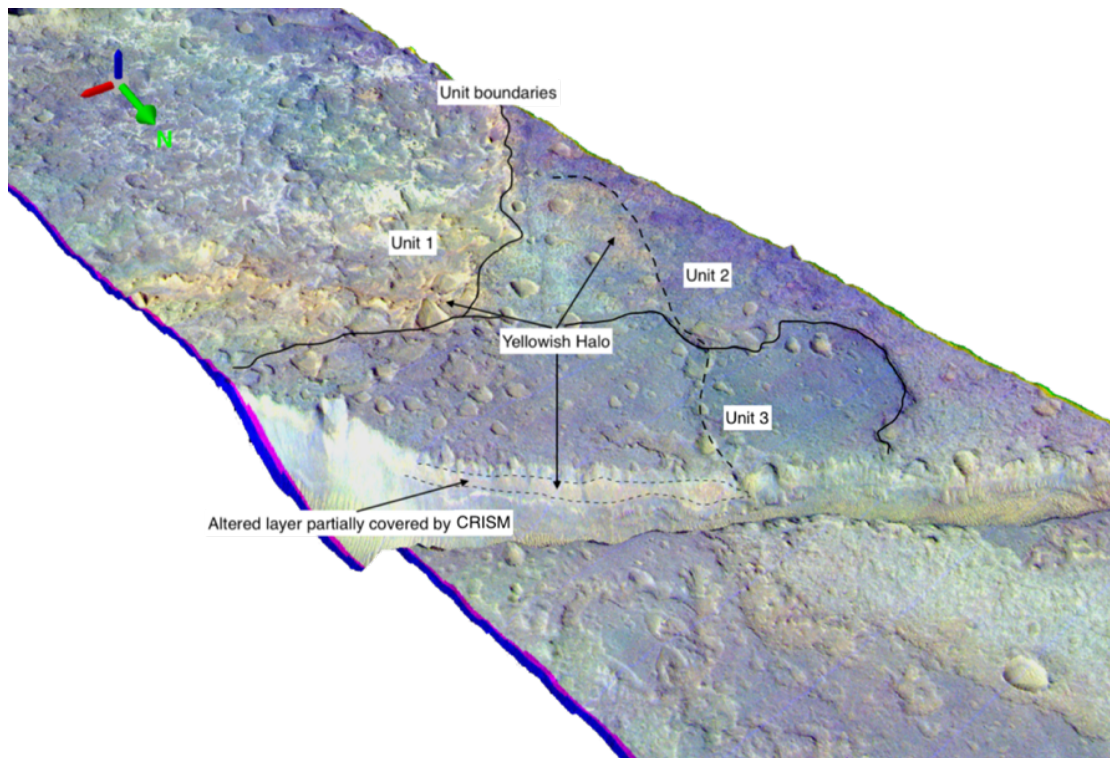


Figure 4. 3D view of the study area. Alteration is evident at unit boundaries and within the oldest unit

References

- [1] Vago, J., O. Witasse, H. Svedhem, P. Baglioni, A. Haldemann, G. Gianfiglio, T. Blancquaert, D. McCoy, and R. de Groot, (2015), ESA ExoMars program: The next step in exploring Mars, *Solar System Research*, 49, 518-528.
- [2] Thomas, N., et al, (2017), The Colour and Stereo Surface Imaging System (CaSSIS) for the ExoMars Trace Gas Orbiter, *Space Science Reviews*, 212, 1897-1944.
- [3] Thomas, R.J., Potter-McIntyre, S.L. and Hynes, B.M. Large-scale fluid-deposited mineralization in Margaritifer Terra, Mars, *Geophysical Research Letters*, 44, 13, (6579-6588), (2017)
- [4] McEwen, A., Eliason, E., Bergstrom, J., Bridges, N., Hansen, C., Delamere, W., Grant, J., Gulick, V., Herkenhoff, K., Keszthelyi, L., Kirk, R., Mellon, M., Squyres, S., Thomas, N., Weitz, C., 2007. Mars Reconnaissance Orbiters's high resolution imaging science experiment (HiRISE). *J. Geophys. Res.* 112, E05S02. doi:10.1029/2005JE002605
- [5] Grant, J.A. and T.J. Parker, (2002), Drainage evolution in the Margaritifer Sinus region, Mars. *Journal of Geophysical Research-Planets*, 107(E9), 5066.
- [6] Wolfinger, D.C. and K.A. Milam, (2014), A Geologic Characterization Of Ladon Valles, Mars, And Vicinity, LPSC, 49, Abstract #2908.
- [7] Milliken, R.E. and D.L. Bish, (2010), Sources and sinks of clay minerals on Mars, *Philo. Mag.*, 90, 2293-2308.
- [8] Roloff, B., Offa, B., and Turner, I.J., (2017) Indentation recovery threshold using the Electrostatic Detection Apparatus, *Canadian Society of Forensic Science Journal*, 50:1, 23-29, DOI: 10.1080/00085030.2016.1222706
- [9] Backer, J.W.,K. Becker, T. Becker, K. L. Berry, K. L. Edmundson, A. Goins, I. Humphrey, C. E. Isbell, L. Keszthelyi, J. Mapel, M. P. Milazzo, C. Neubauer, A. Pacquette, M. Shepherd, S. Sides, T. Titus, L. Weller, K. Williams, and T. J. Wilson, (2018), Updates To Integrated Software For Imagers And Spectrometers (ISIS3). 49th LPSC Conf. Abstract #2083
- [10] Schultz, P. H., Martian intrusions: Possible sites and implications, *Geophys. Res. Lett.* 5, 457-460, 197
- [11] Weitz, C. M., Wilson, S., Irwin, R. P. & Grant, J. A. Geologic mapping to constrain the sources and timing of fluvial activity in western Ladon basin, Mars. in 3rd Planetary Data Workshop 1986 (2017). doi:10.1590/S1516-18462008000300012
- [12] Salvatore, M. R., M. D. Kraft, C. S. Edwards, and P. R. Christensen (2016), The geologic history of Margaritifer basin, Mars, *J. Geophys. Res. Planets*, 121, 273–295, doi:10.1002/2015JE004938.
- [13] Okubo, C. & McEwen, A. S. Fracture-Controlled Paleo-Fluid Flow in Candor Chasma, Mars. *Science* (80-.). 315, 983–986 (2007).
- [14] Ehlmann, B.L., Mustard, J.F., (2012), An in situ record of major environmental transitions on early Mars at Northeast Syrtis Major. *Geophys. Res. Lett.* 39, L11202.
- [15] Bramble, M.S., J.F. Mustard, M.R Salvatore, (2017), The geological history of Northeast Syrtis Major, Mars *Icarus*, 293, 66-93.
- [16] Brown, A.J., S.J. Hook, A.M. Baldridge, J.K. Crowley, N.T. Bridges, B.J. Thomson, G.M. Marion, C.R. de Souza Filho, and J.L. Bishop, (2010), Hydrothermal formation of Clay-Carbonate alteration assemblages in the Nili Fossae region of Mars, *Earth and Planetary Science Letters*, 297, 174-182.

Conclusions

In its entirety, the aim of the research work herein presented was to step forward and widen our knowledge about fluid flows in the Martian upper crust in order to gain new clues for the identification of resurgence centres responsible for methane degassing and water discharge.

As far as we currently know, on Mars, intense circulation and discharge of large bodies of water were recorded during the early evolution stage of the planet (~ 4.6 – 3.7 Ga) when a denser atmosphere allowed the permanence of stable liquid water on the surface. Nevertheless, already during the Hesperian (~ 3.7 - 3 Ga) period such equilibrium begun to be compromised by atmosphere loss resulting in a decrease of atmospheric pressure and temperature possibly induced by a reduction of the volcanic activity. As a result, water started to progressively be less stable on the surface and, although it got partially lost, part of the fluids retreated toward the poles and in the subsurface. From this global climate change onward, water release from the subsurface reservoirs to the surface started to be driven only by outflow channels discharge.

Thus, this thesis includes studies that aimed to understand and enhance the current information available about fluid circulation in the Martian upper crust. A significative relevance has been given to large scale observations rather than single spot observations so to lay solid foundations for future investigation on the processes that lay behind the geomorphological expressions of fluid transport. Understanding the geologically recent hydrothermal circulation represent a key step in the search for environments suitable for life growth and flourish, which could be in turn linked to methane release. Based on this perspective, the investigation of the subsurface is among the cutting-edge frontiers that still remains mostly unexplored due to technical limitation. For such reason we pursued the validation and application of rising methods that could allow to gather information in this sense.

We specifically exploited the observation and analysis of the way percolating fracture networks grow filling the space and drew a relationship between such systems and their surface expressions produced by the accumulation of materials extruded during fluid expulsion. In addition, the presence of such kind of features in correspondence of percolating fractures tipping on the surface makes these environments a crucial astrobiological target due to their high preservation potential

of deep biosignatures. The implementation of fractal analysis played a central role in identifying high-interest area on the Martian surface, characterised by the presence of large pitted mound fields whose morphology alone would have been otherwise easily mistakable due to convergences with other features that lay beyond our interest. In this respect, not only a relationship between network of percolating fractures and the above mentioned mounds was detected, but was recurrently recorded a link between such kind of surface morphologies and the shallowest hypothesised interface between gas hydrate-rich cryosphere and the potential hydrosphere that lays beneath. In fact, in all the fields analysed within this project there is at least one cluster of mounds that appears to be linked to such specific level in the subsurface, hence it is to say that for each one of these areas there are hundreds, and in some cases more than one thousand, mounds related to the clathrate stability zone base. Given the remarkably vast coverage of the investigated regions that could have therefore experienced many different processes that concurred in cracking the crust, the observation of this unequivocal relationship needs to be recognised and set as a starting point for further analyses. A better understanding of the processes, for instance, that led to fracturing or triggered the fluid resurgences is an intriguing pivotal question since by the application of fractal analysis only the existence of such preferential pathways for fluids is verified. We thus approached this general question from two different sides: the investigation of structural asset of fracture systems that experienced fluid flow and the investigation of terrestrial environments that could be analogue to the mound fields under examination. Accordingly, on a smaller scale, we focused on the investigation and reconstruction of the structural asset of Gale crater to identify the driving forces that interplayed leading to the surface cracking and to fluid circulation. The region observed by the rover is significantly smaller than the areas covered by our previous analyses and nonetheless many different features linked to fracturing and sediment mobilisation have been recognised. Many factors can thus concur to these processes, we exploited well-exposed sulfate veins to profitably infer the stress field distribution, but the complexity and the geographical variability must not be underestimated particularly moving toward larger surfaces with diverse geological histories. Concurrently, instead of investigating the driving forces that generated the environments of interest, we approached the topic in the opposite direction that is to say by surveying the environment to detect key traits that can lead to specific formation processes. In this respect, we produced: (i) new spectral datasets of

uncommon materials linked to different fluid circulation phenomena always representative of suitable niches for life hosting, and (ii) we moved on in orbital images investigation implementing the latest tools provided by space exploration, specifically the four-colours CaSSIS camera products that led to the clear identification of alteration features and significantly helped the understanding of the relationship between them.

Overall, this three year project produced innovative and intriguing results by keeping the focus on one defined objective, that is the fluid circulation in the Martian upper crust, by anyway approaching it from different points of view. Nevertheless, new questions arose from these investigations that still have not been answered, such are the broad spectra of new scenarios that could involve clathrates dissociation in the Martian subsurface, that could not only lead to step forward in the reconstruction of the planet evolution, but could be a new cornerstone to start looking into topics that have not been previously considered central and bringing together diverse disciplines that would otherwise work on parallel tracks.

Acknowledgments

I feel entitled to write this section with the intent of being comprehensive rather than succinct. This is probably the last good opportunity to express my gratitude, in writing, to the many individuals who have instructed and supported me throughout my graduate career and formal education.

I firstly want to thank my graduate advisor, Matteo Massironi. During the past years he taught me, guided me and help me to grow as a scientist. I admire and acknowledge his scientific passion and vast knowledge of the field and I am glad he shared these qualities with me throughout all my years in graduate school. He is an intelligent, honest, passionate person genuinely caring about people around him and I am grateful he increasingly supported me along this challenging journey, believing in me also when I did not in the first place. All of these are among the many leadership qualities I admire and plan to emulate in the future when it will be my turn.

I thank my co-advisors, Gabriele Cremonese and Francesco Mazzarini, who helped and advised me as well and contributed in making me a stronger scientist. I especially would like to express my gratitude to Francesco that came a long way to serve in the first graduate committee sincerely supporting me through that first step of the evaluation process I was about to face.

I am also happy I had the opportunity to collaborate with professor Nicolas Mangold. Both the period I spent in Nantes and the further interactions we had enriched my planetary science knowledge and opened up new research horizons.

I am grateful to professors Karoly Nemeth and Matt Balme who reviewed this thesis and gave precious inputs to improve it and useful suggestions for future enhancements and developments.

I had the privilege to work in a research group alongside individuals, young and senior scientists, of great intellectual and human value. Among them, Riccardo Pozzobon deeply influenced my graduate career. Despite all the difficulties that academia had for us, we profitably complemented each other and our projects blossomed into amazing results that we struggled and will struggle to publish. He is a tenacious researcher that can always be counted on to help out and get things done. I am proud to have collaborated with him and I am certain my life in the office would have been miserable without his camaraderie.

It was a rewarding experience being part of the Geosciences research staff at the University of Padova and I feel that the bond which took me here for such many years, since my bachelor to my PhD, will never fade away no matter what the future will be. Here I had the opportunity to meet amazing scientists who I spent my time with during graduate school. While I did not collaborate on projects with all of them, I truly enjoyed working alongside these fantastic people that made the Geosciences department a great place to call home. Among them, Chiara Anzolini, Chiara Ballestrieri, Bruna Borges, Andrea Brenna, Carlotta Cappelli, Manfredo Capriolo, Luca Collanega, Silvia Contessi, Marco Crivellaro, Omar Gianola, Simone Molinari, Jacopo Nava, Livio Ronchi, Elisa Savignano, Tommaso Tacchetto, Luca Toffolo and many others.

I also thank the University of Padova for the fellowships that supported my graduate study and the “Fondazione Ing. Aldo Gini”, the GeoPlaNet consortium, EuroPlanet, European Astrobiology Center, European Space Agency that awarded me scholarships that made possible exceptional international exchanges during my PhD. Part of this work has been also supported by the Italian Space Agency (ASI) (ASI-INAF agreement no.2017-03-17) and the European Union's Horizon 2020 research and innovation program under grant agreement N°776276 (PLANMAP).

I also want to take a look back at several people who pre-dated my time in grad-school and at my friends and family who had a profound influence on my academic pursuits. Words cannot express how deeply grateful I am to my parents that exposed me to all sorts of opportunities as I grew up. They were incredibly encouraging of all I wanted to do both when this meant to watch me succeed, but also when it meant to watch me going through hell and fire to reach my goals. Being parents is not an easy task at all, but they are the best mom and dad that a person could wish for and I am ineffably blessed to have them in my life. A special memory goes also to my grandmother Nonna Elsa who, at the venerable age of almost one century, enthusiastically supported me and my career goals even if these were an alien world for her, more than they were for anybody else.

So many teachers and instructors crossed my way and I owe a little bit of my happiness and pride to each and every one of them. I cannot exempt to thanks Manuel Rigo and Guido Roghi who supervised me during my bachelor's degree and after that never stopped showing me their support me even if our scientific paths diverged.

Outside my geological life I have also been able to draw invaluable support from old and new close friends that made a great difference in my darkest and brightest moments. I have the privilege to count among them Alessandro Agostini who shared with me an apartment and a great flat-mate life and initiated me to the ADI PhD student association where I came to meet a surprisingly large number of splendid human beings that embraced graduate careers as well. I especially want to mention Giulia Binato and Federico Chiariotti who I am now glad to count as good friends. All these deep friendships have meant a great deal to me and periodically restored my faith in humanity.

Any future success that I may enjoy will be built on the love and educational foundation laid by all of those mentioned above. I hope that I will be one day able to pay everyone back and make the world a better place as a heritage from the ones who were and as a legacy for the ones that will be.